Pleiotropic Drug Resistance Type ABC Transporters in *Petunia hybrida*: Novel Roles in Symbiotic Interactions, Branch Development and Herbivory Defense

Dissertation

zur

Erlangung der naturwissenschaftlichen Doktorwürde

(Dr. sc. nat.)

vorgelegt der

Mathematisch-naturwissenschaftlichen Fakultät

der

Universität Zürich

von

Tobias Kretzschmar

aus

Deutschland

Promotionskomitee

Prof. Dr. Enrico Martinoia (Leitung der Dissertation)

Prof. Dr. Beat Keller

Dr. Didier Reinhardt

Zürich, 2009

Table of Contents

Zusammenfassung

Pleiotropische Drogen Resistenz (PDR) Proteine sind Transportproteine der ABC Transporter Superfamilie, die in Pflanzen unter anderem bei Krankheitsresistenz und Schwermetalltoleranz beteiligt sind. Im Allgemeinen scheinen PDR Proteine in vielfältige Reaktionen auf biotischen und abiotischen Stress, sowohl unterirdischer als auch oberirdischer Pflanzenorgane, eingebunden zu sein. Es wird angenommen, dass dabei der Transport pflanzlicher Sekundärmetabolite, wie Terpenoide oder Phenylpropanoide, über die Plasmamembran die auschlaggebende Funktion von PDR Proteinen ist. Pflanzliche Sekundärmetabolite werden zur Zeit als wichtige Signalmoleküle in der Kommunikation zwischen Wurzeln und Mycorrhizapilzen angesehen. Besonders wichtige Substanzen in diesem Zusammenhang sind dabei Strigolactone, die eine entscheidende Rolle bei der initiellen Erkennung der Symbionten in der Rhizosphere spielen.

Mit dem Ziel den Transport symbiotisch relevanter Sekundärmetabolite in Hinsicht auf die Etablierung arbuskulärer Mycorrhiza zu charakterisieren, haben wir mehrere putative Kandidatentranskripte aus den mycorrhizierten Wurzeln von *Petunia hybrida* isoliert. In der vorliegenden Arbeit beschreiben wir PhPDR1, einen ABC Transporter, der spezifisch in mycorrhizierten Geweben der Wurzelrinden induziert ist. Transposon-Insertionsmutanten, die keine funktionellen Kopien von *PhPDR1* besitzen, zeichnen sich durch signifikant reduzierte Kolonisationsraten aus, die zumindest teilweise auf eine Beeinträchtigung präsymbiotischer Kommunikation zurückzuführen sind. Dieser Phänotyp deutet auf eine Einschränkung der Exudation von Strigolactonen hin. In oberirdischen Organen ist die Expression von *PhPDR1* auf die Vaskulatur beschränkt und konzentriert sich im Breich der Nodien direkt unter den Blattachseln. Interessanterweise ist schon lange bekannt, dass ein Apocarotenoid, welches haupsächlich in der Wurzel produziert und über die Vaskulatur in den Spross transportiert wird, in den Blattachseln das Austreiben von Seitenzweigen verhindert. Kürzlich konnte gezeigt werden, dass Strigolactone mit diesem Verzweigungshormon identisch sind. In Übereinstimmung mit unserer Hypothese weisen PhPDR1 Mutanten ein abnormales Verzweigungsmuster auf, und akkumulieren ein exogen verabreichtes syntetisches

Strigolactonderivat in signifikant höheren Mengen als wildtyp Pflanzen. Zusammengenommen unterstützen unsere Daten die Annahme, dass PhPDR1 den Transport von Strigolactonen über biologische Membranen katalysiert und damit wichtig für die spezifischen Allokationen eines neu beschrieben Pflanzenhormons ist.

Ein zweiter in unserem Ansatz identifizierter PDR Transporter, PhPDR2, erwies sich ebenfalls auf Transkriptebene als Mycorrhiza reguliert, aber weder gewebsspezifische Lokalisationsstudien noch die Untersuchung mit RNAi Mutanten deuteten darauf hin, dass das Protein eine für die Symbiose relevante Funktion erfüllt. Im Gegensatz zu PhPDR1 ist PhPDR2 vorwiegend in Blatt- und Stengel-Trichomen sowie Lateralwurzelprimordien exprimiert, wo das Protein vermutlich bei der Exkretion von für Herbivoren giftigen Substanzen beteiligt ist. Pflanzen mit eingeschränkter *PhPDR2* Transkriptmenge scheinen anfälliger gegenüber Fressschäden durch *Spodoptera littoralis* Larven zu sein.

Summary

In plants Pleiotropic Drug Resistance Transporters (PDRs) have been demonstrated to contribute to pathogen resistance and heavy metal tolerance. In general they seem to be implicated in biotic and abiotic stress responses of aboveground and belowground plant organs and are suggested to transport secondary metabolites, such as terpenoids or phenylpropanoids across the plasma membrane. Plant secondary metabolites are currently emerging as powerful mediators in the communication between plants and arbuscular mycorrhizal fungi. A substrate class of particular interest in this respect are strigolactones, which play a dominant role in pre-symbiotic signaling in the rhizosphere.

In an attempt to characterize symbiosis related secondary metabolite transport and its implications in the establishment and function of mycorrhizal interactions we isolated several candidate transcripts from the mycorrhized roots of *Petunia hybrida*. Here we report on PhPDR1, a Pleiotropic Drug Resistance type ABC transporter that is specifically induced in and around mycorrhized cortical tissues. Transposon insertion mutants deficient in PhPDR1 function display significantly reduced colonization patterns that are at least in part due to a dysfunctional exudation of pre-symbiotic signals in the rhizosphere, reminiscent of strigolactone function. In accordance aboveground expression of PhPDR1 is confined to the vasculature with dominant peaks of expression in the nodal regions directly below dormant axillary meristems. Very recently strigolactones have been identified as the long elusive branching hormone that is predominantly produced in the root and moves acropetally in the shoot vasculature to inhibit the outgrowth of lateral buds. Congruently *PhPDR1* transposon insertion mutants display an aberrant branching pattern and over-accumulate exogenously applied synthetic strigolactone derivates. Taken together our findings suggest that PhPDR1 contributes to the translocation of strigolactones across biological membranes and that there are novel yet uncharacterized functions for strigolactones.

A second PDR identified in this screen, PhPDR2, also proved responsive to mycorrhization, but tissue specific localization studies and post-transcriptional silencing did not indicate any symbiosis specific function. Instead *PhPDR2* is highly expressed in foliar trichomes and lateral root primordia, where it is presumed to contribute to the

excretion of herbivore deterring secondary metabolites. Silencing of *PhPDR2* seems to render plants more susceptible to folivory by the generalist caterpillar larvae of *Spodoptera littoralis*.

1 General Introduction

1.1 Pleiotropic Drug Resistance Transporters and White Brown Complex Transporters, the ABCG Subfamily of ATP Binding Cassette Transporters

Pleiotropic Drug Resistance Transporters (PDRs) comprise a sub-family of full size transporters within the family of ATP Binding Cassette Transporters (ABCs). The ABC protein family consists of full size, half size and a few soluble members that all share a cytosolic Nucleotide Binding Domain (NBD), capable of binding and hydrolyzing ATP. The NBD is made up of approximately 200 amino acid (AA) residues and features three defining motifs, the Walker A box ($GX_4GK[ST]$), the Walker B box ($(hydrophobic)_4$ [DE]) and the ABC signature ([LIVMFY]S[SG]GX_3[RKA][LIVMYA]X[LIVFM][AG]), all of which are highly conserved within the family and among homologues across kingdoms. Walker A and Walker B are separated by around 120 amino acid residues and the ABC signature is situated just upstream of Walker B. Together they are thought to compose the binding site for ATP and the catalytic centre for its hydrolysis.

Full and half size members constitute integral membrane proteins that actively translocate a broad range of substrates across biological membranes at the expense of ATP. Since the transport is directly energized by Mg-ATP it is not directly linked to electrochemical gradients across the membrane and the mode activity equals that of a primary active pump. In addition to one or two NBDs, half and full size transporters also contain one or two Trans Membrane Domains (TMDs) respectively. Each TMD is made up of 4-7 membrane spanning alpha-helices that form a pore across the membrane, through which the substrate can be shuttled. Half size transporters are thought to act mainly as homo- or hetero-dimers, making them structural equivalents of full size transporters. In fact two NBDs and two TMDs seem necessary to form a functional unit for transmembrane transport. A comprehensive review on the structure and function of all plant ABC-transporter subfamilies has recently been published (Rea, 2007).

Together with Multi Drug Resistance Transporters (MDRs), Multidrug Related Proteins (MRPs), ABC1 homologues (AOHs) and Peroxisomal Membrane Protein homologues (PMPs), PDRs make up the entirety of full size transporters in plants. They are

characterized by containing two TMDs and two NBDs in an alternating arrangement. Whereas MDRs, MRPs, AOHs and PMPs display a forward domain organization with each TMD preceding a NBD, PDRs have a reverse configuration, featuring first a NBD, followed by a TMD. They share this orientation only with the half size sub-family of White Brown Complex (WBC) proteins, from which they are believed to have arisen through a single ancestral duplication event (Crouzet et al., 2006). Partly because of their close relatedness, a recently unified nomenclature for plant ABC proteins pools PDRs and WBCs into one subfamily, namely the ABCG subfamily (Verrier et al., 2008b). However, since the majority of the functionally described PDRs and WBCs are not of rice or Arabidopsis origin, and thus cannot be reconciled with the new classification system, and since rice and Arabidopsis homologues are generally referred to by their original name in the respective publications, I will refrain from using the newly proposed terminology in this introduction.

Another structural feature that clearly distinguishes PDRs from other ABC transporters, including WBCs, is the presence of four highly conserved PDR signatures of at least six contiguous amino acid residues. PDR signature1 (LLLGPP) and PDR signature2 (GLDSST) flank the Walker A and Walker B box on NBD1, while PDR signature3 (GLDARAAAIVMR) lies just downstream of the Walker B on NBD2 and PDR signature4 (VCTIHQPSI) starts 102 residues downstream of the Walker B on NBD2 (van den Brule and Smart, 2002). The signatures appear to be plant specific and are not conserved in yeast PDRs. No discrete function could yet be allocated to any of the PDR signatures, with the exception of PDR signature3. A single amino acid (AA) substitution in this region causes an increased protein abundance for AtPDR9, which is probably due to enhanced protein stability (Ito and Gray, 2006). It is thus likely that PDR signature3 plays a role in ubiquitin mediated protein turn over.

The most variant domain within the PDR subfamily is found 55 residues upstream of the Walker A box on NBD2. It encompasses a region of 3 (AtPDR2) to 80 (OsPDR15) amino acid residues that seems distinct for each PDR, excluding extremely closely related homologues. With exception of the N-terminus, which also significantly differs in composition and length, it is the only such region in the otherwise structurally highly conserved PDR subfamily. Whether it plays a role in substrate recognition or is merely a

non-functional domain that evolved without any selective restrains remains to be shown. Domain swapping experiments between well characterized homologues and subsequent analysis in regard to substrate specificity might prove a useful approach to address this question.

1.1.1 White Brown Complex Transporters

With 29 members in Arabidopsis and 30 members in rice, the half size White Brown Complex homologues make up the most numerous ABC subfamily found in plants (Verrier et al., 2008a). Considering that half size transporters are thought to form homo or hetero dimers, and can possibly pair up with more than just one partner, the actually number of functional units might be even higher than that. With the exception of Drosophila (15 members), WBCs are scarcely present in eukaryotes of fungal or animal origin. Yeast only contains one member of unknown function and five WBC homologues have been recognized in the human genome (Klein et al., 1999). They have been implicated in sterol and tetrapyrole transport as well as anthracycline resistance.

In Arabidopsis functional analysis of WBCs is restricted to AtWBC11 (Bird et al., 2007; Luo et al., 2007; Panikashvili et al., 2007; Ukitsu et al., 2007), AtWBC12 (Pighin et al., 2004) and AtWBC19 (Mentewab and Stewart, 2005). The former two contribute to cuticle formation, presumably via transporting cuticular waxes and/or their precursors across epidermal plasma membranes (PMs), to which they localize. The latter seems to confer a basal resistance to the aminoglycoside antibiotic Kanamycin. In terms of substrate affinities these functions are strikingly congruent with the ones observed for human WBCs. In a very recent publication OsABCG5, a WBC from rice, has been reported to be implicated in the regulation of shoot branching, adding a novel aspect to the repertoire of plant WBC function (Yasuno et al., 2008).

Histological studies of a collection of wax-lacking Arabidopsis eceriferum mutants (cer mutants) lead to the identification of a WBC with implications in cuticle formation (Pighin et al., 2004). Even though AtWBC12/CER5 is expressed in the epidermal tissues of most plant organs, loss of function mutants display a phenotype which is restricted to the stem epidermis, signifying redundant transport mechanisms in other organs. Stem

epidermal cells of cer5 plants feature laminar cytoplasmic inclusions of lipidic nature and the stem cuticle is depleted in a variety of wax components such as alkanes, ketones and alcohols, giving the stem a glossy bright green appearance. Contrastingly the total amount of epidermal wax, intracellular and cuticular, does not differ between WT and mutant, suggesting that the cytosolic inclusions comprise an accumulation of wax components that are lacking in the cuticle. WBC12 GFP fusion constructs under the control of the native promoter localize to the PM and are able to complement the cer5 phenotype. These findings indicate that AtWBC12 plays a direct role in export and not production or subcellular compartmentation of cuticular waxes and suggest that AtWBC12 is capable of transporting a multitude of wax precursors, with a dominant affinity for nonacosane across the PM. Because the cytoplasmic intrusions are not directly associated with the PM is seems most probable that the substrates are extracted directly from the ER or Golgi originated vesicles, which come into contact with the transporter.

AtWBC11/COF1 transcript is predominantly found in the epidermis of aerial organs, but also in lateral root primordia and root tips. The protein localizes to the PM, where, in congruence to AtWBC12 function, it contributes to the secretion of cuticular waxes, nonacosane in particular. The cuticle is one of the main barriers against non stomatal water loss and thus it is intriguing to find that the water stress related hormone ABA induces upregulation of AtWBC11 (Luo et al., 2007). In combination with an increased biosynthesis of wax and cutin precursors this would result in the fortification of aerial organs against desiccation. Consistent with this finding cof1 mutants are prone to wilting, but also display a pleiotropic growth phenotype, with a marked reduction in growth and fusion of rosette leaves. Similar to cer5, cof1 accumulates cytosolic lipidic inclusions in the epidermis and displays an aberrant cuticle structure. In contrast to cer5, cof1 also displays a significantly reduced cutin load, suggesting cutin precursor fatty acids as additional COF1 substrates.

In order to dissect the overlapping phenotype of cer5 and cof1, double mutants were produced and compared to the single mutant (Bird et al., 2007). Since the double mutants do not exhibit an accumulative phenotype, it was suggested that they either act in the same pathway or form heterodimers, with a strong affinity for cuticular waxes. The

additional phenotypes of cof1 mutants in comparison to cer5 would then suggest that COF1 can form additional dimers with other WBC members or with itself to create a complex with a high affinity for cutin precursor fatty acids.

The Kanamycin resistance conferring properties of AtWBC19 became apparent when T-DNA insertion lines for *AtWBC19* proved sensitive to Kanamycin despite the presence of the bacterial Kanamycin resistance marker nptII (Mentewab and Stewart, 2005). Overexpression of *AtWBC19* in tobacco results consistently in an increased resistance to Kanamycin. The fact that WBC19 is highly specific for Kanamycin transport and unlike nptII does not confer resistance to other antibiotics of clinical importance encouraged the authors to propose AtWBC19 as a novel resistance marker for the creation of transgenic plants. Not only would WBC19 constitute an endogenous plant derived marker, it would also limit resistance properties to the antibiotic Kanamycin were it to be transferred horizontally to potentially pathogenic microorganisms. GFP localization studies target WBC19 to the vacuolar lumen, which is interpreted as a tonoplastic association of the protein, but might also simply be due to degradation and vacuolar sequestration of the fusion protein. Since overexpression of a single WBC member accounts for the observed phenotype it can be assumed that AtWBC19 forms homodimers.

A novel function for WBC proteins was recently discovered when a map based cloning approach on the rice mutant reduced culm number 1 (rcn1) revealed that the inhibition of tiller outgrowth in this branching mutant is caused by aberrant function of OsABCG5, owing to single amino acid substitutions in two independent lines (Yasuno et al., 2008). Apparent phenotypes of rcn1 include a reduced shoot length and a reduced leaf number, but most conspicuously a highly diminished number of tillers. Homozygous double mutants for rcn1 and d3, a high tillering mutant with a defect in branching hormone perception (Ishikawa et al., 2005), display a phenotype comparable to that of the d3 mutants, leading the authors to conclude that rcn1 acts independently of the branching inhibitory pathway well established for rice (D-pathway), Arabidopsis (MAX-pathway), petunia (DAD-pathway) and pea (RMS-pathway). Northern blot and in-situ hybridization experiments localize *RCN1* expression to the root and the basal shoot with dominant peaks of expression in root tips, crown root primordia, shoot apical meristems and axillary meristems. Expression in the axillary meristems might be directly linked to tiller

outgrowth and authors speculate that, in accordance with previously observed WBC function, lipid transport might be involved.

Additional plant WBCs have been identified in the reproductive organs of tobacco, NtWBC1 (Otsu et al., 2004), and elongating cotton fibers, GhWBC1 (Zhu et al., 2003). Ectopic expression of *GhWBC1* in Arabidopsis leads to impaired development of seeds and siliques. Both hint at a role of WBCs in reproductive processes, but it remains to be determined whether this is also associated with the transport of lipids or other highly hydrophopic substances.

1.1.2 Pleiotropic Drug Resistance Transporters

While all major ABC transporter subfamilies are represented in all eukaryotes, PDRs are restricted to the plant and fungi kingdoms. They were first discovered in yeast, where they were recognized as powerful mediators of drug resistance (Balzi and Goffeau, 1995). PDR5/STS1/YDR1 from yeast, the prototype for all PDRs in terms of structure and function, has been intensively studied for its ability to confer resistance to a multitude of structurally unrelated toxic compounds such as the protein biosynthesis inhibitor cycloheximide and the mitochondrial inhibitors chloramphenicol, linomycin, erythromycin and antimycin (Leppert et al., 1990; Meyers et al., 1992). PDR5 encodes a 160kDA protein of PDR typical reverse configuration (Balzi et al., 1994) and localizes to the PM, where it operates as an ATP driven efflux pump.

Whole genome sequencing of Arabidopsis and rice lead to the identification of 15 PDR homologues in the former and 23 members in the latter (Crouzet et al., 2006). This discrepancy of member number is unusual for ABC transporter subfamilies and might hint at the expected function of PDRs as secondary metabolite transporters, which have specialized and diversified in accordance to each species` unique arsenal of secondary compounds. MRP and MDR numbers in rice and Arabidopsis are fairly conserved, and PMPs and AOHs are single copy genes in both. 17 MRPs have been found in rice and 15 MRPs in Arabidopsis, while both species contain 22 MDRs (Verrier et al., 2008a). Most MRPs investigated so far localize to the tonoplast, where they catalyze the sequestration of glutathione conjugates, xenobiotic compounds and anthocyanins into the vacuole

(Klein et al., 2006). MDRs on the other hand are generally targeted to the PM and several of its homologues have been demonstrated to be implicated in auxin transport (Geisler and Murphy, 2006).

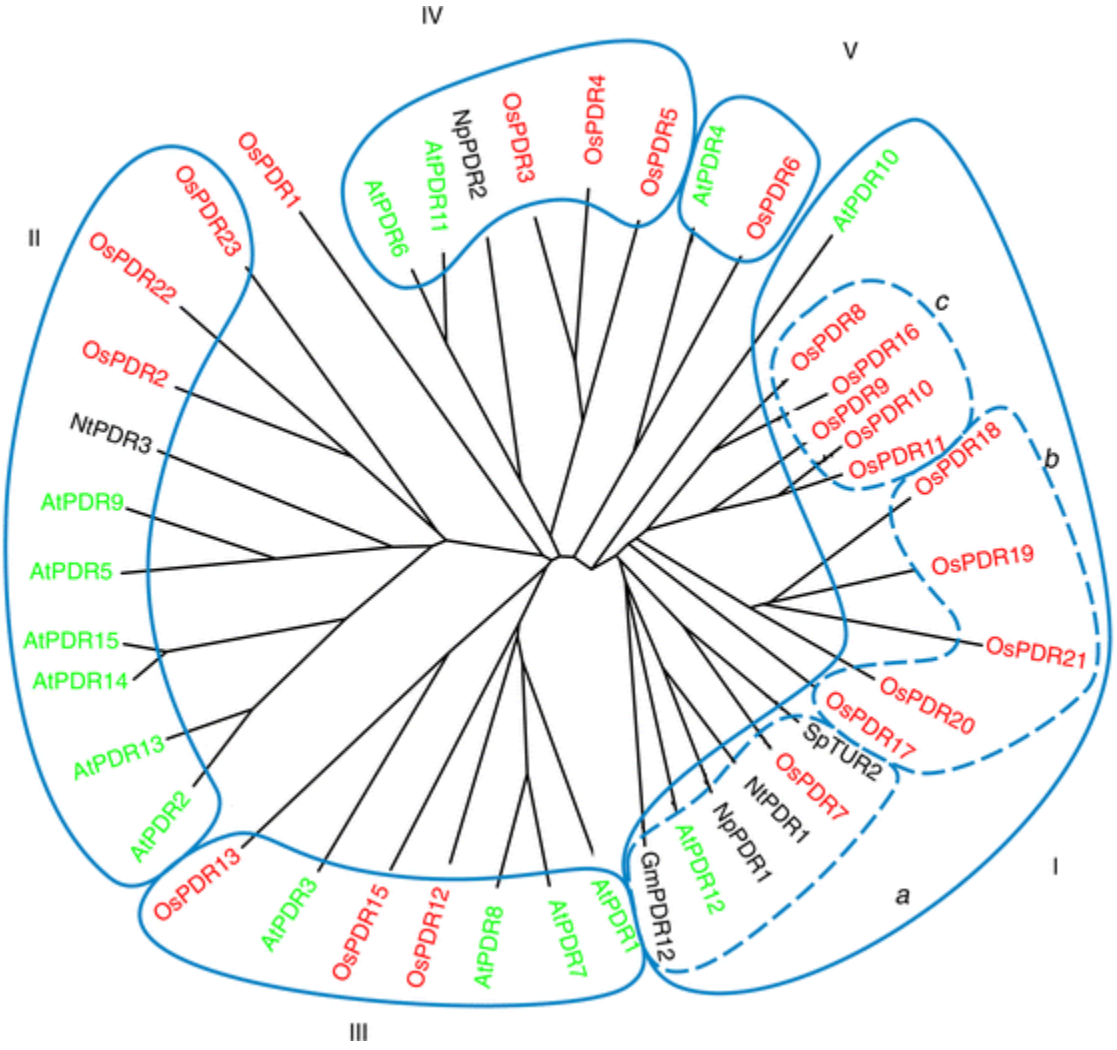

Figure1.1: Phylogenetic analysis of plant PDR proteins taken from Moons (2008).
Phylogenetic tree contains 22 rice homologues (red), 15 Arabidopsis homologues (green) and 6 homologues from unsequenced species (black). Homologues can be grouped into 5 distinct clusters (blue borders numbered I-V which correspond to Cluster1-5 in this introduction). Cluster1 can be further subdivided into 3 subclusters (broken blue borders numbered a-c), which are not further considered in this introduction.

PDRs also appear to be predominantly confined to the PM and putative substrates include substances as disparate as metal cations and lipophilic isoprenoids (putatively even transported by a single member). According to their relative phylogenetic relatedness the subfamily of PDR transporters can be further subdivided into 5 clusters of different size (Fig 1.1). There is a markedly uneven distribution of Arabidopsis, rice and other PDRs within the clusters and so far true structural and functional orthologues between species could not be unambiguously identified within a given cluster or across clusters. Furthermore, no apparent functional patterns have yet emerged within a given cluster that would suggest congruency with the phylogenetic partitioning.

1.1.2.1 PDR Cluster1 Homologues

Cluster1 is by far the largest and, in terms of new discoveries from unsequenced species, the fastest expanding PDR subdivision. It contains 12 members from rice, but only two members from Arabidopsis, namely AtPDR10 and AtPDR12, ofwhich only the latter has been characterized on a functional level. Of the twelve identified homologues from rice (OsPDR7-11, OsPDR14 and OsPDR16-21) only OsPDR9 and OsPDR20 have been partially investigated. Incidentally all but two of the PDRs identified from various other species fall into Cluster1, suggesting that Cluster1 members are either high in abundance or high in transcript levels for the species investigated. This is consistent with the finding that a genome wide analysis of ABC transporters in the model plant *Lotus japonicus* identified an unusually large amount of NBDs and TMDs that cluster with the respective domains of AtPDR12 and therefore can possibly be assigned to Cluster1 (Sugiyama et al., 2006). Furthermore transcripts of 8 putative *Lotus japonicus* Cluster1 members were detected, with most of them being highly expressed in rhizobium inoculated roots. This could either be due to a general responsiveness of Cluster1 homologues to bacterial elicitors or alternatively might hint at a functional role for PDRs in the root nodule symbiosis. Contrastingly, both *AtPDR10* and *AtPDR12* are expressed only marginally in root tissues and reproductive organs and *AtPDR10* was initially believed to be a pseudogene until weak traces of transcript could be detected (van den Brule and Smart, 2002).

SpTUR2 from the aquatic plant *Spirodela polyrrhiza* was the first plant PDR to be identified and characterized (Smart and Fleming, 1996). *SpTUR2* is highly responsive to abiotic environmental stresses such as low temperature and high salt concentrations and induction of *SpTUR* transcript seems to be under the control of ABA dependent pathways. In a follow-up study it could be demonstrated that SpTUR2 localizes to the PM, where it presumably catalyzes the excretion of antimicrobial compounds into the apoplast, thus participating additionally in biotic stress responses (van den Brule et al., 2002). Ectopic expression of *SpTUR2* in Arabidopsis leads to an increased resistance to the antifungal diterpene sclareol, suggesting defense related terpenoids as putative substrates. Consequently SpTUR2 seems to be implicated in both biotic and abiotic stress responses, a reoccurring quality of several PDR type transporters.

Among the most intensively studied plant PDRs is NpPDR1/ABC1. It was isolated from a PM-enriched fraction of a suspension culture of *Nicotiana plumbaginifolia* cells treated with sclareolide, a close analog of sclareol (Jasinski et al., 2001). It could be shown that NpPDR1 resides in the PM, is induced by sclareolide as well as sclareol and that it contributes to the excretion of closely related radiolabled compounds. Functional NpPDR1 characterization was the first report of a plant ABC transporter being implicated in pathogen defense and it can be considered the first acknowledgement of active terpenoid transport in plants. In a later study NpPDR1 function was investigated more closely on the whole plant level (Stukkens et al., 2005). Expression studies revealed that transcript is most abundant in the leaf epidermis, including leaf trichomes, but is also present in root tissues and petals. Both jasmonic acid (JA) and salicylic acid (SA) promote its expression, with the former exerting the stronger effect. Concomitantly a strong response to *Botritis cineria* and *Pseudomonas syringae*, both necrotrophic pathogens, the former a fungus and the latter a bacteria, could be observed. Downregulation of NpPDR1 via RNA interference mediated mechanisms leads to spontaneous and commonly lethal infections with *B. cineria* and renders the plant highly susceptible to exogenously applied sclareol. All these findings clearly indicate a dominant function for NpPDR1 in basal plant defense. Antimicrobial compounds such as sclareolide are deposited via NpPDR1 on the leaf surface and possibly exuded into the rhizosphere, contributing to a constitutive chemical defense barrier. Upon perception of

various pathogens and mediated via JA and SA dependent pathways this mode of defense is intensified locally around areas of infection, so that NpPDR1 mediated modes of action are both of a constitutive and an induced nature .

AtPDR12 has also been demonstrated to be induced by necrotrophic fungal pathogens, with the response being dependent on JA, SA and ethylene dependent pathways (Campbell et al., 2003). SA, a major mediator of systemic acquired resistance (SAR) in plants, exerts the strongest effect, promoting *AtPDR12* expression in most tissues. The SA and ethylene responsiveness clearly distinguishes *AtPDR12* from *SpTUR2*, which is mainly controlled by ABA, and *NpPDR1*, which is predominantly implicated in JA dependent pathways. In accordance to SpTUR2 and NpPDR1 function it was hypothesized that AtPDR12 might contribute to pathogen related defense by equally sequestering antifungal secondary compounds into the apoplast. And indeed the diterpene sclareol, putative substrate of SpTUR2 and NpPDR1, caused a thousand fold induction of *AtPDR12* as observed by real time PCR measurements, even though sclareol is not known to be produced by Arabidopsis. The authors conclude that AtPDR12 might be able to transport a variety of defense related terpenoid compounds and thus displays an affinity for sclareol even though it is not a native substrate. Concordantly, pdr12 mutant plants display an increased susceptibility towards sclareol treatment, manifesting itself in lower germination rates and stunted root growth. However no difference in resistance to pathogens of fungal and bacterial origin could be detected, which might either be due to redundant transport mechanisms or suggest other functions.

Interestingly the same protein seems to confer resistance to elevated heavy metal concentrations, as demonstrated by growth trials with WT and pdr12 mutant plants on plates containing lead (Lee et al., 2005). While *pdr12* knock out plants were more susceptible to lead than the WT, *PDR12* overexpressing plants displayed an increased resistance. Furthermore the authors could show that exogenous lead induced *AtPDR12* expression in roots and that *pdr12* knock out plants accumulate more lead than the WT, while overexpressing lines contained less of the toxic metal. The protein localizes to the PM where it presumably acts directly as a lead extrusion pump. However it is not discussed how the obvious double function of AtPDR12 in biotic and abiotic stress response can be reconciled. Even for a member of transporter class with exceptionally

broad substrate specificity, simulataneous affinities for substances as disparate as complex organic isoprenoids and simple charged inorganic ions are pending for further investigation.

Other Cluster1 members identified from various species seem to support the pattern of function in pathogen defense. *NtPDR1* from tobacco is an elicitor responsive member isolated from BY2 cells (Sasabe et al., 2002). Like *NpPDR1* it is mainly regulated via JA and strongly induced by a variety of fungal and bacterial elicitors. *GmPDR12* isolated from soybean suspension culture is also highly responsive to SA and JA and implicated in defense (Eichhorn et al., 2006). However, because of a lack of *in planta* studies and mutational approaches, no distinct function has yet been allocated to these proteins.

OsPDR9 from rice is absent in shoot tissues and was isolated as a low transcript root specific gene with marked responsiveness to abiotic stress conditions (Moons, 2003). Initially identified as a PEG induced gene it also proved responsive to hypoxia, redox perturbations (induced via DTT and peroxide) as well as elevated cadmium and zinc concentrations. Both ABA and JA stimulate OsPDR9 expression. However, the specific role of OsPDR9 in the reaction to these stresses remains unclear and it is yet unknown which membrane it localizes to.

OsPDR20 from rice seems to be distinct from the above described functions for Cluster1 PDRs. Even though it is markedly induced by the application of SA and transiently up-regulated by ABA, it is postulated to potentially play a role in weak organic acid release, rather than secondary metabolite transport (Moons, 2008). *OsPDR20* transcript is mainly found in the root and its expression is strongly promoted in response to organic acids such as malic acid, citric acid and lactic acid. All of these are commonly found in plant root exudates and serve several functions. Malic acid exuded into the rhizosphere has been repeatedly reported to serve as a powerful chelator of toxic aluminum cations. Citric acid facilitates nutrient acquisition (Pi in particular) and might provide a beneficial soil borne microflora with energy and carbon. Lactic acid sequestration is a common response to hypoxic stress, and similar to *OsPDR9*, *OsPDR20* also responds positively to redox perturbations. Another feature that unifies both rice homologues and distinguishes them from other Cluster1 members is their marked upregulation upon auxin treatment, introducing yet another phytohormone to the list of PDR effectors.

In conclusion, Cluster1 PDR members are generally PM localized and emerge as considerable contributors to plant pathogen responses by mediating the efflux of antimicrobial secondary metabolites, particularly of terpenoid origin, at the interfaces of plant and environment such as the cuticle and rhizosphere. They are predominantly incorporated in JA and/or SA dependent pathways, but several members also respond to a variety of other phytohormones such as ABA, ethylene or auxin. Many Cluster1 homologues show a transcriptional response to various pathogen specific elicitors and many are induced by their own substrates. This is thought to ensure a swift if unspecific response towards presence of the pathogen and concomitantly the cell avoids poisoning itself by over-accumulation of the often cytotoxic compounds. To a lesser degree they seem to be implicated in heavy metal tolerance either directly via extrusion of heavy metal cations or indirectly via the sequestration of chelating organic acids.
Surprisingly, given the fact that JA is a major mediator of plant herbivory defense and that insect deterring secondary metabolites form a strong line of defense against herbivores, no functional role for PDRs in plant insect interaction has yet been observed.

1.1.2.2 PDR Cluster2 Homologues

In contrast to Cluster1, Cluster2 contains only three members from rice (OsPDR2, OsPDR22 and OsPDR23), but six members from Arabidopsis (AtPDR2, AtPDR5, AtPDR9, AtPDR13, AtPDR14 and AtPDR15). With the exception of *AtPDR14*, all of the Cluster2 members of Arabidopsis are predominantly active in below ground tissues. (No expression data exists for AtPDR15.) The same is generally true for *OsPDR2*, whereas *OsPDR22* and *OsPDR23* are restricted to reproductive organs. Interestingly, unlike most other PDRs, *OsPDR22* and *OsPDR23* are insensitive to stress related hormone treatments, insinuating novel yet unidentified functions for PDRs. Despite their abundance in Arabidopsis, with easy access to T-DNA insertion lines, only AtPDR9 has been subjected to closer investigation (Ito and Gray, 2006).
A mutated gain-of-function allele of *AtPDR9* was isolated in a screen intended to identify enhancers in auxin resistance. Interestingly a single amino acid substitution (Ala to Thr at AA 1034) in a highly conserved PDR region (PDR signature3) appears to be

responsible for the semidominant nature of the phenotype. Presumably the mutation causes an increased protein stability resulting in lower turn-over rates and consequently higher protein abundance. Surprisingly AtPDR9 appears to be specific for the non-endogenous auxin derivate 2,4-D, and other closely related phenolic auxinic compounds. The gain of function mutant confers resistance to the analogues, while a null mutant proves to be hypersensitive. Both mutants however display neither alterations in transport or sensitivity to the endogenous auxin IAA, nor do they exhibit any apparent auxin related phenotypes under normal growth conditions. This raises the question of the in planta substrates for AtPDR9. Since the *AtPDR9* transcript is root specific with a marked expression in the root tip and root cap and furthermore strongly stimulated by SA, the authors hypothesize a function in below ground pathogen defense. Several phenolic secondary metabolites with structural resemblance to 2,4-D are known to have antimicrobial properties. Such are vanillic acid, ferulic acid, o-coumaric acid and cinnamic acid, all of which have been discovered in Arabidopsis root exudates, making them putative substrates for AtPDR9. A detailed analysis of root exudates from WT plants compared to both mutants might reveal the nature of AtPDR9 substrates.

Another Cluster2 member, NtPDR3, has been reported from tobacco (Ducos et al., 2005). Originally identified as a JA induced protein in suspension cultured BY-2 cells, it also proved responsive to SA and IAA treatment. Further investigation lead to the presumption that NpPDR3 was involved in iron homeostasis. Iron deficiency conditions in the culture medium strongly induced *NtPDR3* expression and a putative IDE-1 element, commonly found in iron deficiency inducible promoters, was identified upstream of the gene. NpPDR3 appears to localize to the PM and the authors postulate that it might be involved in the exudation of weak organic acids in order to facilitate iron uptake.

In a very recent publication, a novel Cluster2 member was identified as the responsible gene behind a robust and durable pathogen resistance against leaf rust, stripe rust and powdery mildew in wheat carrying functional *Lr34* alleles (Krattinger et al., 2009). LR34 clusters closely together with OsPDR23, but in contrast to the panicle specific rice protein it is predominantly found in adult foliar tissues, particularly the flag leaf. Unlike many other PDRs its expression seems to be modulated by developmental cues rather than stress factors. Whereas it is almost absent in the leaves of two-week old seedlings, it

is moderately expressed in the flag leaf of 7.5-week old plants and yet more transcript is found in the flag leaf of 9-week old plants. Transcript abundance is highest in the leaf tip, and wheat varieties with functional *Lr34* alleles can be phenotypically selected via a leaf tip necrosis developing in adult flag leaves. Despite of its resistance-conferring properties, *Lr34* is not responsive to pathogen inoculation, suggesting rather constitutive than induced pathogen related functions. The authors propose that in analogy to PEN3 (see chapter 1.1.2.3) LR34 might contribute to basal pathogen defense via the excretion of antimicrobial secondary metabolites into cuticular foliar surfaces. However, in contrast to PEN3 function, which seems restricted to nonhost resistance, LR34 is implicated in the defense against several compatible pathogens of fungal origin. In fact it is the only PDR characterized so far that negatively affects the invasion and spread of appropriate pathogens. Considering the appearance of leaf tip necrosis that coincides with functional *Lr34* expression, the authors speculate that LR34 may alternatively be involved in regulated leaf senescence. Indeed nonfluorescent chlorophyll catabolites, indicators of senescence, were only found in the flag tips of *Lr34* carrying varieties. Furthermore HvS40 a marker transcript of leaf senescence in barley (Krupinska et al., 2002), was found to be upregulated only in the presence of *Lr34* in uninfected 9 week-old flag leaves. Interestingly HvS40, under the control of JA and SA dependent pathways, is proposed to play additional roles in pathogen resistance. Senescence related defense mechanisms against obligate biotroph pathogens would constitute a novel function for PDR dependent biotic stress responses, which is presumably unlinked to secondary metabolite transport and might lead to the discovery of yet unknown PDR substrate classes.

1.1.2.3 PDR Cluster3 Homologues

Three PDRs from rice (OsPDR12, OsPDR13 and OsPDR15) as well as four PDRs from Arabidopsis (AtPDR1, AtPDR3, AtPDR7 and AtPDR8) fall within this cluster. AtPDR7 and AtPDR8 are structurally closely related, even on the genomic level. They contain the fewest introns (7 for PDR8 and 8 for PDR7) known for any PDR and share an 84% identity on the AA level. Both are ubiquitously expressed in all plant organs even though *AtPDR7* expression is most pronounced below ground, whereas *AtPDR8* is most

dominant above ground. However, only AtPDR8 has been the focus of several studies, all of which include a phenotype despite likely redundancies. It demonstrates a clear functional divergence regardless of structural and expressional similarities between AtPDR7 and AtPDR8. AtPDR8 is probably the most prominent Arabidopsis PDR homologue in terms of transcript abundance and general distribution.

AtPDR8 was first recognized as a crucial factor in pre-invasive nonhost resistance (Stein et al., 2006). In an extensive forward genetic screen of Arabidopsis mutants for an increased susceptibility to the barley powdery mildew pathogen *Blumeria graminis*, two penetration3 (pen3) lines were recovered and the mutations were mapped to the *AtPDR8* locus. Both mutations proved to be point mutations that lead to single AA substitutions in the ABC signature of NBD1 and the Walker A box of NBD2. Two *AtPDR8* T-DNA insertion lines display equal phenotypes, verifying the implication of PEN3 in nonhost resistance. The finding that single residue mutations in either Walker A or ABC signatures render the protein nonfunctional stresses the importance of these domains for proper PDR function.

Further studies revealed that pen3 mutants were also compromised in their capacity to prevent entry of two nonhost biotrophs (pea powdery mildew and potato late blight) and the necrotroph *Plectoshaerella cucumerina*. Contrastingly pen3 mutants proved hyper-resistant against an appropriate Arabidopsis powdery mildew pathogen, which the authors attribute to a hyperactivation of SA-dependent pathways observed for pen3 mutants. GFP fusion proteins under the control of the native promoter are able to complement the phenotype and target to the PM, with a marked increase of abundance at local infection sites. Taken together and considering the findings for NpPDR1 the authors conclude that PEN3 transports defense related compounds across the PM in a concentrated manner at local infection sites. Lack of PEN3 function would then lead to an accumulation of these compounds within the cell, which in turn activate SA dependent pathways that boost defense against compatible pathogens.

Contemporaneously a reverse genetic approach to investigate the function of AtPDR8 came to similar conclusions (Kobae et al., 2006). Null mutants were observed to develop spontaneous lesions on leaf margins when grown under non sterile conditions. After inoculation with the nonhost potato late blight pathogen, the mutant exhibited enhanced

cell death and macroscopic brown lesions indicative of a successful penetration and propagation of the oomycete. The bacterial pathogen *Pseudomonas syringae* on the other hand was only able to proliferate on the WT lines. *AtPDR8* null mutants reacted with a strong hypersensitive response (HR), causing local cell death at infection sites and thus preventing the spread of the otherwise compatible pathogen. This is consistent with the findings that SA dependent pathways are hyperactivated in pen3 mutants, since HR is SA induced. The authors could furthermore show that PR-1, PR-2, PR-5 and several other defense associated transcripts were upregulated in AtPDR8 mutants when grown in non-sterile conditions, priming the plant against imminent infections. Immunolocalization targets the protein to the PM, confirming the above GFP data. Interestingly promoter-GUS fusion studies revealed a pronounced peak of expression in cells surrounding the stomatal cavities. Since these are preferred sites of entry for several pathogens this finding supports the idea that AtPDR8 exports pathogen deterring, possibly even volatile secondary metabolites. Because of the high basal expression levels of *AtPDR8* one might speculate that it also plays a role in constitutive defense by enriching epidermal cell walls with antimicrobial compounds. Alternatively it might have other unrelated functions.

In a more recent publication (Kim et al., 2007) a prominent role for AtPDR8 in heavy metal resistance was proposed. Based on the observation that *AtPDR8* expression was promoted by exogenously applied cadmium and lead, the authors tested the response of WT plants, *AtPDR8* null mutants, *AtPDR8* silenced mutants and *AtPDR8* over-expression mutants to elevated heavy metal concentrations. A clear positive correlation between transcript abundance and resistance to lead and cadmium could be established, while the susceptibility to high copper concentrations was not affected. Supporting these observations, over-expression lines accumulated significantly less, and silenced lines significantly more cadmium in both root and shoot tissues with respect to the WT. In order to test whether AtPDR8 is directly involved in the export of cadmium ions or cadmium complexes, a ^{109}Cadmium flux assay, utilizing isolated mesophyll protoplast was deployed. Initial uptake rates did not vary between the different mutants, but after one hour of incubation the over-expressing line contained less and the silenced line contained more ^{109}Cadmium than the WT. Whereas uptake of ^{109}Cadmium more or less saturated in the WT and silenced lines after one hour it was clearly reduced in the over-

expression line, when compared to earlier time points, indicating increased export capacities for the over-expression line. This observation was confirmed in ^{109}Cadmium efflux assays with preloaded protoplasts. Moreover two silenced lines and two T-DNA insertion lines exhibited a marked reduction of fresh weight (FW) and root length in comparison to the WT when grown on plates containing either cadmium or lead. In contrast, the over-expression of *AtPDR8* conferred an increased resistance to both, without affecting the susceptibility to high copper concentrations.

1.1.2.4 PDR Cluster4 Homologues

Cluster 4 contains OsPDR3, OsPDR4 and OsPDR5 from rice as well as AtPDR6 and AtPDR11 from Arabidopsis, none of which have been analyzed on a functional level. First attempts to characterize a Cluster4 member have been successful with a candidate from *Nicotiana plumbaginifolia*, NpPDR2 (Trombik et al., 2008). Transcripts have been confirmed in the root and the flower. Closer investigation, utilizing a Promoter-GUS fusion construct, pinpoints the floral expression to the conductive tissues within the style 48h post-pollination. It is argued that NpPDR2 is either involved in pollen tube guidance via the secretion of signaling compounds or in post-pollination specific senescence of stylar tissue. RNA interference mediated silencing of *NpPDR2* however did not result in a detectable phenotype, awhich the authors argue is probably due to redundancy. Interestingly none of the stress related hormones and elicitors known to promote PDR expression show any effect on *NpPDR2*, making it the first characterized PDR whose function seems to be independent from either biotic or abiotic stress response. In terms of spatial expression it might be functionally homologous to its close relative AtPDR11, which seems to be restricted to stylar tissues and ovaries. Thus according to expression profile studies it might be functionally related to the Cluster2 members OsPDR22 and OsPDR23. Functional overlap with members of its own cluster, however, seems unlikely since *OsPDR3* and *OsPDR4* exhibit a more general distribution and *OsPDR5* transcript is highly abundant in rice blast infected leaves.

1.1.2.5 PDR Cluster5 Homologues

This cluster constitutes the smallest subclass of PDRs, with AtPDR4 and OsPDR6 being the only members identified so far. *AtPDR4* appears to be ubiquitously expressed throughout the plant and is insensitive to most of the known PDR effectors (Genevestigator, EFP-browser). *OsPDR6* on the other hand is exclusively found in the panicles and its expression is promoted by ABA treatment, tempting the speculation that it might be involved in the regulation of grain filling under limited water availability.

1.1.2.6 PDR and WBC Conclusion

No apparent functional patterns emerge that are congruent with the phylogenetic clustering. Instead, reoccurring qualities of PDRs such as contribution to pathogen resistance and heavy metal tolerance are found among homologues of several clusters. Transcript profiling of most members in Arabidopsis (van den Brule and Smart, 2002) and rice (Moons, 2008) revealed that a large number of PDRs are predominantly expressed in root tissues. Most PDRs seem to be implicated in either JA and/or SA dependent pathways, suggesting roles in biotic and abiotic stress responses, which could be confirmed on a functional level for several members of Arabidopsis and solanaceaous homologues. Interestingly, whereas ABA does not alter PDR expression in Arabidopsis, it is the main inducer of *SpTUR2* in the aquatic plant *Spirodela polyrrhiza* and exerts influence over several rice homologues.

In recent years plant PDRs have become among one of the most widely investigated subfamilies of full size plant ABC transporters, considering the number of homologues portrayed on a functional level via transcriptional profiling, mutational approaches and reporter gene fusion constructs. Unfortunately in depth characterization of structural properties, functional domain qualities, substrate specificities and putative modulator interactions (such as kinases etc.) are severely hampered by the inability to express PDRs in non-plant heterologous systems such as yeast. Until now no system for a successful heterologous expression of PDRs has been reported. This might be partially due to a particularly high regulated proteolysis mediated turnover rate of PDRs. Having identified

PDR signature3 as a potential target for ubiquitination, site directed mutagenesis of single residues within the domain might prove a useful tool to increase protein stability in heterologous systems. But it must be kept in mind that this specific PDR signature is not conserved in yeast homologues. Apart from heterologous systems, new high throughput mass spectrometry based metabolomic approaches might also give insight into the nature of in planta substrates. However high levels of redundancy, and broad substrate specificities expected for most PDRs might complicate the matter.

There appears to be a functional overlap between WBCs and PDRs in terms of transporting lipophilic compounds across the PM, although this apparent congruence might simply be due to a lack of functional data for WBCs. There are indications that WBCs occur in different endomemebranous systems such as the tonoplast and plastidal membranes, which would clearly distinguish them from the strictly PM residing PDRs. And whereas PDRs are predominantly implicated in stress related responses, WBCs appear to contribute more to structural aspects of plant survival and might also fall within the classical role of ABC transporters as cellular detoxifiers. Because of their shared reverse domain organization and the phylogenetic origin of PDRs within the WBC clade, combining both subfamilies into one seems reasonable, particularly from a historic point of view. The novel unified nomenclature is based on the animal system, where PDRs are simply not present, and the only alternative to assimilation within an existing subfamily would be the creation of a completely new clade.

1.2 Signaling in Arbuscular Mycorrhiza

Arbuscular Mycorrhiza (AM) comprises the mutual symbiotic relationship between soil born fungi of the phylum Glomeromycota and an estimated 80% of all vascular land plants. Thus AM can be considered the rule rather than the exception and is generally regarded to be the most prevalent terrestrial symbiosis, with major impact on ecosystem productivity, biodiversity and global carbon turnover.

The interaction is confined to the roots, where single mature hyphae form simple appressoria, also referred to as hyphopodia, on the root surface of host plants and start to invade the root via epidermal clefts, prepared by the plant at sites of entry (Harrison,

1999). Prior to fungal penetration, as a result of chemical and mechanical stimulation, the about to be invaded cell undergoes profound subcellular reorganization (Genre et al., 2005). First the nucleus migrates to the expected point of entry, where the establishment of the pre-penetration apparatus (PPA) is induced. Microtubules together with microfilaments and ER-cisternae initiate a tubular transcellular structure of cytoplasmic nature, which eventually bridges the large central vacuole and predefines a cytosolic path across the cell. Along this tube the plant plasma membrane (PM) surrounding the invading hypha will invaginate, its expansion supported by membrane vesicles budding off the ER associated with the PPA, guiding the hypha across the epidermal cell. The fungus then continues growing either intracellularly, supported by further PPA structures, or intercellularly towards the root cortex, where it commences to extend longitudinally in both directions. Lateral hyphal branches start to penetrate single cortical cells and dichotomously expand to form extensively branched, tree like haustorial structures, the arbuscles, which ultimately fill out most of the cell. At this symbiotic interface, the invaginated and largely extended PM lies in direct and close contact with the fungal PM. Even though it is continuous with the rest of the PM, it features a unique protein composition and is highly specialized to serve symbiotic purposes. It is referred to as the periarbuscular membrane (PAM) and the small extracellular space between plant and fungal membrane as the periarbuscular space. Most of the exchange of nutrients and possibly the secretion and perception of signaling compounds takes place across it. Despite their complexity and cost-intensity, arbuscles are very short lived and usually senesce within days (Harrison, 1999). It is argued that thus the plant keeps a tight control over the extent of fungal colonization and might selectively favor efficient arbuscles over non-efficient ones by increasing or decreasing its life span.

The major benefit for the symbiotes are photoassimilates, provided by the plant in the form of hexose sugars, in return for inorganic nutrients, predominantly phosphorous, but also nitrogen and possibly others. With its extensive network of very fine extraradical hyphae, and supported by the exudation of soil chemistry altering compounds, the fungus can exploit the mineral and organic resources of the soil much more efficiently than the plant, and a majority of the plant`s phosphorous demands can be met by symbiotic phosphate transfer. The symbiosis exists in such abundance that an estimated 20% of all

photosynthetically fixed carbon is allocated to the fungus, making AM a major contributor to carbon and nutrient cycling of most terrestrial ecosystems, with direct impact on productivity and sustainability (Parniske, 2008).

Consequently lots of effort has been invested in trying to identify the nutrient and sugar transporters that mediate the symbiotic exchange at the level of the PAM. The plant actively controls the allocation of sucrose towards the roots, presumably via JA governed mechanisms. The transporter(s) responsible for the translocation of sucrose into the periarbuscular space have not yet been identified, but it is assumed that plant derived sucrose synthases or acid invertases in the periarbuscular space convert sucrose into hexoses to maintain a sucrose gradient across the PAM and prepare the sugars for uptake via the fungus.

Much more is known about plant derived phosphate transporters in the PAM. Originally identified in potato, a mycorrhiza induced phosphate transporter, StPT3, expressed in cortical cells with close association to fungal structures, was demonstrated to exhibit high affinity transport kinetics for inorganic phosphate in a heterologous yeast system (Rausch et al., 2001)**.** Later studies on the phosphate transporter (PT) family led to the discovery of a close Medicago homologue, MtPT4, which specifically targets to the PAM (Harrison et al., 2002). Abolishment of its function severely impairs mycorrhizal colonization patterns, particularly arbuscle development (Javot et al., 2007), demonstrating that it constitutes an essential component of the symbiosis. Orthologues of MtPT4 were described in tomato, LePT4, and potato, StPT4 (Nagy et al., 2005). Additionally a close homologue from rice, OsPT11, was characterized (Paszkowski et al., 2002), pointing out similarities and differences in symbiotic phosphate acquisition strategies between distantly related species.

AM is a very ancient symbiosis, with fossil records dating the onset of the relationship to the early Devonian period, at least 400 Mio years ago (Remy et al., 1994). Interestingly it coincides with the first major radiation of land plants, suggesting that AM was highly beneficial, if not decisive for the initial colonization of terrestrial habitats. Given the high level of structural organization already present in these fossils and the presence of mycotrophic plants in all of today's terrestrial plant orders, it can be speculated that AM might have already been a characteristic of a common land plant ancestor. Ancestral

Glomeromycota are believed to have been already obligate biotrophs and to this day no single species of this phylum seems to have escaped this dependency. Without successful colonization of a plant root, the fungus is unable to complete its life cycle and form a new generation of spores. Plants on the other hand remain facultative symbiotes and some families have lost the ability to form AM altogether. The extent to which a plant attracts the fungus and allows colonization of its root system seems to be primarily regulated by its nutrient status and it can either promote or inhibit fungal proliferation. Surprisingly the symbiosis appears to be rather unspecific, and at least under laboratory conditions most investigated fungal species exhibit an exceptionally broad host spectrum. Congruently a single plant can be colonized by several different fungal species simultaneously and might selectively favor certain strains only after having assessed its phosphorous providing capacities.

Given the fact that AM fungi (AMF) are obligate biotrophs, it is crucial for their survival that they can sense the presence of a host root within the soil. Furthermore it is of equal importance that they send out a chemical or mechanical cue to the plant, which will clearly mark them as a beneficial symbiote and unambiguously distinguish them from other potentially pathogenic fungi. The plant on the other hand, mostly interested in the establishment of the symbiosis in times of low nutrient availability, would benefit most, if in the possession of a non-constitutive signal to attract the fungus, which can be turned on or turned off, in respect to its current nutritional status. And it certainly needs to be able to recognize a mycorrhizal fungus as such in order to lower its defenses and prepare for the accommodation of the symbiote.

It has long been acknowledged that, in the pre-symbiotic phase of the relationship, the plant excretes one or several diffusible low molecular signals into the rhizosphere, which upon perception by the fungus induce extensive hyphal branching and thus have been dubbed branching factors (BF) (Buee et al., 2000; Akiyama et al., 2002). Phosphate starvation promotes BF exudation (Tawaraya et al., 1998), increasing the plants chance to recruit a mycorrhizal partner and subsequently improve its nutrient status. BFs are thought to activate the AMF metabolism and development in the vicinity of a host plant in order to facilitate contact. However it was not until recently that a BF could be unambiguously identified as a sesquiterpene lactone of the family of strigolactones

(Akiyama et al., 2005). Interestingly those sesquiterpenoids have long been known as germination stimulants of the obligate parasitic weeds *Striga* ssp. and *Orobanche* ssp., which exploit the presence of strigolactones in the rhizosphere as proximity indicators of host roots (Cook et al., 1966; Sato et al., 2005).

In addition to the discovery of branching factors, two tomato mutants, pmi1 and pmi2, have been described, which fail to stimulate germination and growth of several AMF. It was first hypothesized that it was a lack of stimulatory compounds, which created the pmi1 phenotype (David-Schwartz et al., 2001), but later studies suggest, that the pmi1 phenotype is rather due to an increase or the novel production of inhibitory substances (Gadkar et al., 2003). The same seems to hold true for pmi2 (David-Schwartz et al., 2003). These findings stress the fact that it is the fine tuning between positive and negative signals released into the rhizosphere that decides over the initial compatibility of the plant AMF interaction.

Likewise the existence of one or several fungi derived low molecular weight substances that initiate the activation of downstream symbiosis related genes, thus preparing the plant for colonization, has been affirmed in several studies (Kosuta et al., 2003). They are collectively referred to as MYC factors, and a specific, but yet unknown MYC factor receptor is expected to reside in the rhizodermis to perceive and transduce the signal in a similar fashion as NOD factor receptors do at the onset of root-rhizobia interactions. Whether the reception of the MYC factor by the plant also stimulates strigolactone exudation, thus creating a positive feedback loop to facilitate first contact between both symbiotes, remains unclear, but seems plausible. Despite the elaborate pre-symbiotic crosstalk between plant and fungus, a transient SA dependent defense response is elicited in the plant and appears to remain at a basal level throughout the interaction (Garcia-Garrido and Ocampo, 2002). It might in part account for the increased pathogen resistance commonly observed for mycorrhized plants.

Several genes of the signal transduction network required to trigger the profound physiological and developmental changes accompanying successful mycorrhization have been identified and characterized in legume species. Interestingly most of them had been initially recognized as part of the signaling pathway in the root-nodule symbiosis with rhizobia, leading to the acknowledgement that a common symbiosis (SYM) pathway

exists for both fungal and bacterial partners. Since the root nodule symbiosis evolved more recently than the AM symbiosis and is restricted to legumes, it is argued that the former merely utilized the already existing pathway, which then secondarily evolved distinct rhizobia specific components such as the Nod factor receptors. Common SYM genes include a receptor like kinase (SYMRK), two nuclear ion channels (CASTOR and POLLUX), two putative nuclear pore complex components (NUP85 and NUP133), a calcium-calmodulin dependent protein kinase (CCaMK) and CYCLOPS, a nuclear protein of unknown function with a coiled-coil domain. Specific nuclear and near-nuclear calcium oscillation have been identified as intermediate AM induced signals and the function of common sym genes can be classified as either acting upstream or downstream of the calcium signal (Parniske, 2008).

SYMRK is generally accepted as the entry point to the common symbiotic signaling pathway, perceiving a microbial signal with its extracellular receptor domain and transducing it to its intracellular kinase domain (Stracke et al., 2002). However, neither the microbial ligands nor the downstream phosphorylation targets of SYMRK are known, but lack of function mutants display a severe impairment in the intracellular passage of fungal hyphae through the outer cell layers. Calcium spiking is abolished in the mutants and the PPA fails to be induced. SYMRK however is not directly involved in MYC factor related signaling, as one might be tempted to speculate, because *MtENOD11* is activated downstream of MYC factor perception even in SYMRK mutant background (Kosuta et al., 2003). Second-messenger mediated transduction downstream of SYMRK leads to the activation of the nuclear cation channels CASTOR and POLLUX (Kistner et al., 2005). Similar to the SYMRK phenotype, mutations in either gene also lead to a defect in calcium oscillations and failure to induce the PPA. Additionally castor mutants also seem impaired in arbuscle development (Imaizumi-Anraku et al., 2005). Both channels however display only marginal affinity for calcium and are proposed to act as potassium channels that counteract electrochemical imbalances caused by the rapid calcium fluxes during calcium oscillations (Parniske, 2008). The calcium spikes in turn activate CCaMK, whose function is absolutely essential for AM development (Levy et al., 2004). CCaMK mutants display normal calcium oscillations in response to AMF, but fail to initiate epidermal clefts, and display aberrant PPA and arbuscle formation. All of these

phenotypes are in accordance with its proposed essential role in decoding mycorrhiza induced calcium spikes. Abolishment of CYCLOPS, a putative in vivo target of CCaMK, also leads to impairments in the fungal infection process and defects in arbuscle development (Yano et al., 2008). All of the common SYM genes seem to constitute core components of the initial signaling pathway. They lead to the transcriptional activation of downstream genes orchestrating the structural modifications and chemical signaling necessary for successful fungal accommodation. Nevertheless several publications suggest that alternative pathways and additional components in the common SYM pathway exist (Reddy et al., 2007; Gutjahr et al., 2008).

There is increasing evidence, that downstream of the common SYM pathway, plant secondary metabolites play an important role in regulating the dynamics of the developing symbiosis. They might influence important late stage aspects of AM such as apoplastic hyphal guidance within the cortex, arbuscle development and turnover and the steady state extent of the colonization under feedback control of the plant`s nutritional status. In each of the symbiotic steps a multitude of secondary compounds such as flavonoids (Vierheilig et al., 1998b) terpenoids (Fester et al., 2005) and phenolic compounds (Maier et al., 1995) have been demonstrated to be differentially produced and/or excreted. Furthermore some of the key enzymes of the flavonoid pathway, such as PAL (phenyl ammonium lyase) and CHS (chalcone synthase) (Maria J. Harrison, 1994) and of the plastidal non-mevalonate pathway, such as DXS (1-deoxy-D-xylulose-5-phosphate synthase), DXR (1-deoxy-D-xylulose-5-phosphate reductoisomerase) and PDS (phytoene desaturase) (Fester et al., 2002) show a pronounced positive transcriptional response upon mycorrhization, with spatial expression patterns closely correlating with mycorrhizal structures such as arbuscles.

In some species, predominantly monocotyledons, chromophoric apocarotenoids, esterified derivatives of mycorradicin collectively called yellow pigment, accumulate in such vast quantities in mycorrhized parts of the roots that they can be distinguished macroscopically from non-mycorrhized sections by their distinct yellow color. Concomitantly cyclohexenone derivatives, such as blumenin, presumably derived from the same carotenoid precursors as mycorradicin, accumulate in comparable amounts. Whereas mycorradicin is expected to be sequestered to the vacuole, Blumenin appears to

be excreted into the apoplast. However, despite their apparent abundance in mycorrhized roots, the distinct function of these apocarotenoids is yet unknown. Exogenously applied blumenin seems to have an inhibitory effect on mycorrhization, which together with the finding that *DXR* expression seem highest around mature and senescing arbuscles, might suggest that they play a role in arbuscle turnover (Hans et al., 2004). Direct evidence for this hypothesis comes from two recent publications (Floss et al., 2008b; Floss et al., 2008a), which show that post-transcriptional silencing of mycorrhiza inducible *DXS2* or *CCD1* in Medicago, both involved in apocarotenoid production, does not result in a significant change of overall fungal colonization, but instead increases the relative amount of senescent arbuscles.

Despite the identification of a number of early and late mycorrhiza related secondary metabolites via analytical approaches a distinct allocation of function within AM relevant processes has not been achieved so far. Strigolactones prove an exception, since they seem to exert their effect primarily in the pre-symbiotic phase on isolated fungi in the rhizosphere and not on the complex symbiotic network within the root, enabling a functional investigation by means of in vitro bioassays. Furthermore parts of the biosynthetic pathway of strigolactones have been unraveled and it could thus be demonstrated that a lack of endogenous strigolactone production leads to a decrease in colonization rates and significantly reduced hyphal branching (Gomez-Roldan et al., 2008). Effects of exogenous application of later stage induced secondary metabolites are difficult to interpret, because they will always be applied in addition to endogenous levels, but their functionality might be highly dosage dependent, with too little or too much having adverse effects. Specific biosynthetic genes for these compounds are mostly unknown and downregulation or overexpression of key enzymes such as PAL and CHS for flavonoid pathways, or PDS for carotenoid biosynthesis will invariably result in pleiotropic effects, rendering analysis of strictly mycorrhizal aspects difficult. Assuming that these substances are actively transported from the compartments of production to the sites where they exert their effects (such as the periarbuscular space), a useful approach might be to identify the respective transporters. Not only would they make prime targets for mutational approaches, but tissue or membrane specific localization via reporter

constructs would pinpoint precisely where the secondary metabolites of interest are deployed.

It is furthermore expected that a number of phytohormones have an effect on the development of AM (Hause et al., 2007). Exogenous application of either auxins or cytokinins, both major mediators of plant architecture, on mycorrhized roots has a stimulatory effect on the symbiosis. Endogenous levels of both were also found to be higher when roots were colonized by the fungus. This suggests a direct or indirect role for these phytohormones in the process, but no clear mechanisms could yet be determined.

A more detailed picture seems to be emerging for the role of jasmonates in AM. They seem to affect the symbiosis in a dosage dependent manner, typical for hormone actions. Whereas supplemented JA in low dosages enhances the interaction, application of high concentrations over longer periods leads to a drastic reduction. Allene Oxide Synthase (AOS) involved in JA biosynthesis is significantly upregulated in and around arbuscle containing cortex cells as demonstrated by in situ hybridization with mycorrhized barley roots. Moreover, downregulation of Allene Oxide Cyclase in Medicago, resulted in a marked decrease of JA contents and a concomitant delay and overall decrease in mycorrhizal colonization (Isayenkov et al., 2005). *MtPT4* expression, an indicator of functional arbuscles abundance, was reduced by ten fold when compared to mycorrhized WT plants. All these findings indicate a role for JA in early and late stage events. As possible explanations for these observations it is proposed that JA deficient plants might fail to induce mycorrhiza specific secondary metabolite production, for JA is a well known modulator of secondary metabolite pathways. Alternatively JA might influence the sink status of the plant root and thus orchestrate the allocation of carbohydrates intended for the fungus (Tejeda-Sartorius et al., 2008).

1.3 *Petunia hybrida* a Non-Model Model Plant

In recent years Petunia has become increasingly popular as a novel plant model system to study several aspects of plant development, physiology and ecology (Gerats and Vandenbussche, 2005). Petunia forms a genus of around 30 species and subspecies within the family of Solanaceae. Originating from central-eastern South America, Petunia has

become one of the most popular ornamental plants and can be found on balconies and in gardens all over the world. Among plant breeders it is still one of the favorite genera to create differently shaped and colored varieties. The most commonly found Petunias in horticulture and research alike are of the variety *Petunia hybrida*, stemming from a cross of *Petunia axillaris* and *Petunia integrifolia*. Several different *Petunia hybrida* lines are used for different purposes in research. The white odorant W115 line (Mitchell WT), exhibiting superior qualities in terms of fertility (seed setting), transformability and growth, has been used to study scent production (Verdonk et al., 2003; Verdonk et al., 2005), ethylene dependent pathways (Shibuya et al., 2004) and adventitious root formation (Ahkami et al., 2008). The inbred line V26, featuring blue to purple flowers has been used to study flavonoid biosynthesis, flower coloration (Chen et al., 2004) and above ground plant architechture (Simons et al., 2007). The red flowered transposon harboring line W138 has been mainly utilized for forward and reverse genetic approaches in flowers (Vandenbussche et al., 2003) and meristem development (Angenent et al., 2005). Other Petunia species are mainly featured in taxonomic studies and the investigation of pollination syndromes (Galliot et al., 2006). Petunia is particularly interesting in this context because it contains a white odorant species, *P. axillaris*, which is hawk moth pollinated, red scentless species, *P. integrifolia*, which is bee pollinated and potentially hummingbird pollinated species, most of which can be crossed with each other to create hybrid species.

Being a member of the Solanaceae family, Petunia is closely related to important crop species such as potato, tomato, tobacco and capsicum. Certain characteristics qualify it as a future model system to study the physiology and genetics of solanaceous species. Among them are a relatively short generation time of 3-4 months from seed to seed and easy asexual propagation from cuttings or callus. Many varieties are easily transformable and have proved susceptible to *A. tumefaciens*, *A. rhizogenes* and VIGS (Spitzer et al., 2007). Despite having large leaves and flowers to facilitate biochemical studies and studies of floral development, the overall plant size can be kept relatively small when intended for breeding or screening purposes. Large collections of organ and treatment specific cDNA libraries, several BAC libraries and a growing number of annotated ESTs

databases have been created and the transfer of molecular tools as well as knowledge is aided by a dynamic and cooperative research platform (www.petuniaplatform.net).

Most intriguing, however, is the existence of an endogenous highly active transposon system in the W138 line (Gerats et al., 1990). Each W138 individual harbors up to 200 copies of the non-autonomous, highly mobile 284bp transposon dTph1. Transposon insertion in a gene of interest commonly results in a complete lack of function mutation, creating true non-transgenic knock outs. Since dTph1 lacks transposase activity and appears to be under the control of a single "master transposase" at the *ACT2* locus (Stuurman and Kuhlemeier, 2005), it is possible to stabilize a mutant line by crossing out the transposase and thus fixing the transposons in their position. Elaborate screening techniques have been developed for both forward (Van den Broeck et al., 1998) and reverse genetic approaches (Koes et al., 1995; Vandenbussche and Gerats, 2004). In the former a so-called "Transposon Display", adapted from the AFLP technique, allows for the identification of a transposon-tagged gene that co-segregates with the desired phenotype. In the latter, so-called "3D-gDNA Library Screens" allow for the simultaneous PCR-based screen of several thousand W138 individuals for transposon insertions in a desired gene. This method has now been greatly refined by engineering of a method that enables the creation of a database containing transposon flanking regions of large W138 populations (Vandenbussche et al., 2008). Since each transposon flanking region can be allocated to the individual plant it derived from, it has thus become possible to BLAST search for a transposon insertion mutant of interest and retrieve it from a seed stock. The only requirement is to know either the sequence of interest or homologous sequences from other gene family members within petunia or other species. The BLAST approach has the further advantage of concomitantly revealing putatively unknown gene homologues and their respective transposon insertion mutants.

Among the most fruitful topics of petunia related research have been the implications of the MADS-box family of transcription factors in flower development and organ differentiation. The function of other families of transcription factors in meristem function and plant architecture has also been successfully investigated. Large flowers, easily accessible shoot meristems and a highly structured plant body of relatively small size make petunia an ideal candidate for forward genetic screening approaches in this

respect. The biochemical analysis of scent production in flowers and the role of ethylene in flower senescence are two examples of Petunia related research that find direct application in the ornamental flower industry. Because of its conspicuous flowers of different coloration, petunia has become an indispensable tool in the unraveling of flavonoids and anthocyanin biosynthetic pathways with respect to flower pigmentation and the development of reproductive organs. Several biosynthetic and regulatory genes were initially discovered and characterized in petunia.

Not until very recently has petunia research been shifting its focus from strictly aboveground studies to belowground topics. Two areas of interest are emerging from underground. One focuses on the establishment and function of AM (Reddy et al., 2007) and another investigates the molecular mechanisms behind adventitious root formation (Ahkami et al., 2008). Understanding adventitious root formation is of particular importance in horticultural practice, for fast and easy propagation of specimens via cuttings. A holistic approach, focusing on anatomy, gene expression, enzymatic activities and levels of metabolites, is now under way in order to unravel key steps in adventitious root formation in petunia, with the long term goal of applying this knowledge to species that are yet unable to be regenerated from cuttings.

Understanding molecular mechanisms in the establishment and function of AM has been approached using several plant species as model organisms. Foremost of all are legume species such as *Medicago truncatula* and *Lotus japonicus*, since it was discovered that a common SYM pathway exists between the initial signaling events in root-nodule formation and AM establishment (Kistner et al., 2005). Hence many mutants found to be impeded in root-rhizobia interactions were also useful for studying mycorrhiza-specific events. Two attempts have been made to utilize the unique qualities of the transposon harboring petunia line W138 in order to identify mutants impaired in mycorrhization. In a histochemical approach a large population of divergent W138 individuals was screened for aberrant mycorrhiza formation (Reddy et al., 2007). Several mutants were identified and one of them, penetration and arbuscle morphogenesis1 (pam1), was characterized in detail. Pam1 mutants frequently fail to accommodate the fungus already at the epidermal level and the few hyphae that are able to reach the cortex do not manage to form arbuscles, a phenotype reminiscent of common SYM pathway mutants. Even though the

authors could not to identify the transposon tagged gene responsible for the phenotype, they could nevertheless show, that the mutation is independent of the common SYM pathway, hinting at a novel gene member in the complex of mycorrhiza related signaling.

In an attempt to identify signaling components upstream of mycorrhiza specific phosphate acquisition via mycorrhiza-induced phosphate transporters, a bidirectional StPT3 promoter construct, controlling two reporter genes (Luciferase and GUS), was generated, transferred into the W115 background and crossed into a transposon mutagenized W138 population (Wegmuller et al., 2008). Since the promoter is exclusively activated in the presence of mycorrhiza, lack of activity in the presence of mycorrhiza would indicate a lack of function transposon insertion in a gene with implications in the signaling cascade between perception of the fungus and expression of the phosphate transporter. Six putative mutants with deregulated StPT3 promoter activity could be identified and await molecular and biochemical characterization. In one of the mutants, ptd1, it was demonstrated that the endogenous phosphate transporters *PhPT3*, *PhPT4* and *PhPT5* were substantially downregulated under mycorrhizal conditions, verifying the functionality of the system. However no apparent phenotype was reported and the identity of the transposon tagged gene in question remains to be determined

In order to identify candidate genes in the nutritional control of mycorrhization a large scale microarray-based transcriptional approach has been initiated (Reinhardt unpublished) and its findings will certainly trigger further investigation in the field and support mycorrhiza related research in petunia on a broad base.

2 PhPDR1,
Influencing Mycorrhizal Interactions and Plant Architecture

Strigolactones are carotenoid derived sesquiterpene lactones, which were originally identified as germination stimulants for parasitic weeds of the broomrape family. Being present in the root exudates of host and non-host plant species, they signal the vicinity of a plant root and thus induce germination of the parasite only under favorable conditions. Later on it was acknowledged that strigolactones are primarily exuded into the rhizosphere by mycotrophic plants to serve as pre-symbiotic signals in the establishment of arbuscular mycorrhizal interactions. Strigolactones efficiently activate fungal metabolism and induce vigorous hyphal branching, which facilitates initial contact between both symbiotes. Very recently it was discovered that strigolactones are congruent with the long sought after branching hormone that was known to be produced in root and stem tissues and, being acropetally mobile in the shoot vasculature, inhibits the outgrowth of axillary buds.

Here we report on PhPDR1, a Pleiotropic Drug Resistance (PDR) type ABC transporter from Petunia, which exhibits qualities evocative of a strigolactone transporter. Plant PDR-type transporters are plasma membrane intrinsic primary active pumps, known to be implicated in abiotic and biotic stress responses. Several homologues are proposed to contribute to basal nonhost pathogen resistance via the excretion of antimicrobial compounds of terpenoid origin. *PhPDR1* is expressed in various root tissues and the primary shoot vasculature with a pronounced concentration of promoter activity in the nodal areas below the leaf axils. Root colonization by arbuscular mycorrhizal (AM) fungi markedly induces *PhPDR1* expression particularly in and around mycorrhized cortical tissues. Transposon insertion mutants deficient in PhPDR1 function (Phpdr1::dTph1) display significantly reduced AM colonization patterns that are at least in part due to a dysfunctional exudation of pre-symbiotic signals into the rhizosphere. Furthermore Phpdr1::dTph1 individuals are impaired in their ability to inhibit lateral branch development, in a fashion that is partially congruent with strigolactone-biosynthesis-mutant phenotypes. When compared to the wild type, exogenously applied synthetic strigolactone derivates accumulate to a higher degree in the nodal tissues of

Phpdr1::dTph1, suggestive of aberrant strigolactone export capacities in the mutant background.

2.1 Introduction

Pleiotropic Drug Resistance transporters (PDRs) constitute a subfamily of full size ATP-Binding-Cassette transporters (ABC transporters) that is restricted to the fungal and plant kingdoms. While they are limited to a few known homologues within species of the former, they have highly diversified and expanded in number among species of the latter. PDRs are postulated to have arisen from a single ancestral duplication event of half size White Brown Complex transporters (WBCs) that are present in all eukaryotes and are implicated in the transport of pigments, highly lipophilic substances and xenobiotics. In plants PDRs have been demonstrated to act as PM intrinsic secondary metabolite transporters conferring resistance to a variety of non-host pathogens via the extrusion of antimicrobial compounds. They are commonly incorporated in JA or SA dependent defense pathways and a large proportion of PDR homologues are primarily expressed in root tissues and epidermal cell layers. In addition to contributing to biotic stress reactions, they seem to be implicated in abiotic stress responses. Best studied in this respect is their assistance in heavy metal tolerance presumably achieved via actively pumping heavy metal cations from the cytosol into the rhizosphere or apolastic regions, thus preventing cytotoxic over-accumulation. Further roles proposed for plant derived PDRs stretch as far as nutrient acquisition, organic acid excretion, redox state regulation and yet unknown reproductive functions (see General Introduction 1.1 for details).

Plant secondary metabolites are currently emerging as powerful mediators in the communication between plants and AM fungi. Many different compounds mostly derived from terpenoid or phenylpropanoid pathways have been demonstrated to be differentially produced and/or secreted at different stages of the developing symbiosis. But with a few exceptions, the distinct function of most of these substances has not yet been revealed. Specific biosynthetic enzymes for the majority of them are currently unknown, making it difficult to manipulate the levels of production on a genetic level, and exogenous applications on top of naturally occurring concentrations often have adverse or unexpected effects since signaling compounds often work in a dose dependent manner. Assuming that the majority of mycorrhiza specific secondary metabolites are actively transported across the PM to the specific sites, where their activity is needed (e.g. the

rhizosphere, hyphae-containing cortical apoplast or periarbuscular space), a novel approach to unravel their function would be to focus on the respective transporters. Not only would they make prime targets for mutational approaches, but in addition tissue or membrane specific localization via reporter constructs would pinpoint precisely where the secondary metabolites of interest are deployed. A substrate class of particular interest in this respect are apocarotenoid derivatives, such as strigolactones, mycorradicin related compounds and cyclohexenoids. Whereas the former plays a dominant role in pre-symbiotic signaling in the rhizosphere, the latter two have been implicated in the late-symbiotic steps of arbuscle development in the root cortex (see General Introduction 1.2 for details). Considering that certain PDRs mediate stress responses belowground via the extrusion of secondary metabolites into the rhizosphere and that PDRs are so far the only known plant terpenoid transporters, we decided to investigate putative implications of PDR transporters and their respective substrates in the establishment and function of arbuscular mycorrhiza.

Strigolactones comprise a group of structurally related sesquiterpene lactones, known to be produced by a variety of monocotyledonous and dicotyledonous species (Humphrey and Beale, 2006). Examples of naturally occurring derivatives are Strigol, 5-Desoxystrigol, Orobanchol, Alectrol and Sorgolactone. Additionally synthetic analogues such as GR7 and GR24 have been generated (Rugutt et al., 2000). The natural compounds are carotenoid cleavage products consisting of a tri-cyclic sesquiterpenoid, coupled to a C5 lactone via an ether bond (Matusova et al., 2005). They were first identified and described as being germination stimulants for parasitic weeds Striga and Orobanche of the Orobanchaceae (Cook et al., 1966). These hemi- to holoparasitic angiosperms are entirely dependent on their host plants for nutrient and water acquisition and their minute seeds only contain reserves to allow the radicle to protrude for several millimeters. If not reaching a host within this perimeter, they will invariably die from lack of nutrition. Once in contact with a host root the radicle will penetrate the cortex and form a haustorium-like structure to enable exploitation of the host resources. Strigolactones are present in the root exudates of host and non-host plants, and, due to the labile ether bond connecting the sesquiterpenoid to the lactone moiety, subject to spontaneous degradation in the aqueous environment of the soil. Thus they form a steep

concentration gradient within the rhizosphere and signal the dormant parasite seed the immediate vicinity of a plant root, promoting germination only under suitable conditions. However, if exudation of strigolactones results in the attraction of potentially lethal parasites, why does this trait not succumb to negative selective pressure?

Recently it was discovered that strigolactones also act as branching factors for mycorrhizal fungi of the phylum Glomeromycota (Akiyama et al., 2005). It was long known that one or several low molecular diffusible factors of mycotrophic plants stimulate hyphal branching. A dormant Glomeromycota spore is usually capable of germinating spontaneously and extending a germ tube or primary hypha for several millimeters or centimeters into the soil. However if not reaching the vicinity of a host it will arrest its development or even retract its germ tube to reestablish a dormant state. Successive cycles of germination, hyphal extension and retraction have been recorded, allowing the fungus to repeatedly probe its environment without depleting its resources. Perception of a compatible partner is crucial for the fungus since it is an obligate biotroph, depending on root colonization for completion of its life cycle. However, due to the extremely low concentrations being produced and exuded, the nature of this branching factor remained elusive for a long time. Several mycorrhiza-stimulating compounds were identified in the root exudates of different plant species, but it took a large scale approach involving the enrichment of branching factors on an active charcoal filter to unambiguously identify strigolactones as the branching inducing agents.

Picogram to nanogram levels of strigolactones efficiently activate the fungal energy metabolism, induce mitochondrial fissure and increase respiration rates (Besserer et al., 2008). Additionally, strigolactones profoundly influence fungal physiology and development, inducing secondary and tertiary branching as well as hyphal proliferation. It is argued that by actively branching the fungus increases its chances to come into contact with the plant root and initiate colonization. Interestingly phosphate deficient conditions for the plant markedly stimulate strigolactone release (Lopez-Raez et al., 2008). Phosphate has been demonstrated to be the main nutrient provided by the fungus in exchange for photoassimilates. The plant supports a functional symbiosis only in times of scarce nutrients and a differential exudation of strigolactones in regard to its phosphate status might be the first way to achieve this. On the other hand however, this signal

indicates that the plant is weak and thus probably impeded in its capability to withstand parasites, which is perceived by the weeds that efficiently evolved to intercept and decode this call for help. This also explains why the effects of Striga and Orobanche are most devastating in nutrient depleted soils, such as in sub-Saharan Africa. It is now generally accepted that the exudation of strigolactones into the rhizosphere primarily intends to signal the fungal symbiote and aid in the establishment of the symbiosis. The parasitic weeds merely exploit this signaling pathway and for their own benefit. It seems that the overall benefit of attracting a fungal symbiote outweighs the danger of concomitantly attracting a parasite, thus only few varieties impeded in strigolactone related underground signaling have evolved. Additionally novel above ground functions for strigolactones are currently unfolding, expanding the necessity of these compounds beyond the scope of symbiotic signaling.

Very recently it was recognized that strigolactones and/or strigolactone derived compounds play a dominant hormone-like role in shaping above ground plant architecture by inhibiting lateral bud outgrowth into axillary branches (Gomez-Roldan et al., 2008; Umehara et al., 2008). In the past, detailed analysis of several mutants exhibiting increased axillary branching patterns, which are partially independent of auxin related signaling, led to the conclusion that a yet unidentified root derived acropetally mobile and graft transmissible signal of carotenoid origin must exist that inhibits the outgrowth of axillary buds. In Arabidopsis the More Axillary Branching Mutants max3 and max4 proved deficient in Carotenoid Cleavage Dioxygenase AtCCD7 and AtCCD8 activity respectively (Sorefan et al., 2003; Booker et al., 2004). CCD homologues catalyze the conversion of carotenoid precursors into apocarotenoids, leading to the assumption that the novel hormone is an isoprenoid compound. *MAX4* is mainly expressed in the root tip and in cortical tissues of the root, but also in the nodal regions of the shoot and in the hypocotyls. In all cases aboveground expression is less pronounced than belowground expression and no transcript is detectable in the lateral buds. Congruently MAX3 is also predominantly present in root tissues and in the stems of primary and secondary inflorescences. Furthermore, in accordance with its function in carotenoid metabolism, MAX3 was demonstrated to be of plastidal origin (Booker et al., 2004).

Another mutant displaying an identical phenotype, max1, lacks function of a cytochrome P450 family member that supposedly acts downstream of MAX3 and MAX4 in the synthesis of the signaling compound (Booker et al., 2005). *MAX1* is predominantly expressed in the vasculature and vasculature-associated tissues throughout the plant, with an apparent peak of expression in the leaf axis, suggesting that it acts on a mobile substrate. All three mutant shoots can be rescued when grafted on a wild type root stock, suggesting that root derived amounts of this compound are sufficient to fulfill its developmental and physiological roles. Contrastingly max2 mutant scions do not revert to wild type conditions when grafted on a wild type root stock (Stirnberg et al., 2007). *MAX2* encodes an F-Box protein that, as a component of the SCF complex, is implicated in regulated proteolysis via ubiquitination. It is mainly expressed in developing vasculature and in shoot meristems and is thus thought to be involved in the signal transduction downstream of perception at target cells. Consequently all four proteins were proposed to act in the same pathway, but the actual identity of the hormone remained elusive.

Orthologues of AtCCD7 and AtCCD8 have been identified in rice (Arite et al., 2007), pea (Johnson et al., 2006) and Petunia (Snowden et al., 2005). In two landmark publications two scientific groups could demonstrate independently that plants lacking CCD8 function exhibit severely reduced levels of strigolactones (Gomez-Roldan et al., 2008; Umehara et al., 2008). Mutant peas are less colonized by mycorrhizal fungi and their root exudates fail to induce hyphal branching and Striga seed germination. Likewise mutant rice is less susceptible to Striga infection. Micromolar amounts of the synthetic strigolactone analogue GR24 are able to rescue the CCD8 branching phenotype, when added to the soil or directly applied to the axillary buds. Congruently max2 mutants did not revert in the presence of exogenously applied GR24.

In the *Petunia hybrida* line V26, transposon insertion in CCD8/Decreased Apical Dominance (DAD1), results in a bushy phenotype due to vigorous axillary branching (Napoli, 1996). DAD1 mutants commonly produce a lateral branch from each leaf axis, including both cotyledonary nodes, whereas the wild type is restricted in axillary branch production to a zone roughly covering the 3rd to the 8th node on the main shoot axis. As in Arabidopsis the branching phenotype is revertible, when dad1 scions are grafted on V26

root stocks. Furthermore interstock grafting of V26 stem sections in dad1 shoots revealed that the branch inhibiting signal moves strictly acropetally in the stem vasculature (Simons et al., 2007). The V26 interstock is able to inhibit branching out from nodes above the graft, whereas nodes below the graft cannot be converted to the wild type phenotype. Other visible phenotypes of dad1 include aberrant axillary meristem development, delayed leaf senescence, stunted growth, delayed flowering time, decreased flower weight and abnormal adventitious root development (Snowden et al., 2005). All of these findings suggest a hormone like role for strigolactones in several aspects of plant development. Whether dad1 also displays a mycorrhiza specific phenotype remains to be determined.

2.2 Results

2.2.1 Cloning and structural characterization of *PhPDR1*

In order to identify putative implications of PDR type ABC transporters in the establishment and function of AM, a degenerate primer approach targeting conserved PDR domains was applied to the cDNA of mycorrhized W115 Petunia hybrida roots (Fig 2.1). The screen resulted in several partial sequences of PDR origin, that were further investigated in respect to mycorrhization (data not shown). In the case of a positive transcriptional response of the respective candidate gene upon fungal colonization, 3`and 5`RACE PCRs were performed to obtain full length coding sequences.

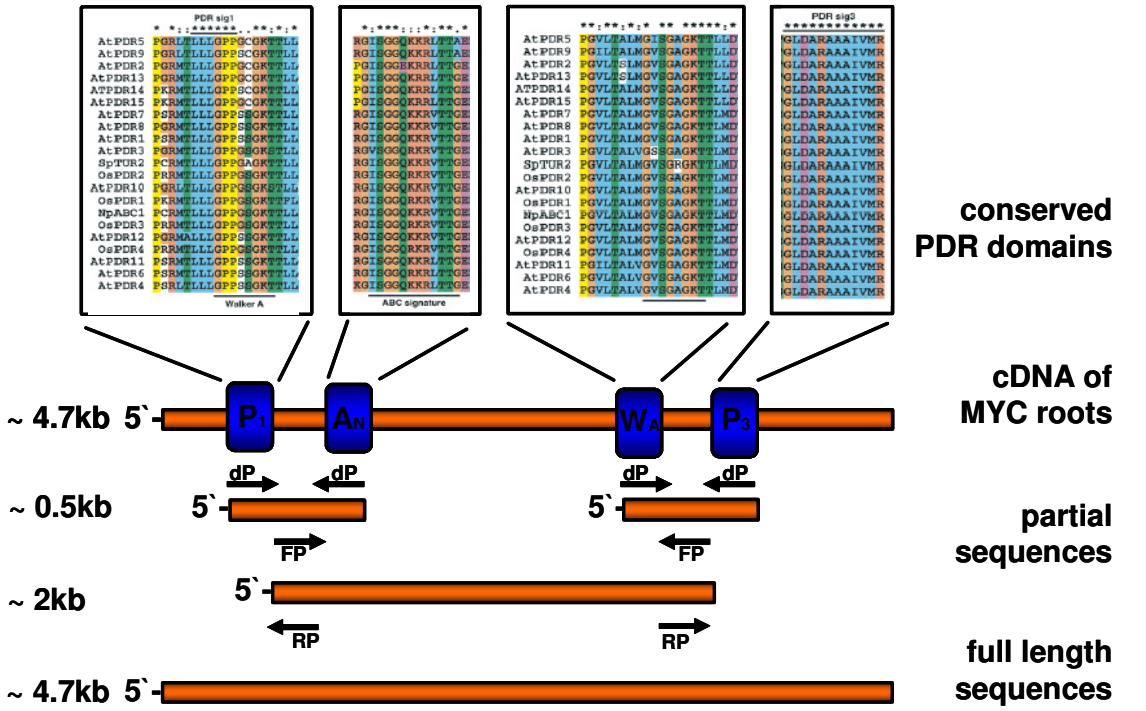

Figure 2.1: Cloning strategy to obtain full length PDR sequences from the cDNA of mycorrhized roots. Degenerate primers (dP) were designed to anneal to highly conserved PDR and/or ABC specific regions, amplifying ~0.5kb fragments from NBD1 and NBD2. On NBD1 PDR signature1 (P1) and the ABC signature (A_N) were targeted and on NBD2 Walker A (W_A) box and PDR signature3 (P3) were targeted. Upper panels display the alignment of the respective regions from several PDR homologues as adapted from van den Brule et al. (2002). The resulting fragments were aligned and non degenerate family specific primers (FP) were designed on the consensus sequence. These yielded amplicons of ~2kb on which RACE primers (RP) were designed to amplify 5`and 3`ends.

The most prominent candidate was dubbed PhPDR1. The 4618bp transcript (Appendix 6.1) encodes an ABC transporter related protein of 1452 amino acid residues (Appendix 6.2) that features a reverse domain configuration (NBD1-TMD1-NBD2-TMD2) specific for the PDR subfamily and contains a predicted number of 13 transmembrane spanning alpha helices (Fig 2.2). Phylogenetic analysis identifies PhPDR1 as a Cluster1 type PDR homologue, closely related to NpPDR1, a PM localized terpenoid transporter implicated in pathogen defense (Stukkens et al., 2005). Its closest homologue in Arabidopsis is AtPDR12, which has been demonstrated to play a role in putatively terpenoid-based pathogen resistance (Campbell et al., 2003) as well as heavy metal tolerance (Lee et al., 2005).

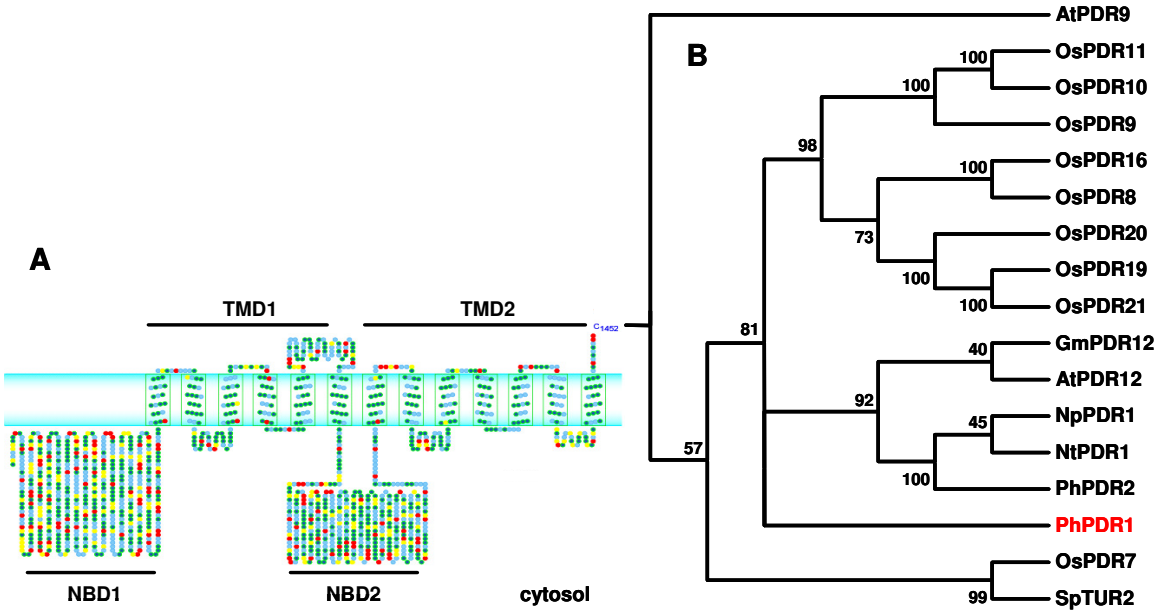

Figure 2.2: Predicted protein topology and phylogenetic analysis of PhPDR1.
(A) Putative transmembrane topology of PhPDR1, featuring a PDR specific reverse orientation with an initial cytosolic nucleotide binding domain (NBD1) followed by 6 membrane spanning alpha helices, which constitute the first transmembrane domain (TMD1). TMD1 is followed by NBD2 and TMD2, the latter consisting of 7 membrane spanning alpha helices. TMDs contain mainly hydrophobic (green circles) and hydrophilic (blue circles) residues, whereas the NBDs additionally contain many positively charged (red circles) and negatively charged (yellow circles) residues.
(B) Position of PhPDR1 within PDR Cluster1 homologues of rice (OsPDRs), Arabidopsis (AtPDRs), tobacco (NtPDR), soy (GmPDR), Petunia (PhPDR), *Nicotiana plumbaginifolia* (NpPDR) and *Spirodela polyrrhiza* (SpTUR). Numbers next to bifurcations represent bootstrap values. Bootstrap supports below 40 were not integrated. Cluster2 homologue AtPDR9 serves as an outgroup.

2.2.2 Expression profile of *PhPDR1*

Based on RT-PCR data, *PhPDR1* seemed to be predominantly expressed in root tissues. Except for a slight presence in stems, expression was absent in above ground tissues such as leaves or flowers (Fig 2.3A). A marked increase in root-specific transcript abundance was observed several weeks after the inoculation with the mycorrhizal fungus *Glomus intraradices* (Fig 2.3A). The finding that more than 28 PCR cycles were necessary to sufficiently detect *PhPDR1* transcript in any untreated tissue, suggested that basal expression levels were either relatively low or confined to very few cell types. Treatment of W115 with various effectors, known to influence PDR transcription, revealed that *PhPDR1* expression was markedly promoted by SA and the synthetic auxin derivate NAA (Fig 2.3B).

Figure 2.3: Semiquantitative *PhPDR1* transcript analysis via RT-PCR.
(A) Relative *PhPDR1* transcript abundance in mycorrhized roots 2-4 weeks post inoculation (2wpi-4wpi), non-mycorrhized roots (Root), whole flowers (Flow), fully expanded leaf tissue (Leaf) and primary stem tissue (Stem) of fully developed W115 individuals. Petunia tubulin (PhTUB) transcript served as a housekeeping control. Cycle number is displayed on the right hand side.
(B) Relative treatment dependent transcript abundance in whole roots and whole shoots of 2 week old W115 seedlings grown on plate after 24h treatment with final concentrations of water (H_2O), 100uM salicylic acid (SA), 5ul/plate methyl-jasmonate (JA), 10 g/l yeast extract (YEX), 10uM abscisic acid (ABA), 25uM alpha-naphthaeneacetic acid (NAA), 250mM Manitol (Man) and 125mM sodium chloride (NaCl). Petunia glycerin-aldehyde-3-phosphate dehydrogenase (PhGAPDH) transcript served as a housekeeping control. Cycle number is displayed on the right hand side.

Auxin, probably among the most versatile of all known phytohormones, regulates a multitude of developmental processes and has a dominant impact on both above ground and below ground plant architecture (Teale et al., 2006). SA is required for the mediation of systemic acquired resistance (SAR) and hypersensitive response (HR), that both play a pivotal role in pathogen defense (Bari and Jones, 2008). Thus it was rather surprising that yeast extract, serving as a general fungal elicitor, had no effect on *PhPDR1* transcript levels. Also JA, commonly found to affect PDR abundance and regarded as a powerful modulator of secondary metabolite productions (Wasternack, 2007) seemed to have no influence on *PhPDR1* expression. Inducers of abiotic stress responses, such as high salt (NaCL) concentrations, enhancers of osmotic pressure (Manitol (Man)) and ABA also had no effect on the transcription of *PhPDR1* (Fig 2.3B). The same held true for other known modulators of PDR expression, such as several types of heavy metal cations (data not shown).

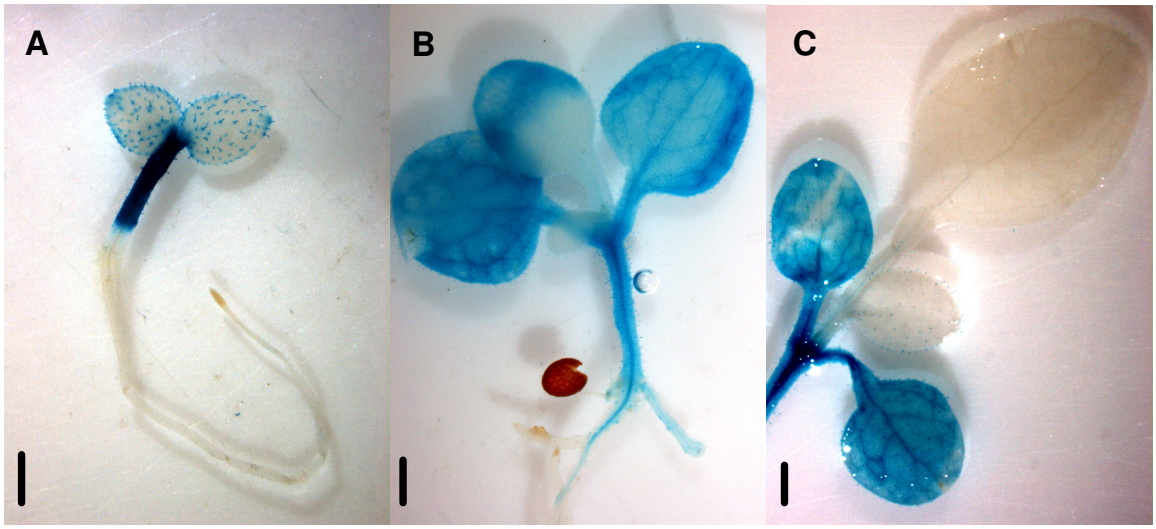

Figure 2.4: Tissue specific *PhPDR1* expression analysis in developing seedlings via *PhPDR1* promoter-GUS fusion constructs in the W115 background.
(A) At the cotyledon stage expression is restricted to the hypocotyl and cotyledonary trichomes.
(B) At the stage of the first true leaf expansion promoter activity is detectable in the hypocotyl (particularly the the vasculature), the primary root vasculature, the whole cotyledons (particularly the vasculature) and the tip of the first leaf. The just emerging second leaf is devoid of signal.
(C) At the stage when the first true leaf is fully expanded signal is restricted to the hypocotyl and cotyledons, predominantly in vascular tissues.
Scale bars = 1mm

In order to get a more detailed and tissue specific understanding of *PhPDR1* expression patterns, a *PhPDR1* reporter construct was created by fusing a 1.8kb genomic fragment containing cis-regulatory elements upstream of the *PhPDR1* gene (Appendix 6.3) to the GUS reporter gene and stably transforming it via *Agrobacterium tumefaciens* mediated mechanisms into the W115 background.

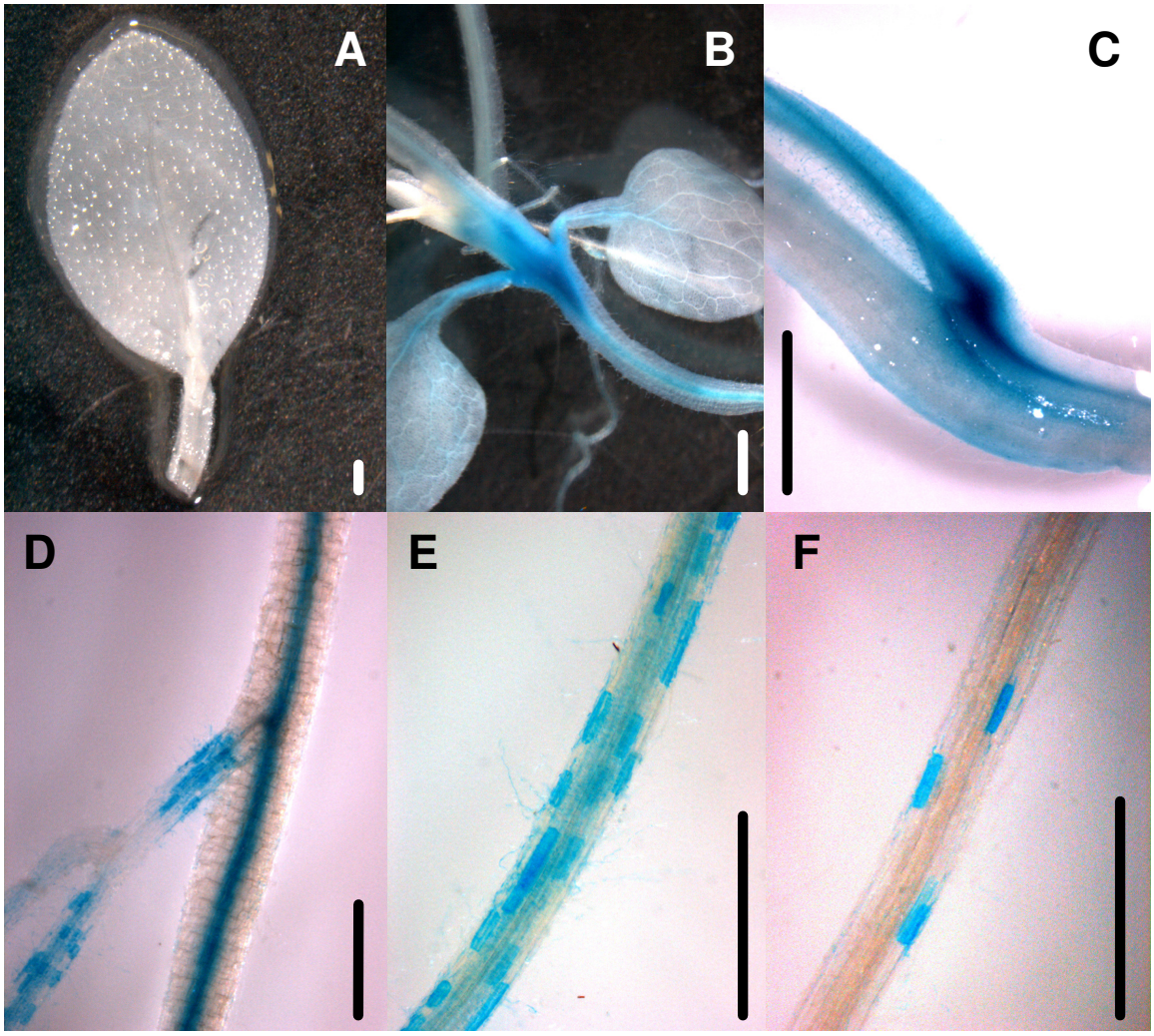

Figure 2.5: Tissue specific *PhPDR1* expression analysis in developing plants via *PhPDR1* promoter-GUS fusion constructs in the W115 background.
All true leaves are devoid of any detectable GUS signal **(A)**. In the shoot *PhPDR1* promoter activity is confined to the main stem vasculature with dominant peaks below the cotyledonary nodes **(B)** and below the leaf axils **(C).** Belowground expression is detectable in the vasculature of the primary root **(D)** as well as in single cortical and epidermal cells (including trichoblasts) throughout the root system **(D-F)**. Scale bars = 1mm

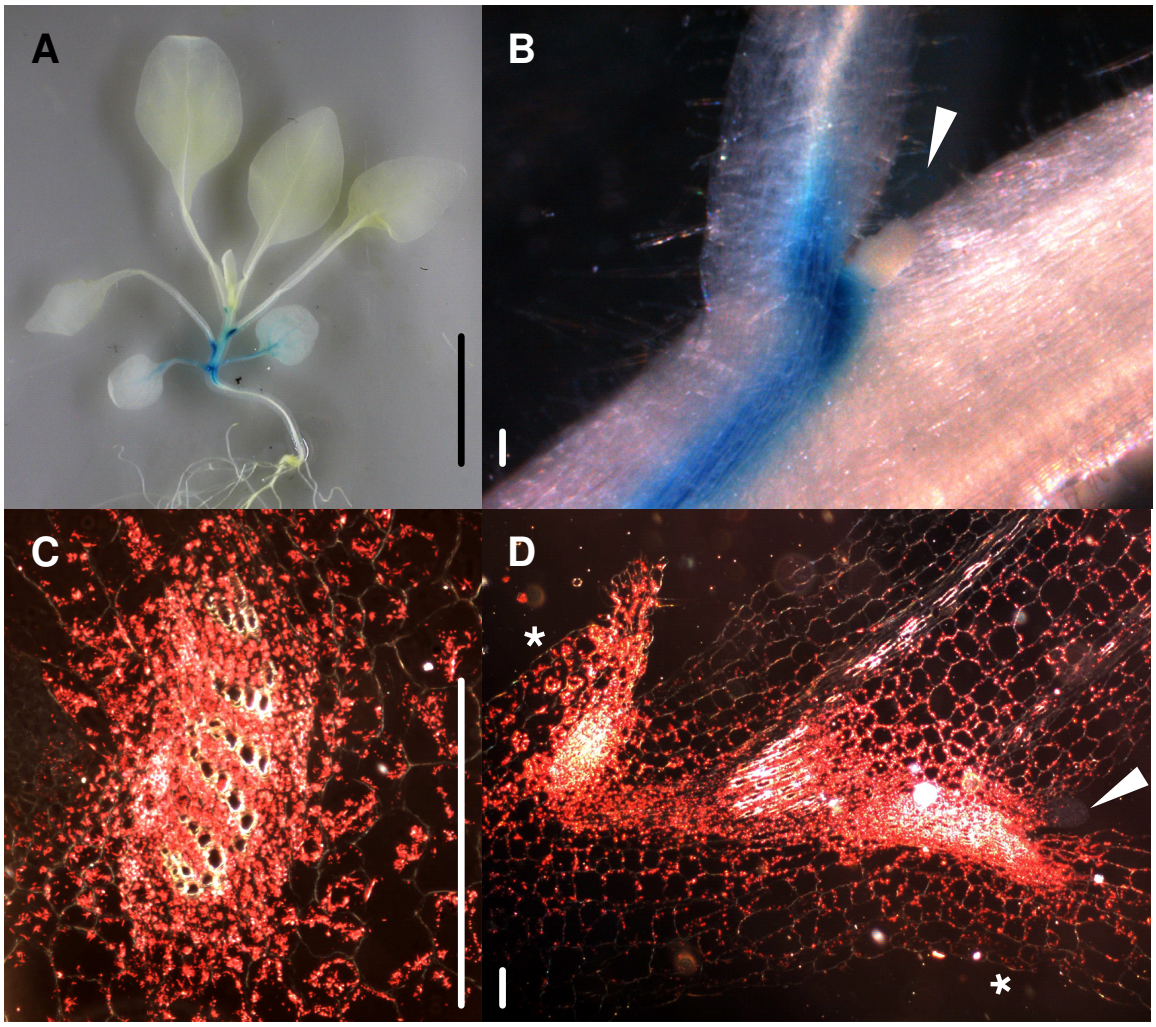

Figure 2.6: Tissue specific *PhPDR1* expression analysis in developing plants via *PhPDR1* promoter-GUS fusion constructs in the W115 background.
(A) At the four leaf stage expression is most pronounced in the vasculature of the nodal regions. Scale bar = 1cm
(B) A close-up of the first true leaf axil reveals that whereas *PhPDR1* promoter activity is strongest directly below the leaf axil and the associates vasculature, it is completely absent from the dormant axillary bud, which is indicated by a white arrow. Scale bars = 0.1mm
(C) Transversal section of a petiole base in the first leaf axil. Image shows a vascular strand as visualized under polarized light. GUS signal appears red to brown whereas tracheary elements are white. Scale bar = 0.1mm
(D) Longitudinal section of a cotyledonary node as visualized under polarized light. GUS signal appears red whereas tracheary elements are white. White asterisks indicate cotyledonary petioles. White arrow indicates cotyledonary meristem. Scale bar = 0.1mm

In terms of seedling development, *PhPDR1* expression was restricted to the elongated hypocotyls of newly germinated seedlings (Fig 2.4A), with the exception of cotyledonary trichomes that also displayed a signal. *PhPDR1* promoter driven GUS expression

remained absent from the radicle and developing primary root for several days, but started to extend into the cotyledons, and the emerging first true leaf, where abundance appeared to be highest in the developing vasculature (Fig 2.4B). At this stage transcript also started to appear in the vasculature of the primary roots directly below the hypocotyls (Fig 2.4B and Fig 2.5D). In emerging lateral roots and towards the tip of the primary root GUS, signal was restricted to distinct single cells, which appeared to be of epidermal and cortical natures (Fig 2.5E-F). As soon as the first true leaf expanded beyond the size of the cotyledons, the GUS signal started to disappear and all following leaves were devoid of any detectable signal (Fig 2.4C and Fig 2.5A). In the developing root system the signal remained in the vasculature close to the root shoot junction (Fig 2.5D) and patches of single cortical or epidermal cells with a strong signal were present throughout the primary and lateral roots (Fig 2.5E-F). These cells appeared to be fewer in number towards the root tips, but occasionally a signal could be detected in the root elongation zone or the root tips. In the growing shoot expression became increasingly restricted to the vasculature. Interestingly a marked peak of expression could be observed in the vasculature of the leaf axil right below the dormant buds of axillary branches (Fig 2.6A-B). However the GUS signal seemed to be completely absent from the meristems themselves (Fig 2.6B). Longitudinal and transversal sections of the nodal regions showed that *PhPDR1* is specifically expressed in the parenchymatic tissues surrounding tracheary elements, which appears particularly pronounced adjacent to the base of axillary meristems.

Since we were primarily interested in the putative implications of PhPDR1 in symbiosis-specific processes, we investigated GUS expression under the control of the *PhPDR1* promoter in mycorrhized roots. Consistent with previous RT-PCR data, we were able to detect a significant increase in GUS staining several weeks after the initial inoculation with the fungus, when compared to non-inoculated plants of the same age (Fig 2.7A). Large patches of adjacent cortical and non-cortical cells displayed staining of different intensity when colonized by the fungus. Most prominently a GUS signal could now be commonly detected in the root elongation zone and the root tip, which were often devoid of any detectable signal in the absence of mycorrhiza (Fig 2.7B). However, above ground expression patterns of *PhPDR1* remained unaffected by myorrhization (data not shown).

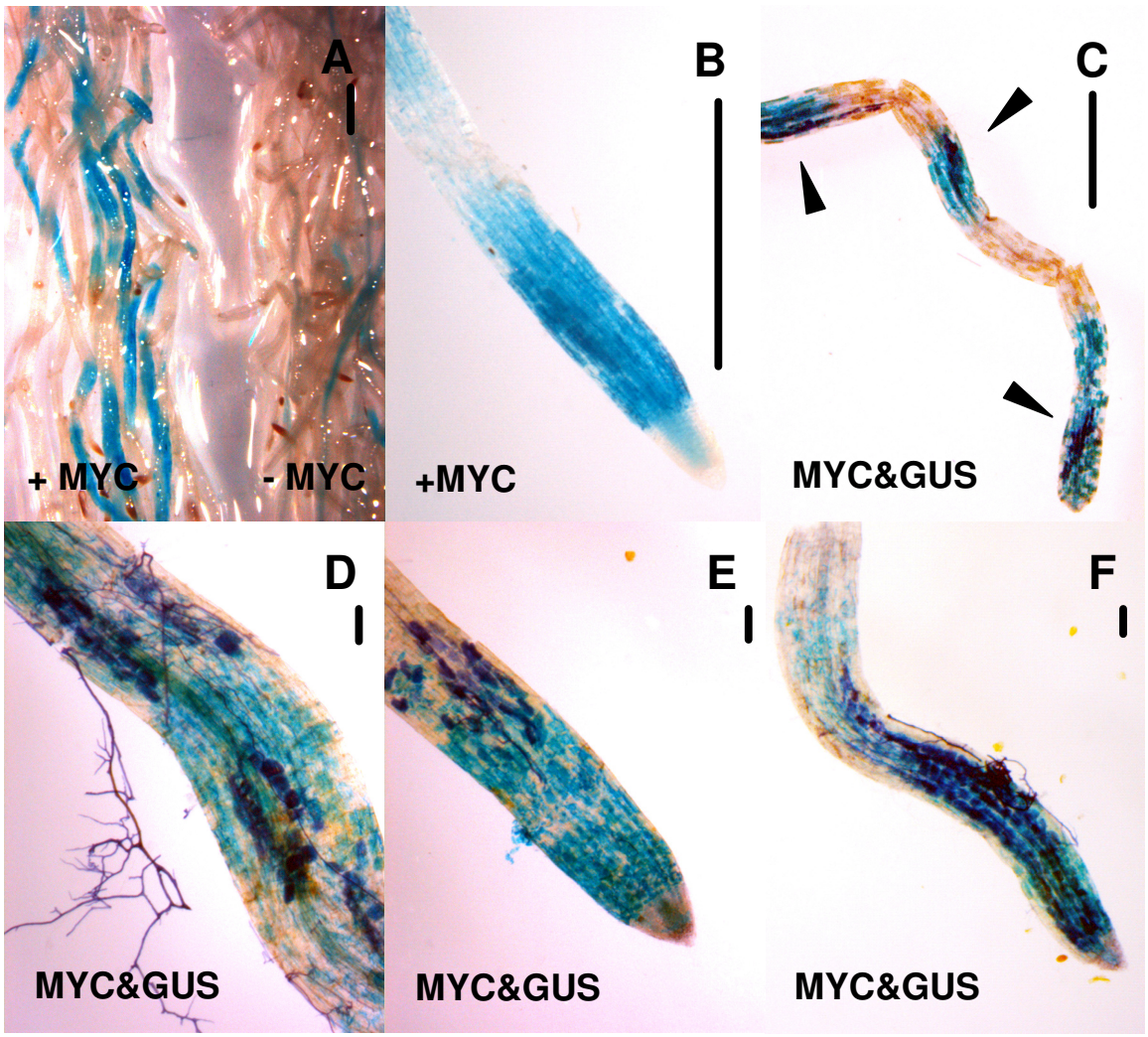

Figure 2.7: Tissue specific *PhPDR1* expression analysis in roots via *PhPDR1* promoter-GUS fusion constructs in the W115 background.
(A) Differential *PhPDR1* promoter activity in mycorrhized roots 8wpi (+MYC) and non mycorrhized roots (-MYC). Scale bar = 1mm
(B) Expression in root tips is induced in mycorrhized roots. Scale bar =1mm
(C) Co-staining for GUS signal and mycorrhizal structures (black triangles) shows substantial overlap. Scale bar =1mm
(D-F) Close up of co-stained root segment depicts that *PhPDR1* promoter activity is strongest around arbusculated cells and the regions flanking colonized sections. Black filamentous structures represent hyphae. Black globular structures represent arbuscles. Scale bars = 0.1mm

In order to investigate, whether the areas of intense *PhPDR1* promoter activity were overlapping with areas of mycorrhizal colonization we performed a co-staining to visualize both simultaneously. Even though areas could be found that were either only accommodating hyphal structures or only exhibiting *PhPDR1* promoter activity, the prevailing picture was that of a co-localization. In most cases the presence of mycorrhizal

structures, particularly arbuscles, were accompanied by GUS stained cells (Fig 2.7C). Interestingly GUS expression seemed to be strongest around arbuscle containing cells and not within them. Furthermore GUS stained patches ofte appeared to be flanking the mycorrhized sections, suggesting that *PhPDR1* promoter activity either precedes or follows fungal colonization (Fig 2. 7D-F). Often the GUS expression resembled a checkerboard pattern of stained and unstained cells (Fig 2.7C). Interestingly, clearing of mycorrhized roots with 10% KOH often revealed a similar pattern of brighter and darker colored cells. The darker ones are presumably metabolically more active and thus contain compounds that are difficult to clear (Fig 2.7C). Also commonly observed were GUS-stained sections that did not contain any internal hyphal structures, but were covered by one or several apressoria forming external hyphae. Again it was not clear whether the GUS signal was cause or effect of the presence of external hyphae.

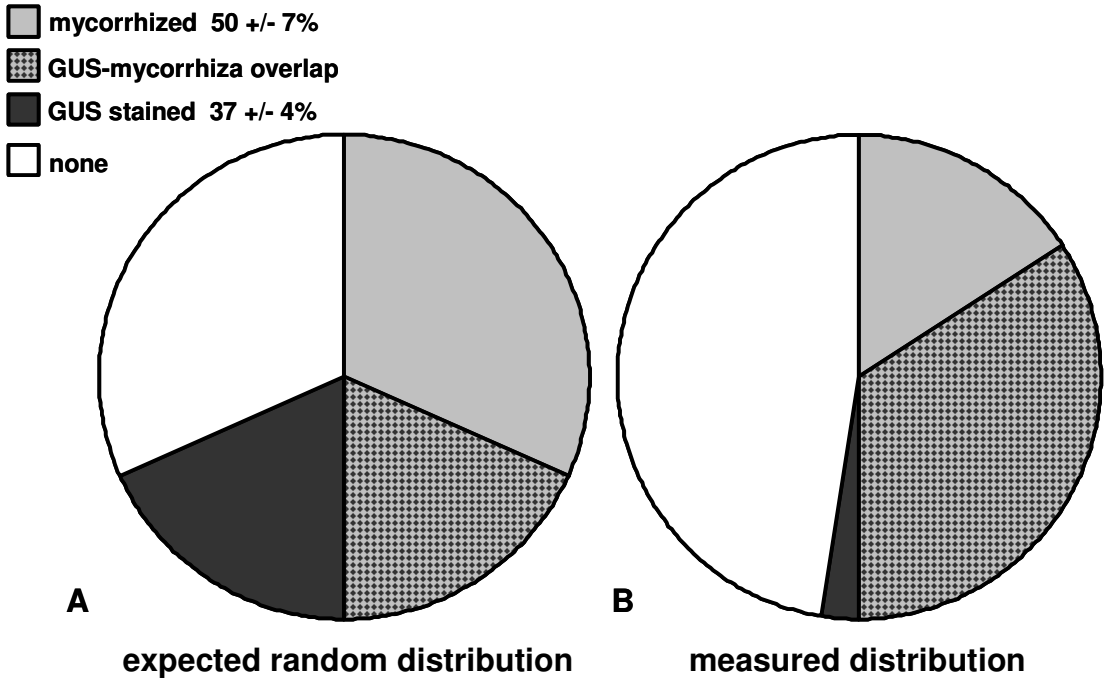

Figure 2.8: Quantification of mycorrhized sections and GUS stained sections in whole root systems of mycorrhized W115 plants 8wpi (n=3) via the grid line intersect method.
(A) Expected mycorrhiza and *PhPDR1* promoter activity overlap (light grey and dark grey checkerboard pattern) if 50% of total colonized root (light grey) sections and 37% of total GUS stained root sections (dark grey) were to be randomly dispersed over 100% of total root system.
(B) Actual recorded overlap of mycorrhized and GUS stained sections (light grey and dark grey checkerboard pattern) as well as only mycorrhized sections (light grey) only GUS stained sections (dark grey) and root sections devoid of both mycorrhiza and *PhPDR1* promoter activity (white).

To rule out that the increase of GUS expression in mycorrhized roots was only a secondary effect and that the overlap of stained cells and mycorrhized tissue did not follow a random distribution, we quantified patches that contained GUS only, patches that contained mycorrhiza only and patches that contained both. By comparing the observed distribution (Fig 2.8B) to a distribution expected if the total amount of mycorrhized patches and the total amount of GUS stained patches were randomly distributed over the root area (Fig 2.8A), it became apparent that a strong correlation between both exists. These data confirmed that *PhPDR1* expression was highly induced in mycorrhized tissues and that there was a tight spatial and temporal correlation between the two. However it did not become apparent from these observations whether PhPDR1 and its respective substrate(s) have a stimulatory or inhibitory effect on internal fungal proliferation. Both scenarios can be deduced from the prevalent patterns. By flanking colonized patches of root, *PhPDR1* expressing cells might restrict fungal expansion via the extrusion of inhibitory substances in a comparable fashion as it would try to confine the invasion of a fungal pathogen. Alternatively, the sequestration of stimulatory secondary metabolites might aid fungal differentiation and proliferation in a similar matter as strigolactones exuded into the rhizosphere do. By doing so the plant would actively guide the growing fungus towards yet un-colonized root sections.

2.2.3 RNAi Mediated Silencing of *PhPDR1* and Screening for Transposon Insertions in *PhPDR1*

In order to resolve this issue we decided to silence *PhPDR1* expression via RNA interference mediated mechanisms in the W115 background. Concomitantly by utilizing the unique properties of the transposon containing line W138, we attempted to screen for a mutant with a transposon insertion in the *PhPDR1* gene, which might result in a complete lack of function. Investigation of mycorrhization in a line impaired in PhPDR1 function might allow us to determine whether its substrate(s) has/have a promoting or inhibitory effect.

Two RNAi constructs were created, one targeting a highly variable region, with no apparent homology to other known PDRs, within NBD2 of PhPDR1 (Phpdr1-C), the

other targeting the 3`UTR and parts of the 3`end of the transcript (Phpdr1-R) (Fig 2. 9A). Both were transformed into the W115 background and the selfed T1 generation of several lines analyzed via RT PCR for their efficiency in silencing *PhPDR1* expression (Fig 2.9B). Two independent lines for each construct, with the highest degree of *PhPDR1* downregulation, were chosen for further investigation, Phpdr1-C-107 and Phpdr1-C-108 for the internal target and Phpdr1-R-101 and Phpdr1-R-104 for the 3`target.

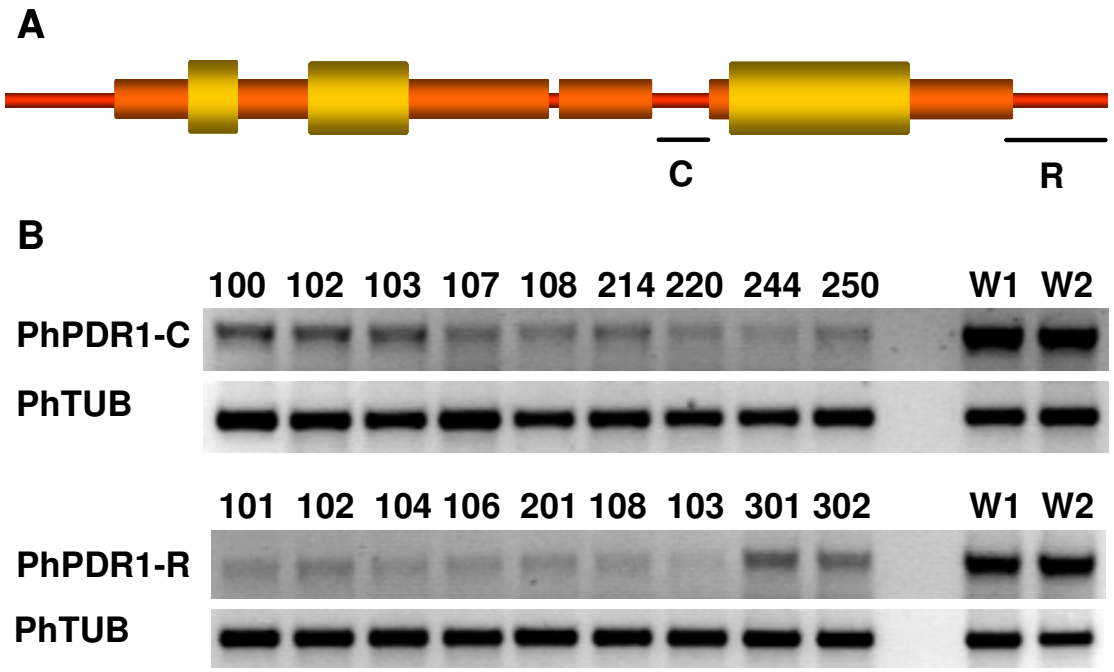

Figure 2.9: Design and evaluation of *PhPDR1* RNAi constructs in the W115 background.
(A) Schematic representation of the level of conservation among PDR transcripts from highly conserved (yellow) to highly variable (red). Target regions of the C-construct (C) and R-construct (R) were chosen in highly variable regions to avoid background silencing of other PDR homologues.
(B) Semiquantitative analysis of residual *PhPDR1* expression in several independent W115 lines transformed with either the Phpdr1-C (100-250) or Phpdr1-R (101-302) silencing construct. Two independent non-transformed W115 individuals (W1 and W2) were used as negative control. Petunia tubulin (PhTUB) served as a housekeeping control.

The highly mobile, non-autonomous, 284bp transposon dTph1 is represented by a number of around 200 copies per individual in petunias of the variety W138. Transposon insertion in the coding region of a gene of interest frequently results in the complete loss of function of the respective gene (Koes et al., 1995). An elaborate PCR based screening approach has been developed that allows for the simultaneous screening of several

thousand W138 individuals for a transposon insertion in the desired gene (scheme in Fig 2.10B).

Fig 2.10A shows the positive result, identifying the W138 individual at the co-ordinates X-10, Y-9 and Z-7 as a potential candidate for containing a dTph1 insertion in *PhPDR1*. All three bands were then cut out from the gel, reamplified and sequenced. Alignment of all three sequences with the cDNA sequence of *PhPDR1* revealed that all three sequences perfectly align to each other and that their respective exons match *PhPDR1* cDNA (Fig 2.10C).

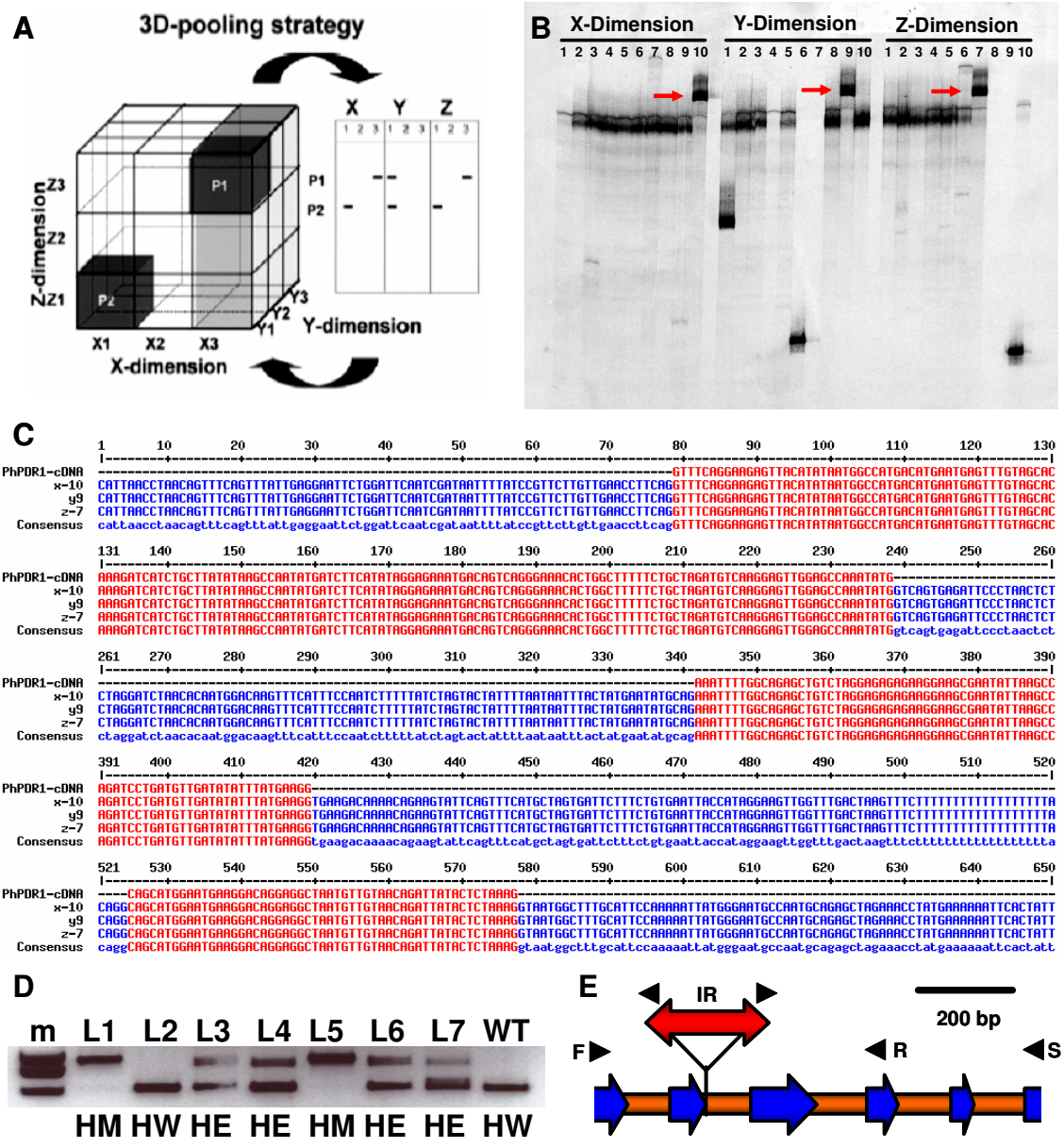

Figure 2.10: PCR based 3D-gDNA library screen for W138 individuals with dTph1 transposon insertions in the *PhPDR1* gene.
(A) Schematic representation of the three dimensional pooling strategy adapted from Vandenbussche and Gerats 2004. W138 individuals with divergent dTph1 distributions are arranged in a cube like fashion and sliced into sections according to the X-Y and Z dimension. The genomic DNA of all individuals in each slice is pooled and used as a template for a PCR reaction with dTph1 inverted repeat specific primer and a radiolabled gene specific primer. Three single congruent bands, one in each dimension indicate a positive hit and the slice number of each dimension gives the exact coordinates of the W138 individual of interest within the original cube.
(B) Screening result of a 10x10x10 3D-gDNA library for a dTph1 insertion in *PhPDR1*. Red arrows indicate single congruent bands in X-10, Y-9 and Z-7, which represent the coordinates for a putative *PhPDR1* knock out mutant
(C) Alignment of the re-amplified and sequenced X10, Y9 and Z7 genomic fragments with the respective *PhPDR1* cDNA fragment. Red areas correspond to the consensus of exons with the *PhPDR1* cDNA and blue areas correspond to the consensus of introns within the three genomic fragments.
(D) Homozygosity PCR with transposon flanking primers over the dTph1 insertion site on gDNA of the selfed T1 progeny of the X10-Y9-Z7 individual. L1-L7 are seven daughter lines either homozygous for the *PhPDR1* transposon insertion allele (HM), homozygous for the assumed *PhPDR1* wild type allele (HW) or heterozygous for both alleles (HE). A W115 individual (WT) served as a homozygous wild type control. „m“ represents the marker lane containing a ladder with 200bp increments.
(E) Schematic representation of the dTph1 insertion (red double arrow) in an intron (orange bars) exon (blue arrows) border of the *PhPDR1* gene. Black triangles indicate the forward (F) and reverse (R) transposon flanking primers used for the homozygosity PCR, as well as the inverted repeat (IR) and gene specific (S) primer used for the library screen. Scale bar equals 200bp.

Fig 2.10E schematically depicts the exact location of the transposon insertion at an intron exon border within the *PhPDR1* gene. Since the W138 individual was expected to be heterozygous for the dTph1 insertion, it was selfed and a number of the resulting T1 individuals were tested for homozygosity with transposon flanking primers. Homozygous wild types are expected to produce one band, congruent with the wild type allele (L2 in Fig 2.10D). Homozygous mutants should produce one band, 284bp larger than the wild type band, due to the presence of dTph1 (L1 and L5 in Fig 2.10D). Heterozygous lines should produce two bands, one representing the wild type allele and the other representing the mutant allele (L3, L4, L6 and L7 in Fig 2.10D).

However sequencing of both mutant and wild band revealed that the matter was more complicated than originally anticipated. The sequence of the mutant allele displayed a 284bp insertion that exactly matches the reverse complement sequence of dTph1 at the expected site, verifying a reverse oriented transposon insertion. Furthermore the mutant allele contains a 7bp target site duplication flanking the transposable element.

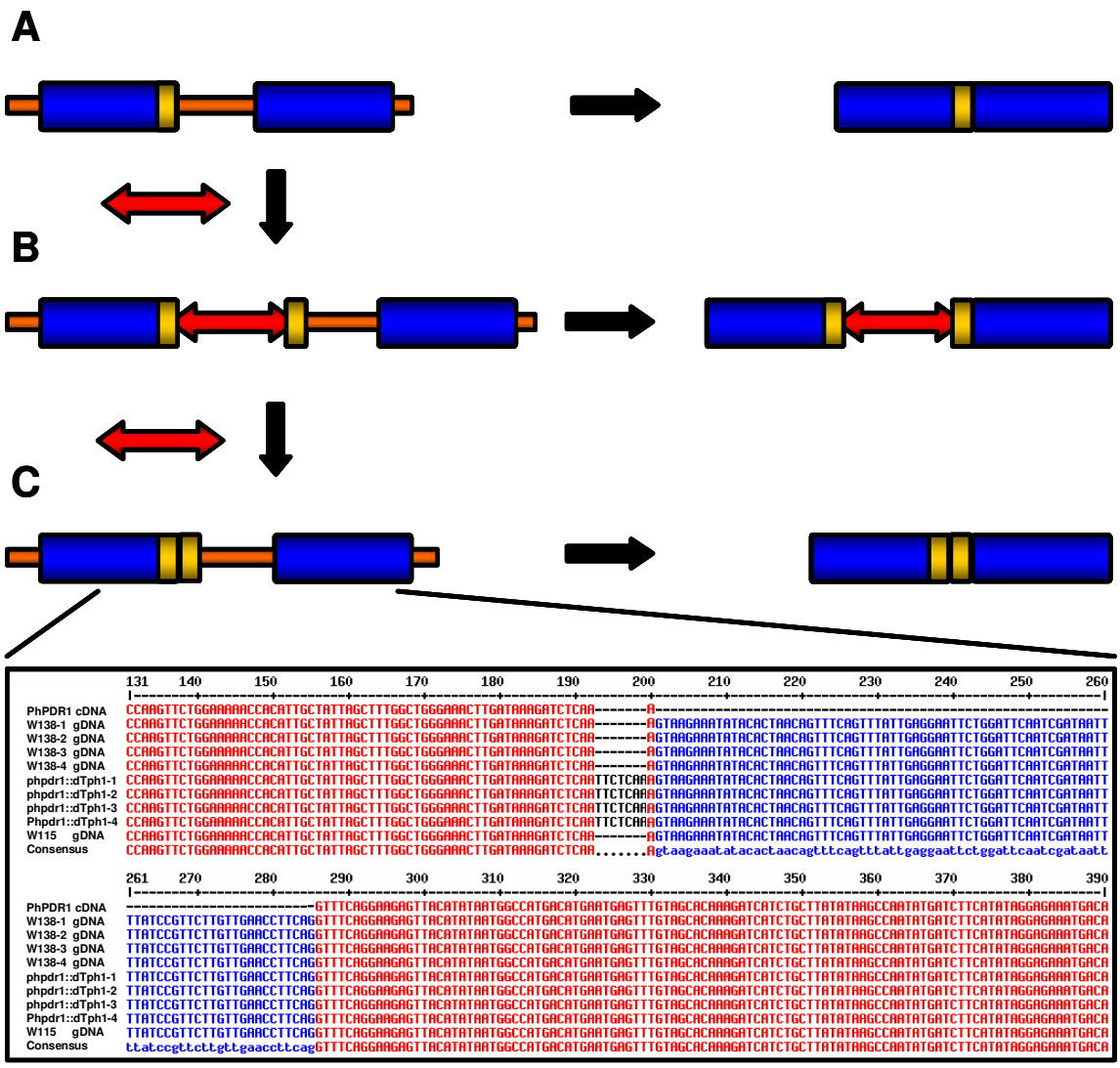

Figure 2.11: Schematic representation of dTph1 transposon insertion and excision events in the *PhPDR1* gene and its ramifications on the *PhPDR1* transcript.
(A) Wild type alleles of *PhPDR1* consisting of exons (blue bars) and introns (orange bars) result in functional transcripts after splicing (A right side). Yellow bar indicates the target site for dTph1.
(**B**) Transposon insertion (red double arrow) into the gene is accompanied by a target site duplication (second yellow bar). Transcription of the gene will result in a non-functional mRNA due to the presence of the transposon and a concomitant frame shift
(C) Upon excision of dTph1 the target site duplication, consisting of 7bp remains in the gene as a footprint. Consequently the transcript contains a 7bp insertion which causes a frameshift and results in a non-functional mRNA. The lower panel shows an alignment of *PhPDR1* cDNA derived from W115, *PhPDR1* genomic fragments from four independent W138 lines not containing a footprint, *PhPDR1* genomic fragments from 2 revertant alleles, previously homozygous mutants (Phpdr1::dTph1-1 and -2) and two homozygous footprint lines, previously believed to contain two wild type alleles (Phpdr1::dTph1-3 and 4), as well as a *PhPDR1* genomic fragment derived from W115. Red sections depict exon consensus, blue section depicts intron consensus and black section comprises the 7bp footprint.

However, the expected wild type allele was not completely congruent with the *PhPDR1* sequence. It contains a 7bp insertion at exactly the transposon insertion site, indicative of target site duplication as a remnant of a previous transposon insertion and subsequent excision. Consequently the original W138 individual derived from the screen was not heterozygous for one transposon insertion allele and one wild type allele, but heterozygous for one transposon insertion allele and one revertant allele, carrying a target site duplication derived footprint (Fig 2.11). Since the 7bp footprint leads to a frameshift within the coding sequence of *PhPDR1*, both insertion and reversion alleles are de facto mutant alleles. This makes it impossible to obtain a *PhPDR1* wild type plant with exactly the same genetic background in respect to other dTph1 insertions via crossing-out of the mutant allele. To circumvent this problem homozygous W138 dTph1 transposon insertion lines and homozygous footprint lines, collectively referred to as Phpdr1::dTph1, were compared to two independent closely related W138 lines containing two copies of the true *PhPDR1* wild type allele, referred to as W138 or PhPDR1 lines, in all subsequent experiments. Comparison of homozygous dTph1 insertion lines to homozygous footprint lines did not reveal any significant differences under all experimental conditions. Likewise both independent W138 lines did not differ significantly in any experimental setup (data not shown). Crossings of transposon insertion alleles and footprint alleles into the W115 background are under way in order to receive true mutant and true outcrossed wild type lines for comparative studies. Furthermore crossing the Phpdr1 mutation into the W115 background is expected to result in improved seed set and improved general plant fitness of the new hybrid lines, owing to the superior quality of the W115 background.

Despite the presence of dTph1 or the 7bp footprint in both *PhPDR1* alleles, *PhPDR1* transcript levels of homozygous mutants, as checked via RT PCR, appeared to be of regular abundance. However sequencing of the cDNA-derived transposon or footprint spanning fragments verified inclusion of either dTph1 or the footprint in the respective transcripts, rendering them non functional. Transposon excision from the *PhPDR1* gene was commonly observed, but in all investigated excision events the footprint remained present, making Phpdr1::dTph1 a de facto stable mutation.

2.2.4 Mycorrhization Trials

To determine whether the spatial and temporal overlap of fungal accommodation and *PhPDR1* expression has functional significance on the quality or quantity of the symbiosis Phpdr1::dTph1 and PhPDR1 lines in the W138 background were inoculated with the mycorrhizal fungus *Glomus intraradices* and the extent of mycorrhization quantified at several time points (wpi=weeks post inoculation). No difference was detected between two divergent PhPDR1 lines (data not shown). Likewise both the Phpdr1::dTph1 and the PhPDR1::footprint line exhibited similar patterns of mycorrhization (data not shown). Comparison of Phpdr1::dTph1 lines to PhPDR1 lines on the other hand disclosed a profound difference in the degree of mycorrhizal colonization. At all observed time points the mutant contained significantly less mycorrhized root sections as quantified via the line intersect method. The overall morphology of the internal and external structures however did not seem to vary between the two genotypes. The fungus produced hyphopodia, intracellular hyphae, intercellular hyphae, arbuscles and vesicles on and in mutant roots that could not be histologically distinguished from their respective counterparts on wild-type roots (data not shown). The disparity seemed to manifest itself mainly in fewer entry sites and lower expansion rates at given entry sites, synergistically contributing to the observed overall decrease in fungal colonization. Concordantly the relative difference was most pronounced at earlier time points post inoculation, before the mycorrhiza reached a steady state level. After 4wpi around 15% of wild type roots were mycorrhized under the given conditions, whereas the mutant contained fungal structures in only around 5% of its root stock (Fig 2.12A). This implies that the wild type is three times more effective in attracting and/or accommodating its symbiotic partner. At a later time point, 8wpi, the relative difference was decreased but still pronounced, with a little less than 50% of colonization recorded for the wild type and around 25% for the mutant (Fig 2.12A). Taken together these data allow for the assumption that PhPDR1 transports substrates have stimulatory effects on mycorrhization. Furthermore it can be speculated that they act both pre-symbiotically and during the later stage of development of the interaction within the root cortex.

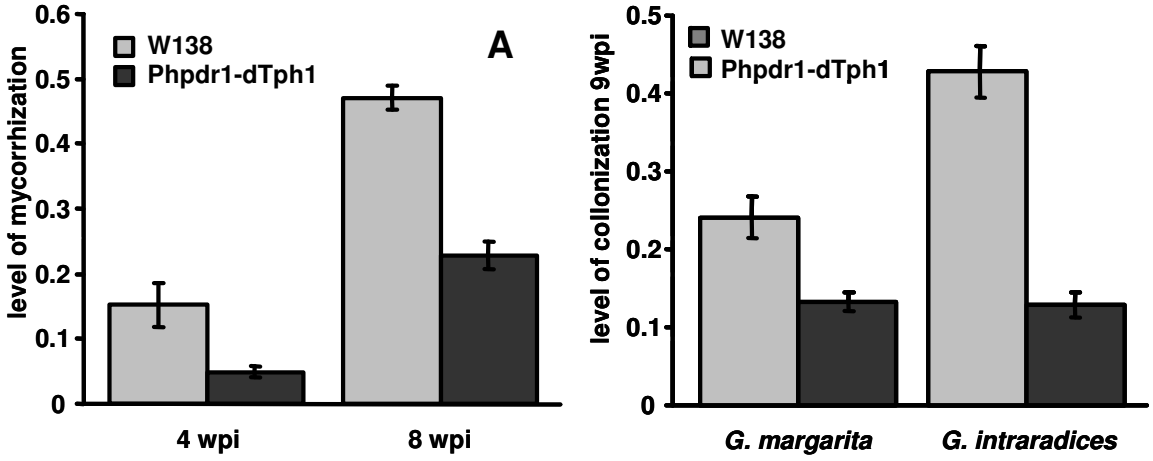

Figure 2.12: Quantification of colonization of W138 and Phpdr1::dTph1 lines by *Glomus intraradices* and *Gigaspora margarita.*
(A) Relative amount of W138 root sections (light grey columns) and Phpdr1::dTph1 root sections (dark grey columns) colonized by *G. intraradices* 4 weeks post inoculation (4wpi) and 8 weeks post inoculation (8wpi). Error bars indicate standard error (n=15-26).
(**B)** Relative amount of root sections colonized by *G. intraradices* or *G. margarita* 9 weeks post inoculation. Error bars indicate standard error (n=17-24).

Glomus intraradices, of the order Glomerales, is commonly utilized in laboratory practice because of its easy propagation and vigorous colonizing behavior. It branches and elongates its extraradical hyphae profusely within the vicinity of a host root and once within the root cortex infects large patches and develops an abundance of arbuscles. Minute spores are either produced intraradically or very close to the host root in large quantities and once germinated, primary hyphae usually do not extend beyond several millimeters before they are either aborted or start branching again in response to host recognition. But the phylum of Glomeromycota consists of several recognized orders of AM fungi that differ substantially in their pre-symbiotic and symbiotic morphology and development. Quite different in appearance and behavior from the Glomerales are members of the Diversisporales like the Gigasporaceae. They produce fewer, but, as their name suggests, gigantic spores with substantial reserves. Once germinated, elongating primary and secondary hyphae can bridge many centimeters of soil without receiving any branching cues from potential hosts. But even close to the root and within range of the BF, they will only branch moderately and only infect small local patches of root (Parniske, 2008). In order to test whether PhPDR1 function is necessary for phylogenetically distinct Glomeromycotes and whether divergent colonization patterns

are affected differently by a lack of PhPDR1 function, we investigated infection rates of *PhPDR1* wild type and mutant plants after inoculation with the Diversisporales member *Gigaspora margarita*. As expected the overall colonization of *Gigaspora margarita* was less pronounced than for *Glomus intraradices* in the wild type, reaching a steady state level of around 24% compared to an estimated 43% for the Glomerale. However *Gigaspora margarita* was able to invade mutant roots to levels above half of that recorded for the wild type at 9wpi, while *Glomus intraradices* colonization was restricted to levels below one third (ca. 13%) in the mutant background (Fig 2. 12B). Apparently *Gigaspora margarita* is less dependent on PhPDR1 transported signals for its development than *Glomus intraradices*. Still PhPDR1 function is necessary for the establishment of the symbiosis to its full capacity for both fungi. Furthermore it must be noted that levels of colonization, even though they are quite stable in the wild type background, show large levels of variation between independent experiments in the mutant background, which we attribute to slight differences in the initial inoculum concentration and age. Because of the presumed delay of invasion and lower rates of colonization in Phpdr1::dTph1, small deviations in terms of initial fungal abundance and vitality might lead to large differences at later time points, whereas these effects become negligible in the wild type background.

2.2.5 Hyphal Branching Assays

It has long been established that in the pre-symbiotic phase mycorrhizal plants exude one or several stimulatory compounds, collectively referred to as branching factors (BF), into the rhizosphere. This results in the induction of hyphal branching and the activation of fungal metabolism, which consequently facilitate the initial contact of both symbiotes. Recently a group of sesquiterpene lactones of carotenoid origin, called strigolactones, have been unambiguously identified as a crucial component of BF (Akiyama et al., 2005). For a detailed analysis of BF capabilities, intricate in vitro hyphal branching assays have been designed and successfully applied in several studies (Nagahashi and Douds, 1999; Buee et al., 2000). Considering that Phpdr1::dTph1 mutants display a potential impairment in the pre-symbiotic development of the AM fungus, root exudates from wild

type and mutant plants were collected and their efficiency to induce hyphal branching was tested in vitro. The synthetic strigolactone analogue GR24 was used as a positive control and since *Gigaspora margarita* had been previously demonstrated to be susceptible to the Phpdr1::dTph1 phenotype in mycorrhization trials, all assays were performed on spores of this species.

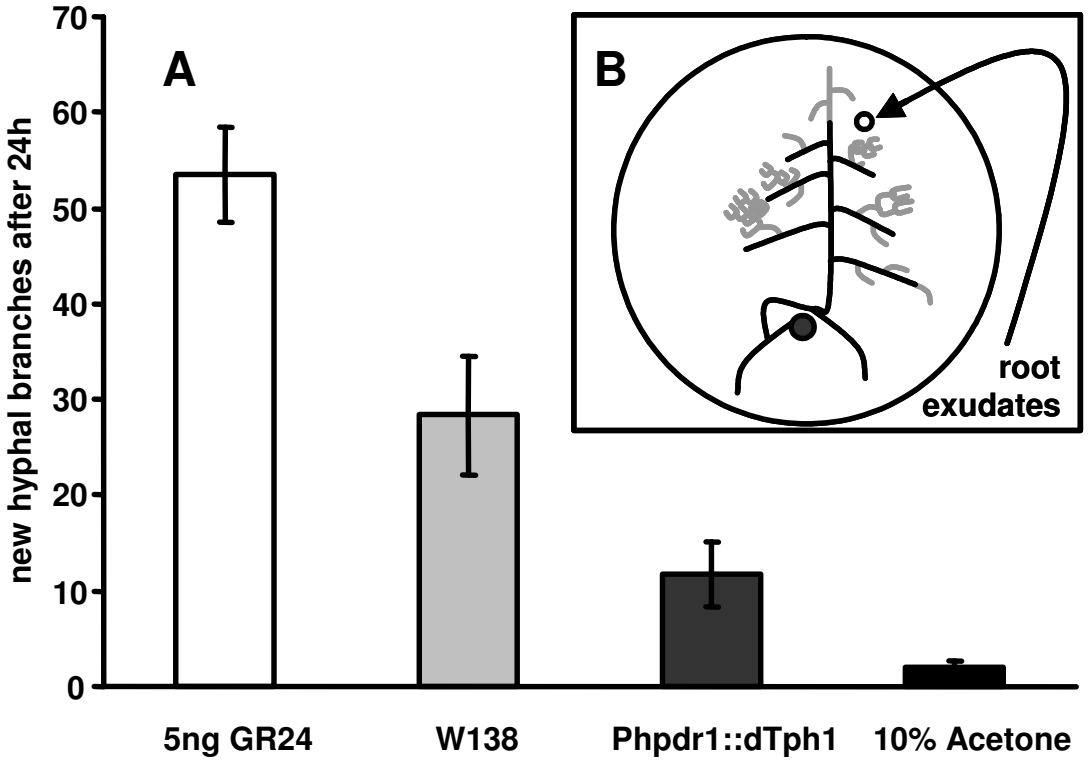

Figure 2.13: *Gigaspora margarita* hyphal branching assay with root exudates of W138 plants and Phpdr1::dTph1 plants.
(A) Quantification of newly formed hyphal apices on secondary hyphae of *Gigaspora margarita* after 24h of exposure to an equivalent of 20mg root FW acetone soluble root exudates of W138 plants (light grey column) and Phpdr1::dTph1 plants (dark grey column). 5ng of the synthetic strigolactone analogue GR24 served as positive control (white column) and the solvent of 10% Acetone (black column) served as negative control. Error bars indicate standard error (n=5-12).
(**B)** Schematic representation of the experimental set up. Spores of *Gigaspora margarita* (dark grey spot)were germinated on plate (big black circle) and incubated vertically for 6-8 days until a secondary hypha growing in a negatively geotropic manner had produced several stunted branches (black lines). Root exudates were applied close to the tip of the secondary hypha (small black circle) and new hyphal apices (light grey lines) counted after 24h of exposure.

Hyphal branching was most pronounced in the presence of 5ng of GR25, with an average of more than 50 new hyphal apices being detected after 24h of exposure (Fig 2.13). Application of the solvent alone (10% acetone) did not result in a detectable reaction of the fungus and the few recorded additional branches can be attributed to normal fungal development within 24h rather than a stimulatory effect of the solvent. Both control assays support the suitability of the in vitro system. Application of an equivalent of total acetone soluble root exudates of 20mg W138 root FW lead to the formation of around 30 novel branch sites per germinated spore (Fig 2.13). The score is significantly lower than that observed for synthetic branching stimulant GR24 that most likely signifies the maximum stimulatory capacity. However, saturating amounts of root exudates were not intended to be applied, since a putative quantitative difference in branching stimulation for both genotypes is expected to be detectable predominantly under non-saturated conditions. And indeed a significant reduction by more than 50% in newly formed hyphal apices was monitored when secondary hyphae of *Gigaspora margarita* were subjected to equal amounts root exudates of Phpdr1::dTph1 plants instead of the respective exudates of wild type lines (Fig 2. 13). This finding is indicative of PhPDR1 dependent exudation having an impact on pre-symbiotic signaling and is likely to explain in part the observed diminution of overall mycorrhization in the Phpdr1 mutant background. However it must be considered that *PhPDR1* promoter activity is most pronounced in late stage symbiotic interactions suggesting that the colonization phenotype is also in part due to impairments in cortical accommodation or guidance.

2.2.6 Axillary Branching Patterns of Wild Type and Phpdr1 Mutant Plants

The overall mycorrhiza specific phenotype of Phpdr1::dTph1 appears to involve a lack of symbiosis promoting secondary metabolites at the root AM fungus interface that is strikingly congruent with the mycorrhiza related phenotype reported for the rms1/ccd8 mutant in pea (Gomez-Roldan et al., 2008). Thus we decided to test the hypothesis that PhPDR1 is implicated in strigolactone transport. Strigolactones are potent inhibitors of axillary bud outgrowth. Being predominantly produced in the root, they are thought to be translocated to target sites via the vasculature. *PhPDR1* expression under non-

mycorrhizing conditions is restrained to single cells within the root cortex and epidermis as well as the primary root vasculature (Fig 2.5). In the shoot, promoter activity is detectable in the vasculature with very prominent sites of activity in the direct vicinity of dormant axillary buds (Fig 2.6). The finding that above ground expression is highest precisely below axillary buds, but completely absent in the meristematic tissues of the respective bud particularly supports the strigolactone transporter hypothesis. In this case we would expect a deregulation of PhPDR1 mediated strigolactone accumulation in the axillary meristems of Phpdr1 mutant plants and consequently an aberrant branch production.

W138 and Phpdr1::dTph1 plants were grown under optimal nutrient and long daylight conditions for 50 days and were then investigated for their capacities to develop lateral branches. Lateral bud outgrowths were considered as branches according to definitions developed for the investigation of petunia Decreased Apical Dominance mutants (Snowden and Napoli, 2003). W138 plants produced an average of 2.7 branches per plant under the given conditions, whereas Phpdr1::dTph1 individuals developed an average of 5.8 branches (Fig 2.14A). Moreover Phpdr1::dTph1 consistently produced very large branches that exceeded the main shoot in length, giving the pant a very open, disc like appearance with stunted height (Fig 2.15). W138 lines lacking *PhPDR1* transposon insertion had a more dominant main axis and only rarely produced lateral branches that became longer than the main shoot. Additionally Phpdr1::dTph1 mutants differed slightly in their distribution of lateral branches along the main plant axis (Fig 2.14B). The graph shows the distribution of lateral branches of 49 individual plants of each genotype for the first 14 nodes of the main plant axis, starting with CN, the cotyledonary node. The height of the bar is indicative for the probability that a single individual will produce a branch from this node and hence the graph displays the branching capacity for W138 lines and Phpdr1 mutant lines. As it becomes apparent W138 lines and Phpdr1::dTph1 lines did not develop outgrowths that could be considered branches from the cotyledonary node and no branches were recorded between node 13 and the last node before the first flower producing node (data not shown). The majority of lateral branches in W138 lines sprouted from node 4 to node 11, but only from node 6 through node 9 did more than 40% of all W138 plants produce a branch, indicating a window of highest branching

capacity. This is consistent, with data previously reported for petunia V26 lines (Snowden and Napoli, 2003).

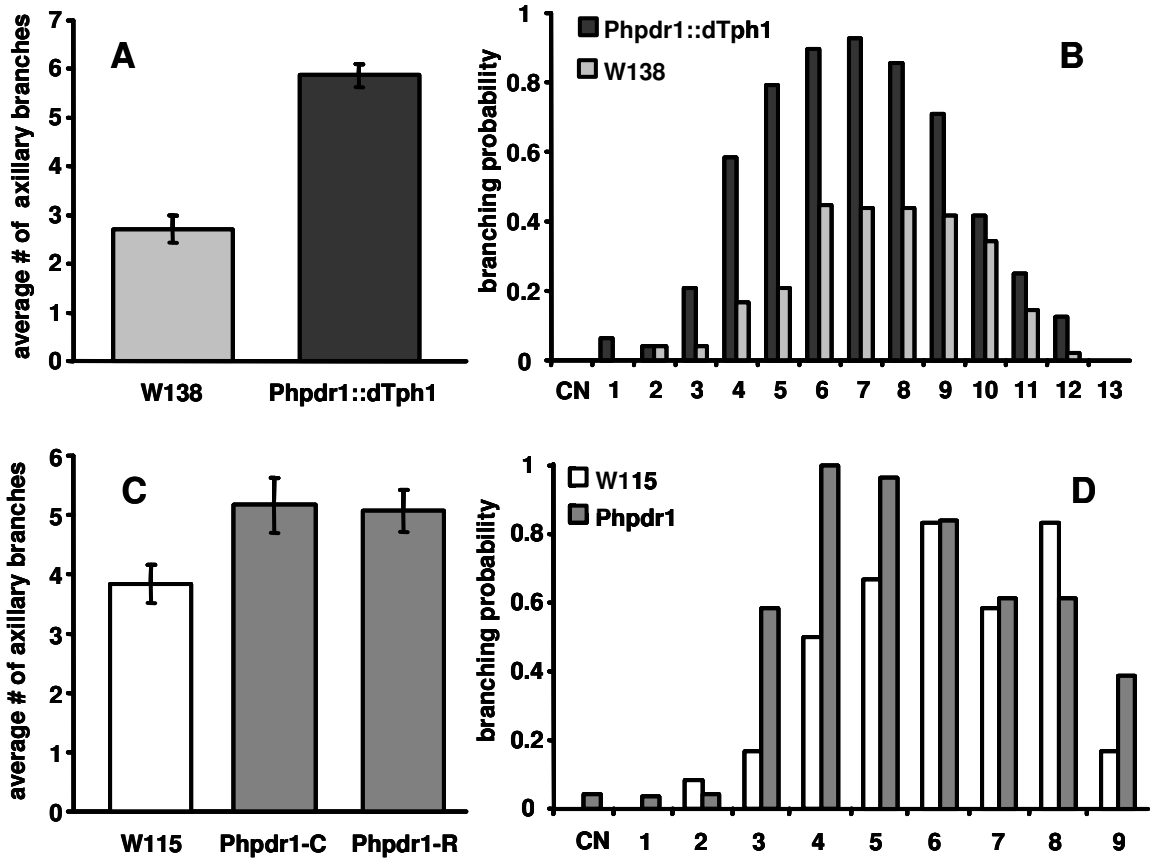

Figure 2.14: Quantification of axillary branch production of W138 individuals, Phpdr1::dTph1 individuals W115 individuals and Phpdr1-C as well as Phpdr1-R RNAi lines 50 days post seedling transplantation.
(A) Average amount of fully developed axillary branches on W138 (light grey column) and Phpdr1::dTph1 individuals (dark grey column). Error bars indicate standard error (n=49).
(B) Probability to produce a full branch for each node (starting from the cotyledonary node CN) of W138 (light grey columns) and Phpdr1::dTph1 individuals (dark grey columns). Error bars indicate standard error (n=49).
(C) Average amount of fully developed axillary branches on W115 (white column) and Phpdr1-C as well as Phpdr1-R individuals (grey columns). Error bars indicate standard error (n=24).
(D) Probability to produce a full branch for each node (starting from the cotyledonary node CN) of W115 (white columns) and Phpdr1 (C and R lines are pooled) individuals (grey columns). Error bars indicate standard error (n=24-48).

W138 lines lacking PhPDR1 function displayed an overall higher probability of producing a lateral branch on all nodes, and from node 6 through node 9 the chance to for a branch to develop was approximately doubled, when compared to W138 line. On the

nodes higher than the main branching window the difference was not as pronounced (with the exception of node 12). The biggest discrepancy in branching behavior however was found on nodes 3 through 5, below the main branching window. Here the probability for a Phpdr1 mutant plant of producing a branch was about four times higher than for PhPDR1 wild-type plants. On node 1, the first node of a true leaf, no W138 was recorded to produce a branch, but 6% of all Phpdr1 mutants did so. In conclusion the probability for Phpdr1 mutants to produce a branch within the main window was higher than for PhPDR1 wild type lines and the window was slightly wider. Most prominent were changes in branching probabilities on the lower nodes. Together they resulted in an approximate doubling of total branch number in the mutant background.

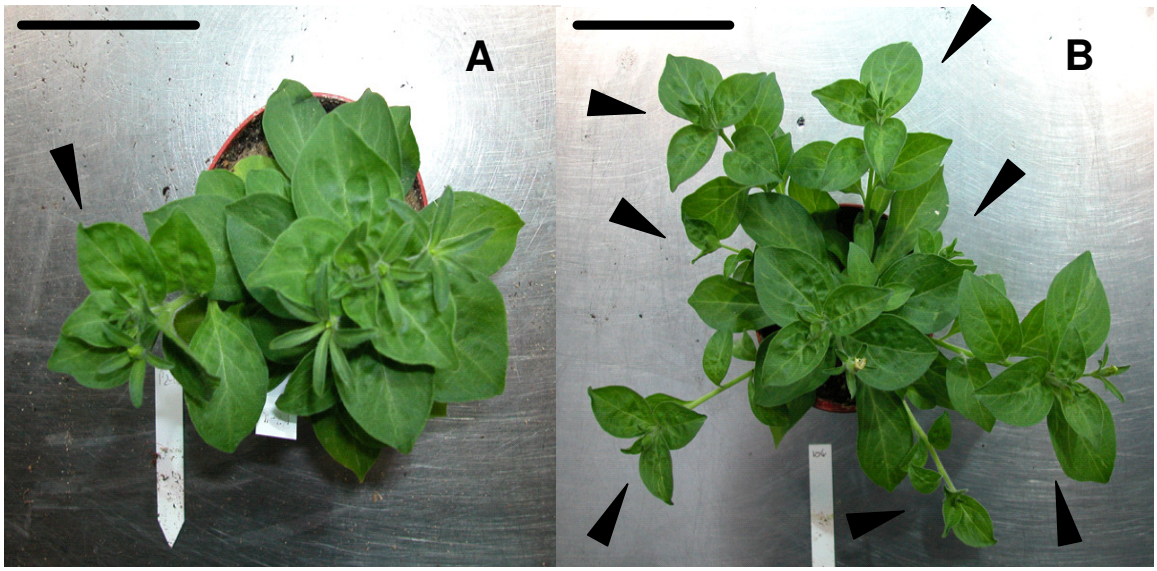

Figure 2.15: Branching phenotype of Phpdr1::dTph1.
Exemplary W138 individual **(A)** and Phpdr1::dTph1 individual **(B)** shown 50 days post seedling transplantation. Black arrows indicate clearly visible lateral branches.
Scale bars = 10cm

The overall change in branching pattern of Phpdr1::dTph1 lines most resembled that of the partial loss of DAD1 function mutants dad1-2 and dad1-3 in the V26 background (Snowden et al., 2005). While dad1-2 contains a single amino acid substitution in the CCD8 gene due to a point mutation, dad1-3 contains an insertion of three AAs, owing to a footprint remaining after a transposon excision event. The branching phenotype of dad1-1, a complete lack of DAD1 function mutant, is by far more prominent than what

was observed for Phpdr1::dTph1 lines. Dad1-1 commonly produces a lateral branch from each node, including both cotyledonary nodes.

Branching trials comparing W115 lines with *PhPDR1* silenced lines yielded similar if less distinct results. With an average of around four branches per plant, W115 lines displayed an overall higher tendency towards producing lateral branches than W138 lines (Fig 2.14C). Downregulation of *PhPDR1* did result in an increased branching capacity in the W115 background, but the effect was rather marginal for both Phpdr1-C108 and Phpdr1-R105, raising the average from around 4 to around 5 branches per plant (Fig 2.14C). As for transposon insertion lines, the difference in branching behavior between W115 and Phpdr1 RNAi lines was most obvious at nodes below the main branching window. The probability was around 4 times as high at node 3 and twice as high at node 4, which together accounted for the observed difference in the total amount of branches.

2.2.7 ^{3}H-GR24 Transport Assays with W138 and Phpdr1::dTph1 Lines

In order to investigate whether loss of PhPDR1 function impairs the transport of strigolactones at the whole plant level, W138 and Phpdr1::dTph1 plants of similar weight and size that had developed four clearly distinguishable nodes above the cotyledonary node were incubated in a medium containing 0.15µCi of ^{3}H radiolabled GR24.

After 1h and 3h, the tissue around the axillary buds, corresponding to the tissue with strongest *PhPDR1* promoter activity (Fig 2.16A), was separated from the main plant body and quantified for its accumulation of ^{3}H-GR24 (Fig 2.16B). Regardless of the genotype, GR24 concentrations decreased at nodes higher up on the main plant body and were lowest within the leaf mesophyll. After 1h Phpdr1::dTph1 plants contained significantly more ^{3}H-GR24 in its nodal tissues than W138 plants. The relative difference was most pronounced for node 1 (N1) and node 2 (N2), with the mutant having accumulated more than double of the synthetic strigolactone than the wild type. Phpdr1::dTph1 plants also accumulated more ^{3}H-GR24 in the cotyledonary node (CN) and node 3 (N3). Interestingly even in the mesophyll of the second true leaf (L2) there seemed to be a slightly increased accumulation of GR24 even though no *PhPDR1* expression was detectable. After 3 hours of incubation a difference in ^{3}H-GR24 content

was no longer discernable at the nodes or leaves of both genotypes, except at N3, which still displayed a slightly higher concentration in the mutant (data not shown). This finding might be indicative of a saturation of GR24 in the nodal tissues after 3h that cannot be counteracted by the presence of PhPDR1. Notably after 1h of incubation the amount of GR24 measured per mg fresh weight in the cotyledonary nodes and nodes of the first true leaves of Phpdr1::dTph1 exceeded the amount of radiolabled GR24 per mg incubation medium, which was calculated to be 3,72pg/µl, clearly supporting the hypothesis that active transport mechanisms for strigolactones exist.

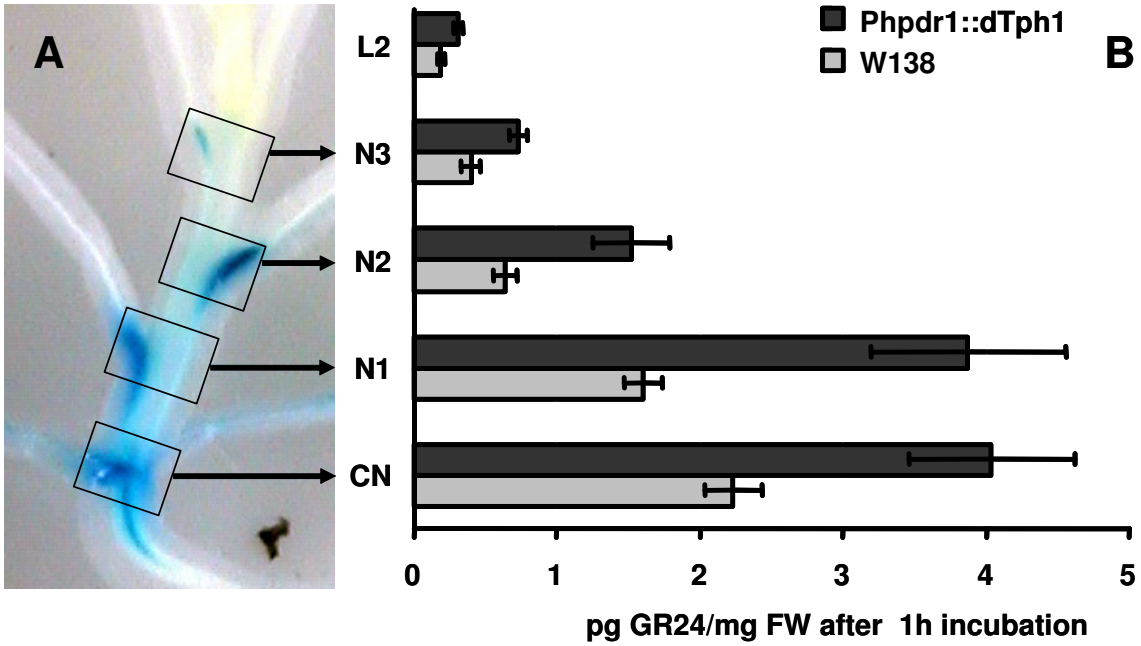

Figure 2.16: Quantification of ^{3}H-GR24 accumulation in the nodal regions of W138 individuals and Phpdr1::dTph1 individuals.
(A) *PhPDR1* promoter-GUS signal in the nodal regions of a W115 individual for an exemplary display of areas with *PhPDR1* expression. Black boxes indicate sections that were used for tritium quantification.
(B) Accumulation of radiolabled GR24 in the nodes of W138 (light grey columns) and Phpdr1::dTph1 individuals (dark grey columns) after 1h of incubation in a medium containing 3.73 µg/l ^{3}H-GR24 (12.9 µM ^{3}H-GR24). CN = cotyledonary nodes; N1-N3 = nodes of the first to the third true leaf, L2 = mesophyll of the second true leaf. Error bars indicate standard error (n=8).

2.2.8 Phpdr1::dTph1 Wilting Phenotype

Apart from mycorrhiza-specific and branching-specific phenotypes recorded for W138 lines lacking PhPDR1 function, another seemingly unrelated phenotype was commonly observed. Mature Phpdr1::dTph1 plants generally well within the flowering stage often started wilting despite ambient water supply. Sometimes one or a few major branches were affected, but more often the whole plant would start to desiccate and could not be rescued by addition of water to the soil or growth medium (Fig 2.17).

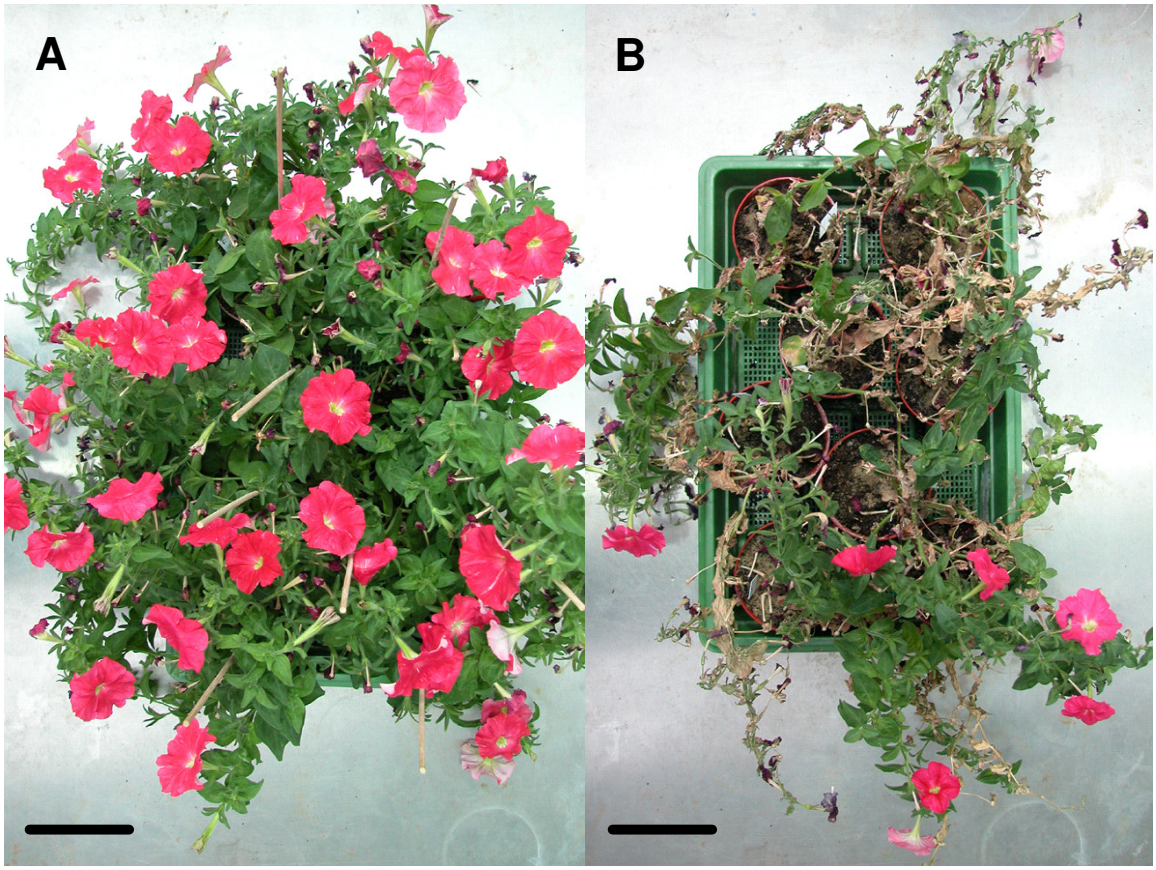

Figure 2.17: Wilting phenotype of Phpdr1::dTph1.
W138 individuals (A) and Phpdr1::dTph1 individuals (B) were grown for three months after seedling transplantation under optimal nutrient and long day conditions. Scale bars = 10cm

However, not all individual seemed to be prone to wilting. After two months under optimal growth conditions around 20% of a given population did completely succumb to desiccation. If kept significantly longer most, but not all, individuals showed signs of

wilting. None of the inspected W138 lines with a functional *PhPDR1* allele ever displayed a similar phenotype. First it was thought that the wilting was pathogen related, but no apparent infection of the root system or vasculature could be observed (data not shown). Furthermore two or more Phpdr1::dTph1 plants could be grown in the same pot and started wilting independently of each other or did not wilt at all, and transfer of a fully turgescent mutant plant to a pot with a fully desiccated plant did not necessarily induce wilting (data not shown). On the other hand, if a partially desiccated branch of either transposon insertion mutant or RNAi line was severed from the main plant body and placed into a container with water it would regain turgor within an hour (Fig 2.18 insets).

Figure 2.18: Wilting phenotype of Phpdr1::dTph1
Mature Phpdr1::dTph1 individual **(A)** and mature Phpdr1-C RNAi individual **(B)** showing clear signs of wilting despite ambient water supply. Insets show a single lateral branch of the same plant two hours after separation from the main plant body. Scale bars = 10cm

To further investigate this phenomenon, we took seedlings ranging from 60-120mg in FW, and monitored their evaporative water loss under high light and high temperature conditions over time (Fig 2.19). Both wild type and mutant initially lost around 2% of their initial FW in water over the first 2 hours. But whereas the wild-type managed to

balance its water loss at around 2% and appeared to recover within the last hours of the 6 hour incubation time, the mutant kept loosing increasingly more water, resulting in a total water loss of more than 5% after 6 hours of incubation. The apparent inability of Phpdr1::dTph1 lines to replenish evaporative water loss via vascular conduction from the bathing medium furthermore lead to apical turgor loss in the newest emerging leaves and the tips of older leaves, giving the plant a wilted appearance (data not shown).

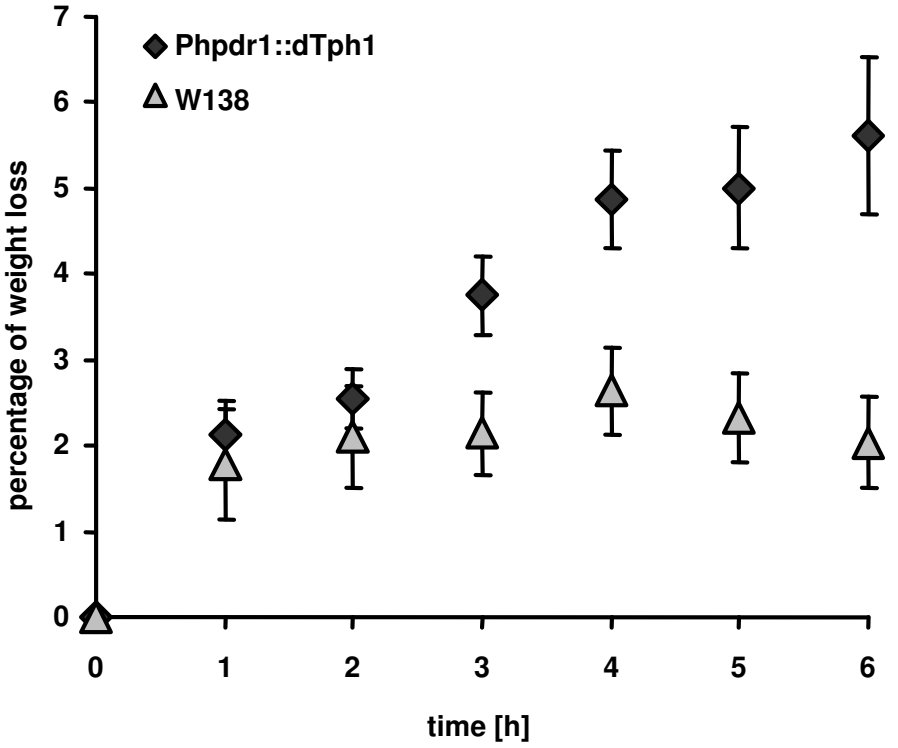

Figure 2.19: Wilting phenotype of Phpdr1::dTph1.
Percentage of relative water loss over time of W138 seedlings (light grey triangles) and Phpdr1::dTph1 seedlings (dark grey diamonds) of an average weight of 91mg exposed to high light at 31°C. Error bars indicate standard error (n=12).

Taken together these observations suggest that the wilting phenotype of Phpdr1::dTph1 is due to aberrant root or vasculature development, restricting water allocation to the whole plant body in fully developed plants and in seedlings under high evaporative conditions. Interestingly, rms2, a branching mutant in pea where the responsible mutation is yet unknown, also displays a wilting phenotype under conditions of increased water demand (Dodd et al., 2008).

2.3 Discussion

PhPDR1, a novel full size PDR-type ABC transporter isolated from mycorrhized roots of Petunia, is suggested to have functional implications in plant development and symbiosis-related signaling. Assuming that, in accordance with general PDR localization, PhPDR1 targets to the PM (data outstanding), expression profiling and phenotypic analysis of mutants impaired in PhPDR1 function allow for the conclusion that belowground it is involved in pre-symbiotic signaling events in the rhizosphere as well as post-entry accommodation and/or guidance of AM fungi. Aboveground it apparently contributes to the inhibition of lateral branch outgrowth from axillary buds, thus influencing general plant architecture. PDR homologues are present throughout the fungi and plant kingdoms, and in the latter serve predominantly as ATP-driven and PM-intrinsic secondary metabolite extrusion pumps (Crouzet et al., 2006). Among the proposed substrates for PDR type transporters are antimicrobial terpenoids (van den Brule et al., 2002; Campbell et al., 2003) and phenolic acids (Ito and Gray, 2006). PhPDR1 falls within Cluster1 of the PDR subfamily, which is well characterized in terms of pathogen defense, heavy metal resistance and response to abiotic stresses originating from belowground (see General Introduction). Many Cluster1 homologues are preferentially expressed in root tissues and even though PDRs commonly appear in symbiosis-related transcriptome profiling studies, no functional relationship in mutualistic interactions was ever insinuated.

2.3.1 PhPDR1 and Mycorrhization

Currently it is becoming increasingly apparent that plant secondary metabolites play an important role in mycorrhiza-specific signaling events, both in the pre-symbiotic phase and the later arbuscular phase. Among several groups of mycorrhiza related secondary compounds, plastid derived apocarotenoids are emerging as key components in the crosstalk between both symbiotes (Akiyama, 2007). Strigolactones, a group of C15 apocarotenoids coupled to a C5 lactone moiety, are exuded into the rhizosphere, where they play a pivotal role in the induction of hyphal branching, facilitating the initial contact between AM fungi and the host root Other apocarotenoid complexes such as

mycorradicin related compounds and cyclohexenoid derivates are produced in vast quantities in mycorrhized roots and seem to be involved in arbuscle development and turnover. However, it is currently unknown whether these substances are actively transported across biological membranes. But the highly regulated manner in which strigolactones are exuded and the sheer abundance of mycorradicins and cyclohexenoids that need to be sequestered or excreted would imply that the underlying mechanisms are rather related to active transport than simple passive diffusion.

PhPDR1 transposon insertion mutants display aberrant mycorrhizal colonization patterns that do not resemble the impairments commonly observed for mutants of the common SYM pathway. Fungal invasion upon hyphopodia formation, crossing of epidermal and sub-epidermal cell layers to reach the root cortex and arbuscle formation appear unaffected and symbiotic structures are of normal morphology. Thus PhPDR1 dependent signaling is likely to be independent from common SYM pathway related signaling events. Strong *PhPDR1* expression in and adjacent to arbusculated root sections and lower colonization rates in roots with Phpdr1 mutant background insinuate that PhPDR1 and its substrate(s) are necessary for an optimal accommodation and/or expansion of the fungus in cortical regions.

Apocarotenoids related to mycorradicin and blumenin make interesting candidates for PhPDR1 substrates in this respect. However they have been suggested to play a role in arbuscle development rather than intraradical spread of the fungus. *PhPDR1* expression as visualized by GUS is strong in arbusculated regions and adjacent to them, but cells actually containing arbuscles do not display any apparent *PhPDR1* specific signal (Fig 2.7). Furthermore RNAi mediated downregulation of *CCD1* in Medicago substantially impairs mycorradicin and cyclohexenoid production, without significantly affecting the overall mycorrhization capacities of the plant (Floss et al., 2008a), signifying no phenotypical overlap between CCD1-derived apocarotenoids and PhPDR1 function. Similar results have been obtained for the knock-down of the symbiosis specific DXS2 transcript in Medicago, which acts upstream of CCD1 (Floss et al., 2008b).

At the late arbuscular stage, invasion of new areas by the fungus is predominantly achieved via intercellular growth that is independent of PPA like structures and presumably not directly linked any further to common SYM pathway related processes. It

is still plausible, however, that the fungus continuously needs stimulatory chemical cues from the plant in order to advance towards yet un-colonized sections. For the plant the prerequisite of such chemical guidance would be of benefit, since it would allow for a positive control over the extent of mycorrhization in a spatial and temporal manner. Intraradical hyphae could be directed in accordance to the plants general nutrient status and the roots current sink status and prevent the fungus from becoming a threat to the plants` tissues and/or resources.

It has long been argued to what degree the plant controls the relationship and to what degree the fungus remains an opportunist seizing possibilities to increase its intraradical proliferation (Kogel et al., 2006). In case of an opportunistic, almost hemi-parasitic fungus, the plant would rather have to exert a negative control over the fungal spread by restricting its growth, similar to that of a pathogen (Paszkowski, 2006). Our data on the other hand seems to support the notion that the fungus is more of a benign nature and suggests that the plant controls its development within the root via enticing rather than repelling actions. But to conclusively resolve this matter from a PhPDR1 point of view it will be necessary to develop a non-invasive online system that enables the simultaneous monitoring of fungal spread and *PhPDR1* expression in vitro. Attempts will be made with *PhPDR1* promoter GFP constructs stably transformed in W115 root organ cultures and fluorescent chitin-specific dyes in an on-plate set-up customized for inverse fluorescence microscopy.

Since extraradical hyphal branching of AM fungi is also negatively affected in the Phpdr1::dTph1 background, PhPDR1 substrates are believed to exert their stimulatory effects not only within the root but also throughout the rhizosphere. But given the broad substrate specificity of many ABC transporters, it is quite possible that the PhPDR1 transported compound(s), which stimulate intraradical growth, are not identical with the respective compound(s), which promote extraradical hyphal branching. Pre-symbiotic signaling precedes the common SYM pathway and is postulated to be mainly regulated via the plants current nutrient status. Low phosphate availability in particular stimulates the exudation of secondary compounds into the rhizosphere that attract AM fungi via activation of fungal development and metabolism (Tawaraya et al., 1998; Akiyama et al., 2002; Besserer et al., 2008).

Strigolactones are potent inducers of hyphal activity in the rhizosphere and hence would make putative substrates for PhPDR1. Presuming that PhPDR1 is a PM intrinsic exporter, abolishment of its function would inevitably result in a decrease of strigolactone exudation and could account for the observed reduction in newly formed hyphal apices, when secondary hyphae are exposed to root exudates of Phpdr1::dTph1 plants as opposed to W138 plants (Fig 2.13). The fact that the decrease in mycorrhization only averages around 50% can be explained by the presence of other yet unidentified BFs and residual passive strigolactone excretion. In the pea strigolactone biosynthesis mutant rms1 the reduction in hyphal branching by around 30% is even less pronounced (Gomez-Roldan et al., 2008), indicating the presence of other branching stimulants. Striga germination on the other hand, which is completely dependent on strigolactones, is reduced by around 75% when rms1 root exudates are applied. Furthermore the lipophilic qualities of strigolactones make the existence of a substantial diffusible component quite likely, that might account for the presence of strigolactones in root exudates despite impaired transport mechanisms.

However not much is known about the function of strigolactones post invasion and thus it is not clear whether the observed induction of *PhPDR1* expression in mycorrhized cortical tissues (Fig 2.7) can also be linked to strigolactone transport. It is believed that strigolactone production is lowered after colonization as a negative feedback effect of an improved phosphate status. But considering the profound effects strigolactones have on fungal metabolism it is quite likely that the fungus would also benefit from non-exuded strigolactones to boost its intracortical development. The report that overall fungal colonization in pea with a non-functional *CCD8* allele is reduced by more than two thirds (Gomez-Roldan et al., 2008) is concordant with our observations, but it remains to be shown whether it is solely due to an absence of pre-symbiotic signaling or whether inner cortical signaling is also affected. So far strigolactone production has only been monitored indirectly via quantification of exudation. Most focus has been given on differential exudation is response to phosphate availability in the growth medium (Lopez-Raez et al., 2008). However this was exclusively examined in non-mycorrhized plants. Split-root experiments suggest that once a certain level of mycorrhization is reached, novel invasion of yet un-colonized parts of the root system is actively suppressed

(Vierheilig, 2004) and, the authors later argue that this might be due to a decrease in strigolactone exudation (Steinkellner et al., 2007). Supporting this hypothesis is the finding that the strigolactone induced germination of Striga seeds is reduced in the presence of root exudates obtained from mycorrhized plants (Matusova et al., 2005). But one must consider the possibility that strigolactones excreted into cortical apoplastic regions at sites of fungal proliferation are mainly scavenged by the fungus and consequently do not reach the rhizospere in substantial amounts. To our knowledge the kinetics of strigolactone contents throughout mycorrhizal development within the root have not been investigated so far.

Also noteworthy in this concern is the strong induction of *PhPDR1* expression in the root tip area and elongation zone during mycorrhization. *CDD8* expression and hence strigolactone synthesis appears to be highest in root tips of both Arabidopsis and Petunia, but *PhPDR1* expression is only moderately detectable in the tip region under non-mycorrhizing conditions. In mycorrhized roots however, roots tips are commonly found to exhibit high *PhPDR1* promoter activity, even when no attached or invading hyphae are discernible. This raises the question of whether *PhPDR1* expression close to the root tips precedes fungal contact, or whether expression is induced secondarily upon infection. The rapidly extending root elongation zone appears to be a primary site of initial hyphal invasion and it is reasonable to assume that strigolactone exudation is locally increased in this region at times of imminent colonization. But assuming that PhPDR1 indeed transports strigolactones into the rhizospere at these sites, and its expression precedes actual fungal contact, it must be induced by a diffusible fungal signal such as the still elusive MYC factors. Upon perception of the fungal signals the plant would respond by locally increasing strigolactone exudation at preferred entry sites, thus guiding the fungus in the right direction. In addition strigolactone regulated activation of fungal metabolism and proliferation might result in an enhanced presence of MYC factors in the vicinity of the developing interaction, which in turn could boost strigolactone exudation even further. The consequence would be a positive feedback loop in the excretion of the main pre-symbiotic plant and fungal signaling compounds that could cause strong gradients and local peaks of concentration as directional cues for both partners and hence substantially increase the chances of a swift contact, after both symbiotes have perceived the initial

"calls" for each other. Unfortunately a GUS based reporter system to monitor PhPDR1 expression is not very suitable to test this hypothesis, because the analysis is highly invasive and does not allow for the spatial reconstruction of the original configuration of AM fungus and root tip. A PhPDR1 promoter-GFP or promoter-Luciferase constructs transformed into root organ cultures of petunia might enable an in vivo online visualization of these processes on plate. In addition they might give further insight into the exact roles of PhPDR1 for the intraradical development of the fungus.

The apparent sensitivity of *PhPDR1* expression to SA treatment is consistent with the observation that PDRs in general are commonly incorporated into either SA or JA dependent pathways, but is not easily reconciled with the proposed function of PhPDR1 as a strigolactone transporter. One possible explanation would be that SA (or JA) responsiveness is an attribute of ancestral PDRs that has no more functional implications for PhPDR1. On the other hand SA governed pathways are powerful mediators of SAR, several abiotic stress responses and are at least initially and transiently involved in mycorrhization processes. It is generally argued that the early increase in SA concentrations upon mycorrhization is a sign for an AM fungal induced pathogen response and that this leads to the priming of plant defense pathways, which makes mycorrhized plants more resistant to subsequent pathogen attacks (Pozo and Azcon-Aguilar, 2007). Considering however, that strigolactones were just recently acknowledged as bona fide plant hormones and that their characterization in regard to developmental and functional aspects is so far restricted to branch inhibition and symbiotic signaling, it is quite possible that there are novel yet unidentified roles for strigolactones that might be overlapping with SA dependent pathways. Alternatively the role of SA in the development of AM might not yet be fully understood and overlaps partly with strigolactone specific functions. It can probably be ruled out that *PhPDR1* upregulation upon SA treatment is pathogen defense related, particularly since *PhPDR1* is not responsive to general fungal elicitors present in yeast extracts and since abolishment of PhPDR1 function does not render the plant more susceptible to spontaneous non-appropriate pathogen attacks as observed for other PDR knock-out or knock-down plants.

2.3.2 PhPDR1 in Lateral Branching

Three plant hormone families with a dominant effect on above ground architecture are generally acknowledged; auxins, cytokinins and strigolactones (Ongaro and Leyser, 2008). Best understood is the role of auxin, which is produced in the shoot apical meristem (SAM) and moves basipetally down the main axis. The transport is mediated by PIN1 efflux carriers at the basal part of xylem parenchyma cells. It indirectly inhibits the outgrowth of lateral branches in a process known as apical dominance (Leyser, 2005). In contrast cytokinins produced in the root and shoot can move in a polar manner with the transpiration stream in xylem vessels and tracheids and actively promote bud outgrowth.
Strigolactones are produced predominantly in the root and the stem, from where they move (basipetally within the root vasculature and) acropetally within the shoot vasculature in a yet uncharacterized fashion. They are proposed to directly inhibit development of axillary buds into branches. Perception of strigolactones within the meristems leads to MAX2 mediated regulation of gene expression via regulated protein degradation. *CCD8* expression in roots and stems is promoted by auxin treatment, indicating that auxin stimulates strigolactone production and thus might contribute in this way to the inhibition of lateral bud outgrowth (Bainbridge et al., 2005). Interestingly *PhPDR1* expression is also highly promoted by treatment with the synthetic auxin analogue NAA, suggesting that auxins positively influence the transport of PhPDR1 specific substrates.
Strigolactone specific pathways are currently an area of intense scientific focus. Several genes implicated in production and one gene involved in perception have been identified (Leyser, 2009). But to date nothing is known about putative strigolactone transporters, and whether extracellular strigolactone receptors exist. Furthermore the potential signaling cascade between initial strigolactone reception and downstream MAX2 SCF mediated target protein ubiquitination has not been elucidated. However, it cannot be ruled out that strigolactones simply diffuse across the PM and through the cytosol into the nucleus where they could directly interact with the MAX2/F-box protein.
Since strigolactone target sites identified so far are locally confined to axillary primordia (and possibly developing vasculature) and in vivo strigolactone contents are minute

(Umehara et al., 2008), it must be assumed that active transport from the vasculature into the leaf axils concentrates strigolactone sufficiently to allow for a reaction in dose dependent manner typically observed for phytohormone actions. Altenatively simple passive diffusion could allocate strigolactones to target sites where highly specific receptors monitor strigolactone quantities and transduce the signal in a dose dependent manner. In the latter case, the majority of all strigolactones produced would evenly disperse throughout the shoot without apparent function and large differences in production would yield only minute differences in concentration at target sites. Moreover young axillary buds are not vascularly connected to the main stem where strigolactone transport is thought to take place, denying direct access to the bud to the strigolactone stream. Strigolactones have every attribute of a typical plant hormone, including, specific sites of production, very low ambient concentrations, profound effects at highly specific target sites and directed transport between sites of production and sites of perception. Thus we propose that strigolactone translocation is mediated via active import and export mechanisms rather than passive or facilitated diffusion to be the more likely scenario. For example auxin transport is governed by at least three independent transporter families. PINs and PGPs, each containing several members with high affinity for auxin, catalyze auxin efflux in specific tissues and often in a polar fashion (Blakeslee et al., 2007). Members of the AUX/LAX auxin influx carriers mediate the symport of auxin and protons from the apoplast into the cytosol (Kramer, 2004).

Given the current model of the strigolactone pathway, transport would be required at several points:

First of all export might be imperative at sites of strigolactone production. Active transport seems especially important in cells that synthesize strigolactones, since *CCD8* activity seems to be under negative feedback control. Mutated versions of the transcript unable to be translated into the protein product are nevertheless detectable in high abundance, indicating that a low strigolactone concentration can be sensed and reacted to via transcriptional up-regulation of biosynthetic genes (Snowden et al., 2005). Thus export procured simply via diffusion might lead to intracellular build up of product, inhibiting further novel production. In any case a feedback-controlled fine tuning of production almost certainly requires an evenly controlled transport process. Furthermore

transport away from sites of production needs to be achieved (possibly independently) into two directions. On the one hand strigolactone needs to enter the root and stem vasculature if intended to serve as a branching inhibitor, on the other hand root originated strigolactone needs to be exuded into the rhizosphere and putatively into AM fungus colonized cortex regions to fulfill its role as symbiotic regulator.

Second, active transport might be of equal importance for long distant transfer through the vasculature, depending whether strigolactones are passively conveyed via transpiration-mediated conduction in xylem vessels and tracheids or whether they are actively transported via xylem or phloem parenchyma. In the latter case active polar transport mechanisms (possibly analogous to the well investigated auxin transport) would be indispensable to ensure the strict acropetal flow of strigolactones in the shoot. Besides a polar distributed export protein, vasculatory parenchyma transport would also require a strigolactone import mechanism.

Third, strigolactones must be translocated from the vasculature through several cell layers into tissues which are dependent on strigolactone perception for their development. Most prominent in this case are dormant buds of lateral branches in the leaf axils of the primary shoot. There a certain strigolactone concentration seems necessary to keep the buds in a dormant state. At the base of the meristems, specific transport would serve to provide the meristematic tissues with sufficient amounts of strigolactones and possibly prevent reflux into the vasculature.

PhPDR1 expression, as investigated via a *PhPDR1* promoter-GUS fusion construct in the W115 background, can be reconciled with most of the locations where strigolactone transport is postulated to be obligatory. *PhPDR1* promoter activity is found in single putative cortical cells throughout the root system, in root tips and within the root vasculature. Furthermore it is present in the shoot vasculature and is unequivocally strongest in the leaf axils below the undeveloped buds of lateral branches. Consequently *PhPDR1* promoter activity is highly congruent with sites of strigolactone production, translocation and perception. In detail, shoot specific *PhPDR1* promoter activity in scions developed beyond the seedling stage is highly confined to the vasculature with an evident concentration in areas directly below dormant axillary buds (Fig 2.5A and B). This expression pattern coincides in part with the patterns observed for *MAX2* expression,

which is also most abundant in the shoot vasculature. But instead of being highly active below the axillary branch meristems, *MAX2* promoter activity is concentrated within the meristems themselves. This matches the proposed function of MAX2 as an intranuclear strigolactone signal transducer at sites of strigolactone perception as opposed to the putative function of PhPDR1 as a strigolactone transporter at specific sites of strigolactone translocation. Strigolactone is expected to be primarily produced within the root system and subsequently translocated via vascular transport mechanisms to susceptible plant organs. *MAX3/CCD7* and *MAX4/CCD8*, which are both encoding enzymes essential for strigolactone biosynthesis, are consequently mainly expressed in root and stem tissues. However, particularly in Petunia, *DAD1/CCD8* is also very active in hypocotyls, as interstock experiments with WT hypocotyls grafted between dad1 internodes demonstrate. Whereas the dad1 scion above the interstock reverted to WT conditions, nodes below the interstock still exhibited a mutant branching pattern. These findings furthermore underline that strigolactone strictly moves acropetally. Consistent with a high *DAD1* expression in hypocotyls, *PhPDR1* is also highly expressed in the hypocotyls of seedlings and the vasculature of hypocotyls of older plantlets. In contrast dad1 expression is highest in the root tip, intermediate in root mid sections and almost absent at the root base, while *PhPDR1* expression displays a reverse gradient with highest expression at the base and only moderate presence in the tip region. Interestingly *PhPDR1* expression is strongly induced in the root tip upon mycorrhization.

Since dad1 and Phpdr1::dTph1 both originate from Petunia, albeit from different varieties, a direct comparison of branching behavior is possible. Dad1 (in the V26 background) commonly produces lateral branches from each node, including both cotyledonary nodes, leading to an extremely bushy phenotype and reduced overall height. In contrast Phpdr1::dTph1 (in the W138 background) does not branch from the cotyledonary axils and rarely produces outgrowths that can be considered full branches from the first two true leaf axils. In fact Phpdr1::dTph1 branching capacity only marginally extends over the defined area in which W138 individuals produce branches, and which is to a significant degree congruent with the branching window, named Zone2, described for V26. Still for every given node within the Zone2 equivalent of W138 varieties, the capacity of Phpdr1::dTph1 plants to produce a branch is higher, resulting in an overall

doubling of fully developed branches in two-months old-individuals. The effect is most pronounced at lower nodes and least pronounced at higher nodes within the window. The most obvious argument to explain the discrepancies between the dad1 branching phenotype and the Phpdr1::dTph1 branching phenotype is the fact that Phpdr1::dTph1 is merely impaired in strigolactone transport and probably possesses production rates comparable to the wild type. Since strigolactones are reasonably hydrophobic substances, they are expected to be able to diffuse across membranes to a certain degree, causing decreased but not fully abolished (as is the case for dad1) strigolactone contents throughout the plant. Moreover with impeded transport a precipitous concentration gradient can be assumed in Phpdr1::dTph1 lines. And since strigolactones have been demonstrated to exclusively move acropetally, concentrations should be highest at the base of the shoot and decline towards the tip. This might explain why Phpdr1::dTph1 individuals still have control over branch inhibition in the cotyledonary and first true nodes. However this does not explain why there is no apparent difference above Zone 2, where the difference in strigolactone concentration between Phpdr1::dTph1 lines and W138 lines ought to be the most drastic. A possible argument is that auxinic control of apical dominance, though partly intertwined with strigolactone controlled branch inhibition, “moves” basipetally down the shoot from the SAM and thus might be more influential at nodes higher up on the main plant axis. In this concern it must also be noted that petunia branching behavior changes drastically with the appearance of the first terminal flower. Branch production becomes highly likely in an area starting from one node below the first flower, and the underlying mechanisms have not been subjected to closer investigations. Another scenario that might account for the obvious dissimilarities between dad1 and Phpdr1::dTph1 is the possible presence of redundant strigolactone transport mechanisms. ABC transporters in general have been demonstrated to often possess an exceptionally broad substrate specificity that can overlap among closely related homologues. However, the existence of a redundant close PhPDR1 homologue is rather improbable, considering that *PhPDR1* was cloned via a degenerate primer approach targeting the entirety of PDR transcripts present in mycorrhized roots. Still it is possible that for example WBC homologues display strigolactone affinities.

The postulate that PhPDR1 transports strigolactone suggests that the conclusions derived for rcn1 (Yasuno et al., 2008), a branching mutant in rice with an abolished WBC function, should be reconsidered. WBCs are ancestral to PDRs and an overlap in substrate affinity is quite possible. Rcn-1 mutants are inhibited in tiller outgrowth, suggesting that RCN-1 is positively involved in the control of lateral branching in rice. Since double mutants with an additional mutation in D3, an F-box protein, orthologous to MAX2 and presumably implicated in strigolactone perception, display a d3-specific increased branching phenotype it is argued that RCN1 is independent from the strigolactone pathway. *RCN-1* is mainly expressed directly in crown root and tiller meristems, tissues where strigolactones are proposed to be either produced or exert their function. If, in analogy to PhPDR1, RCN-1 did indeed transport strigolactones, either across the PM into the apoplast or across the tonoplast into the vacuole, then abolishment of function would cause a build-up of strigolactone in the respective cells that would elegantly explain the decreased branching phenotype observed in rcn-1. Then, even though both ABCG homologues exported strigolactone from the cytosol, their tissue specific expression, *PhPDR1* in the vasculature and below axillary buds and *RCN-1* in axillary buds, would lead to the observed opposite phenotypes in the respective lack of function mutants.

2.3.3 ^{3}H-GR24 Uptake

To shed further light on the notion that PhPDR1 might contribute to the translocation of strigolactones we monitored the accumulation of exogenously applied tritium labeled GR24 (a synthetic strigolactone analogue) in the nodal tissues of W138 plants and Phpdr1::dTph1 plants. Because *PhPDR1* is most strongly expressed in conductive tissues around the cotyledonary nodes and the nodes of the first true leaves, we focused on the time dependent accumulation of ^{3}H-GR24 in the respective tissues of developing plants (Fig 2.15Aand B). Independent of incubation time and genotype, a steep gradient of GR24 distribution prevailed between ascending nodes, indicating that GR24 allocation and accumulation is not restricted to transpiration dependent conduction within the xylem and subsequent diffusion in the surrounding tissues. This is supported by the fact that

concentrations of GR24 in nodal tissues can exceed the concentration of GR24 within the incubation medium. Moreover this gradient inversely reflects the branching probability of both wild type and mutant which increases at axils further up the primary stem, indicating a differential transport in a node specific manner. Around the first four nodes including the cotyledonary node, Phpdr1::dTph1 plants accrued significantly larger amounts of GR24 than the wild type (Fig 2.15B). In congruence with *PhPDR1* promoter activity, which decreases with increasing node number, the relative difference in GR24 content between the respective genotypes diminished at higher nodes. The finding that the discrepancies between wild type and Phpdr1 mutant recede with increasing time might indicate a saturation of the system.

Taken together these data not only suggest that PhPDR1 contributes to the export of GR24 from certain cell types in the vicinity of the axillary meristems, but furthermore insinuate that a strigolactone import mechanism, responsible for the observed nodal GR24 accumulation must exist. Strigolactone has been demonstrated to move exclusively acropetally within the shoot, allowing for the speculation that its long distance transport is achieved via xylem specific conduction. Xylem directed long distance transport could also account for the rapid distribution of GR24 throughout the plant, but it must be kept in mind that due to the experimental set up the roots of the assayed plants were cut back to a uniform length. The observed rapid circulation of ^{3}H-GR24 might thus not reflect the in vivo transport mechanism responsible for endogenously produced strigolactone allocations. Xylem vessels and tracheids however are dead cells incapable of actively importing or exporting substrates and given concentrations of solutes are entirely dictated by the properties of convective flow. Transport of solutes from and into the xylem is achieved via living xylem parenchyma cells that surround xylem vessels and tracheids. Particularly in nodal regions and close to axillary buds, specialized xylem transfer cells that feature extensive cell wall invaginations to amplify the PM surface are present to facilitate the exchange of solutes. Hypothesizing the presence of a yet unidentified strigolactone importer with a similar spatial expression pattern as *PhPDR1* in the nodal regions, xylem-mobile strigolactones would be imported into the xylem parenchyma and then exported again via PhPDR1 in a polar fashion that directs transport towards the leaf axil meristems. Subsequent contiguous polar import and export would result in a

concentration of xylem-derived strigolactones in the meristematic tissues, which are devoid of *PhPDR1* expression (but ought to be expressing the hypothesized importer) in order to avoid reflux or sequestration into the meristematic apoplast. In plants lacking PhPDR1 function, xylem concentrations of strigolactones are already expected to be low due to impeded export from strigolactone producing cells. However accrual in xylem associated tissues is still possible owing to the presence of the postulated importer. Still the strigolactones extracted from the xylem sap are not able to be directed towards the axillary buds because of impairments in directed PhPDR1 dependent export. Strigolactones rather accumulate in the xylem associated nodal tissues, as observed for the exogenous application of ^{3}H-GR24 to Phpdr1::dTph1 plants.

In order to support this hypothesis, detailed localization studies either utilizing highly specific antibodies for immuno-histological approaches, or native promoter full length PhPDR1 GFP fusion constructs for stable transformation are crucial. Both approaches are currently being pursued. Furthermore it is important to verify the acquired transport data with strigolactone efflux studies on protoplasts overexpressing *PhPDR1*. If PhPDR1 does indeed transport strigolactones from the cytosol across the PM then cells overexpressing *PhPDR1* should not be able to retain pre-loaded ^{3}H-GR24 as well as non-transformed cells.

2.3.4 PhPDR1 and Wilting

Phpdr1::dTph1 mutant lines are prone to desiccation especially during late development. The wilting phenotype sometimes affects independent branches, but more commonly the whole plant will show clear signs of turgor loss despite saturated water conditions. Loss of turgor can only be reverted by cutting off affected scions and placing them into water (Fig 2.18). We postulate that this phenotype is not pathogen related but rather due to impairments of water acquisition owing to deviant root or vasculature structures. Small Phpdr1::dTph1 plantlets transferred from soil into a nutrient solution and exposed to high temperature and strong light are more prone to apical and foliar wilting than the wild type (Fig 2. 19), suggesting that the convective restrictions already apply to the mutants early in development. Since the rootlets were cropped in this experimental set up and the

addition of EDTA aided to prevent callose formation, ensuring direct water uptake through exposed vascular strands, the observed phenotype is more likely due to aberrant vascularization than defects in root system expansion.

Interestingly a branching mutant from pea, rms2, also displays a wilting phenotype, particular under conditions of increased evaporative demand (Dodd et al., 2008). Analysis of mutant plants revealed that they have a drastically decreased hydraulic conductivity owing to a decrease of xylem vessel diameter despite an overall increase in xylem vessel number. However the authors conclude that the vascularization phenotype is strictly shoot controlled, because reciprocal grafting experiments with WT plants did not alter the phenotype. Still RMS2 is expected to be implicated in the RMS pathway, which can now be considered to be identical with the strigolactone pathway. These findings are congruent with our observations for PhPDR1 whose above ground lack of function is not expected to be rescued by a wild type rootstock. Since none of the biosynthesis mutants display a comparable phenotype it is possible that the aberrant xylem development observed in rms-2 is also related to transport and that the responsible gene might even be orthologous to PhPDR1.

Taking the overaccumulation of exogenously applied ^{3}H-GR24 in the nodal tissues of Phpdr1::dTph1 plants into account, we speculate that strigolactone exerts a negative effect on xylem differentiation in respect to tracheary element size and conductive properties. High concentrations in procambial strands and expanding xylem cells would then favor the development of smaller but more numerous vessels as observed in the rms2 mutant background, whereas low concentrations improve conductivity by promoting the development of fewer but larger vessels. This would also explain why the majority of branching mutants do not seem to suffer from a lack of transpiration despite significantly increased demands due to the presence of numerous foliated branches. From a developmental point of view a double function of strigolactones in branching control and conductive tissue differentiation appears plausible, because both processes are interdependent and need to be brought in accordance in order to avoid xylem over- or under-representation in the expanding plant. It is well documented that auxin exerts control over procambial maintenance and influences xylem differentiation in a concentration dependent manner (Uggla et al., 1996; Bhalerao and Bennett, 2003). PIN

mediated basipetal auxin transport through procambial strands is necessary for procambial maintenance (Carlsbecker and Helariutta, 2005) and mutants deficient in auxin signaling display clear deficits in early vascular development (Sieburth and Deyholos, 2006). Given the significant overlap of auxin and strigolactone dependent signaling in branch development, it is intriguing to speculate that strigolactones contribute in a similar manner to vascular specification and differentiation. Auxin and strigolactone flows are antidromic in the shoot with auxin, produced in the SAM, flow strictly basipetal in procambial strands and xylem parenchyma and strigolactones, mainly produced in the roots, moving strictly acropetal in the shoot in a yet unidentified fashion. It can be expected that both signals thus create discrete gradients and pockets of particularly high or low concentrations along and across the shoot vasculature that are then integrated to regulate vascular specification and differentiation. Distinct overlapping gradients of several plant analogues of animal morphogens are proposed to play an important role in general pattern formation (Bhalerao and Bennett, 2003) and strigolactones might emerge as a novel morphogenic component. We assume that in this respect strigolactones are of particular importance in the development of novel vascular strands in emerging lateral buds.

Supporting a putative role of strigolactones in vasculature development are the findings that MAX2, implicated in strigolactone perception is very active in developing vasculature. *PhPDR1* expression is also strong in the vasculature, particularly in the hypocotyls and cotyledons of plants in the early seedling stage when vasculature differentiation is important. If vasculature differentiation indeed proved to be strigolactone reliant, but is only discernable in Phpdr1::dTph1 and rms2 mutants, then the phenotype would be due to an over-accumulation and not a lack of strigolactones in certain cells, making strigolactones negative regulators of both lateral branch outgrowth and vascular development.

Certainly more detailed analysis of this phenomenon is necessary to elucidate its background. We are currently trying to compare and quantify the amount and structure of conductive tissues in transversal thin sections of W138 and Phpdr1::dTph1 lines, to verify whether, in analogy to rms2, Phpdr1::dTph1 also exhibits an overall increase in xylem vessel number at the expense of single vessel diameter, negatively affecting total

conductivity. Additionally, presuming that lack of PhPDR1 function might lead to a local accumulation of strigolactones in the vasculature, we are trying to mimic impairments in strigolactone export via the exogenous application of GR24 in the W115 background, which is expected to lead to an over-accumulation in the vasculature. First trials with exogenous application of GR24 to W115 seedlings seem to support our hypothesis, since it results in an impeded growth and foliar wilting, reminiscent of impaired water allocation (data not shown). Together these two experimental approaches might help to evaluate the validity of the strigolactone transport hypothesis and relate Phpdr1 dependent wilting phenotypes to rms2 related impairments in branching control and xylem differentiation.

2.3.5 Putative PhPDR1 Orthologues in Arabidopsis and Rice

PhPDR1 appears to play a pivotal role, not only in the development of arbuscular mycorrhiza, but also in the inhibition of lateral branching, suggesting strigolactones as putative substrates. Mutants for strigolactone biosynthesis and perception are known and well described both in Arabidopsis and rice. Thus at least the branch controlling strigolactone pathway seems to be conserved between monocotyledons and dicotyledons, and it is therefore surprising to find that no apparent PhPDR1 orthologues can be easily detected from phylogenetic analysis, expression profiles or in depth studies of homologues in either Arabidopsis or rice. The closest homologues in terms of sequence similarity in Arabidopsis are AtPDR10 and AtPDR12. Not much data exists for AtPDR10. Formerly annotated as a pseudogene, it was nevertheless detected by RT-PCR approaches in roots and siliques (van den Brule and Smart, 2002), but expression levels are very low, particularly in roots, and it is completely absent from stem tissues. Consequently it is a very unlikely candidate for a true PhPDR1 orthologue, but should nevertheless be included in reverse screening approaches. AtPDR12 on the other hand has been intensely studied with respect to pathogen resistance (Campbell et al., 2003) and heavy metal tolerance (Lee et al., 2005). Expression patterns and the observed phenotype in AtPDR12 mutant lines are not congruent with our data obtained for PhPDR1 and hence rule out AtPDR12 as the Arabidopsis PhPDR1 orthologue. Possibly a functional

equivalent to PhPDR1 can be found in other clusters of the AtPDR clade, particularly since so far analysis of PDRs does not support an overlap of primary structure and function. Also, since Arabidopsis is a non mycotrophic plant, it might completely lack a PDR with high affinity for strigolactones and depends on different mechanisms for transmembrane transport.

Rice however is mycotrophic and at least in regard to structural homology and expression profile a putative orthologue might exist. Rice contains 12 PDR homologues that fall within Cluster1, but only *OsPDR9* and *OsPDR20* are predominantly expressed in roots (no expression data is available for OsPDR10*, OsPDR11, OsPDR19* and *OsPDR21*) and exhibit a profound responsiveness to SA and auxin treatment (Moons, 2008). Of these two, OsPDR20 can be regarded as the more likely candidate, since the highly variant region close to the Walker A domain on NBD2 of OsPDR20 shows closest homology of any OsPDR to the respective region of PhPDR1 (data not shown). However *OsPDR20* expression is also promoted in the presence of weak organic acids and redox perturbations, leading the author to conclude that it might be implicated in carboxylate exudation into the rhizosphere (Moons, 2008).

In Lotus, which is both mycotrophic and susceptible to rhizobia infection, at least seven Cluster1 members have been identified, that are predominantly expressed in the roots and are upregulated upon nodulation (Sugiyama et al., 2006). Even though this might just reflect a general elicitor responsiveness of the respective genes, the authors nevertheless propose a symbiosis specific role for lotus Cluster1 homologues. It is currently not known whether strigolactone specific symbiotic effects extend beyond mycorrhization. In comparison to mycorrhiza, the root-rhizobia symbiosis evolved rather recently and many aspects of mycorrhiza specific signaling were recruited and slightly modified to suit and assist nodule formation (Kistner and Parniske, 2002). The common SYM pathway is shared for both mutual interactions and it cannot be ruled out that either specific signaling compounds such as strigolactones or symbiosis specific transport mechanisms such as the one we propose for PhPDR1 are likewise shared. Data mining of existing nodule specific Lotus or Medicago ESTs might allow for the recognition of putative PhPDR1 homologues in legumes.

Given the important role we propose for PhPDR1 in symbiotic signaling as well as lateral branch inhibition, it might seem surprising to the point of being suspicious that in extensive and elaborate forward genetic screens for mutants either impaired in the development of mutualistic relationships or with aberrant branching patterns, no transporter was ever identified to be involved. However it must be kept in mind that that phenotypes owing to deficiencies in transport of given endogenous substances are commonly not as pronounced as phenotypes associated with their biosynthesis or, in case of signaling compounds, perception at target sites. The less polar the substance the more membrane diffusible it becomes, creating literally leaky transport phenotypes. Additionally in a number of branching mutants in pea and rice the responsible genetic alterations have not been mapped. Mutants like rms2 in particular, that display a high overall phenotypic similarity including facets that are absent in other branching mutants, might eventually support our strigolactone transport hypothesis.

2.3.6 PhPDR1 Conclusion

In a very simplified model, strigolactones control the development of above ground plant architecture in accordance with the plants` nutrient status, while at the same time adjusting the plants nutrient status via recruitment of beneficial symbionts. In the case of nutrient deficiencies, strigolactone production and excretion is enhanced, leading to a strong inhibition of secondary shoot development within the plant body and to the attraction of AM fungi within the rhizosphere. In times of saturated nutrient availability strigolactone production is lowered, allowing the plant to invest in new lateral outgrowths, while at the same time the symbiosis with AM fungi is less supported. Since the development of novel branches and associated leaves increases transpiration related demands on the conductivity of the vascular tissues, we postulate that strigolactones, concomitant with controlling lateral branching, influence the development of the vascular tissue through which it is transported. High strigolactone concentrations are postulated to lead to the development of more but relatively smaller xylem tracheids and vessels, whereas low strigolactone concentrations induce the development of fewer but larger

vessels with enhanced conductivity to ensure sufficient water allocation to the expanding plant body.

Mycorrhization is expected to lead to a decrease in strigolactone production or release, and the positive growth effect commonly observed for mycorrhized plants is in part due to an improved nutrient acquisition and in part due to a decrease in above ground strigolactone content that leads to increased lateral branching. In contrast we observe a strong upregulation of *PhPDR1* upon mycorrhization, suggesting that strigolactones are not the sole substrates of PhPDR1 at least in and around arbusculated root sections, or that alternatively cortex confined strigolactones play a yet unrecognized role in late mycorrhizal development.

In a scenario, which aims to integrate most of the above data with what is already known about the MAX pathway, we postulate that strigolactones are produced in specialized cells within the root and possibly the stem. From there they are actively exported either into the apoplastic regions of the root cortex and rhizodermis to carry out their function as symbiosis related signaling compounds, or into the apoplastic regions of the vasculature, from where they are actively taken up by parenchyma cells. In accordance with the prevailing theory, they then move in a polar fashion towards the shoot, either directly via convective flow within xylem vessels and tracheids or via directed polar transport within the xylem or parenchyma. Local accumulation of strigolactones in the nodal regions is achieved via import of strigolactones from the xylem via xylem parenchyma or xylem transfer cells, which then export strigolactones, again in a polar manner, to direct strigolactone flow towards the axillary meristems. There they accumulate due to the absence of export mechanisms (that would cause reflux into the vasculature) and, depending on the overall concentration, inhibit the outgrowth of axillary buds via the activation of MAX2 mediated ubiquitination of target transcription factors. At least in petunia primary stems, the antidromic gradients and directions of transport for auxins and strigolactones might elegantly explain the presence of a central branching window covering several nodes (Zone2), which is flanked on both sides by zones of inhibited branching. Zone1, below Zone2, dominantly guarded over by high nodal strigolactone concentrations and Zone3, above Zone2, mainly under the influence of SAM derived auxins.

Impairment of strigolactone export as observed in the Phpdr1 background results in a decrease of mycorrhization owing to a decreased exudation of the symbiosis promoting compound into the rhizospere and the root cortex. Above ground it causes an under-representation of strigolactones in the axillary meristems, negatively affecting the inhibition of lateral bud outgrowth. In addition we speculate that reduced export also leads to an accumulation of strigolactones in xylem associated cells and possibly cambial tissues that shifts the development of tracheary elements towards smaller and more numerous vessels, limiting the capacities for transpirational flow. This has the effect that, despite increased water demand owing to numerous branches, the vasculature remains under-developed, causing the plant to wilt when fully expanded or under high evaporative demands.

Stigolactones are currently emerging as bona fide phytohormones and symbiotic signaling compounds, with multiple roles in plant development and plant-environment interactions. The full extent of strigolactone function, particularly in concurrence with auxin-dependent pathways is now just beginning to be understood. The discovery of PhPDR1 as a putative strigolactone exporter constitutes a crucial component in the comprehension of strigolactone-dependent signaling in a space and time related manner.

2.4 Materials and Methods

2.4.1 Plant Growth Conditions

All Petunia lines were grown under long day conditions with 16h of continuous light and 60% relative humidity at 25°C. Plants were either grown in soil (ED 73 Einheitserde) or in clay granules (Oil Dry US Special from Damolin) supplemented once a week with 1x Hoagland solution. Depending on the experiment pot size ranged from 294ml to 1500ml. For mycorrhization trials 2 week old seedlings, germinated and grown on clay granules, were transplanted onto a mycorrhization mix of 4 parts soil 4 parts clay granules 1 part sand and 1 part mycorrhizal inoculum. Inoculum was prepared from previously *Glomus intraradices* inoculated substrate (kind gift of Didier Reinhardt, University of Fribourg) by growing *Plantago lanceolatum* for at least 3 months in 5l pots containing mycorrhization mix and subsequently letting the plants dry out in the pots. Crude homogenate of roots and substrates served as inoculum and was stored for up to 1 year at room temperature. *Gigaspora margarita* inoculum was prepared as described above with commercial *Gigaspora margarita* inoculum (obtained from AGRAUXINE, France) as the initial culture. On plate plants were grown on growth medium containing 2.2g/l MS (M0222.0050 Duchefa, The Netherlands) and 15g/l sucrose, supplemented either with 9g/l PHYTO AGAR (Duchefa, The Netherlands) or 4.5g/l Phytagel (Sigma, Switzerland) under long day conditions with 16h of continuous light. Prior to plating seeds were surface sterilized for 3min in 70% ethanol and rinsed four times with sterile distilled water.

All transgene lines were selected for T-DNA insertion either on plates containing 10mg/l Glufosinate Ammonium or in soil by spraying newly germinated seedlings 3 times with a BASTA (BASF, Germany) solution containing 320µM Glufosinate Ammonium over a period of 1 week. Non-transformed wild type lines served as controls for positive selection.

2.4.2 *PhPDR1* Cloning Strategy

Partial sequences of putative PDR transcripts were amplified from total cDNA obtained from the roots of W115 individuals 4 weeks after inoculation with the AM fungus *Glomus intraradices*. NBD1 amplicons of around 0.5kb were obtained with the following degenerate primers: 5`-MGWATGACTCTDYTKYTKGGACCTCC targeting PDR signature1 and 5`-GYTTCYTYTGNCCHCCHGAAATWCC targeting the ABC signature. NBD2 amplicons of around 0.5kb were obtained with the following degenerate primers: 5`-GGGWGTYAGTGGWGCWGGWAARAC targeting the Walker A box and 5`-CTCATNACAATDGCWGCWGCTCTWGC targeting PDR signature3. Fragments for the respective NBDs were aligned and the following consensus primers were designed to amplify putative PDR coding regions spanning NBD1 and NBD2: 5`-tattgggacttgaaatttgtgccgatac and 5`-gctccactaacacccatcagagctgtc.
Amplification of upstream and downstream sequences of *PhPDR1* full length transcript was achieved via 5`RACE and 3`RACE PCRs using the SMART-RACE cDNA Amplification Kit (Clontech, Takara Bio Company, USA) according to the manufacturer's specifications. 5`RACE primer and 5`nested RACE primer had the following sequence: 5'-ctcgagtacattttctggggaccttgg and 5'-ccatttcgtctccaacaatggtatcgg. 3`RACE primer and nested 3`RACE primer sequences were: 5'-gtcctcaagagtaggaagcatcactgcg and 5'-accgaggaccggcttgaactcttgagag.

2.4.3 *PhPDR1* promoter-GUS construct and GUS staining assay

Amplification of a 1.8kb promoter fragment upstream of the *PhPDR1* gene was accomplished via use of the Genome Walker Universal Kit (Clontech, Takara Bio Company, USA) with the primer 5`-agttggaagtttctcaagtgcagccca and the nested primer 5`-ccctaaagagttcttcaccaccctccat. The fragment was T/A cloned into pGEM-T-Easy vector system (Promega, USA) and subsequently reamplified with the primer 5'-catgaagcttgcacccagaagaagattaggc containing a HindIII restriction site (underlined) and the primer 5'-tcgatctagacacattaagaggaaagtaggtac containing an XbaI restriction site

(underlined). The respective restriction sites were used to clone the *PhPDR1* promoter fragment into the GUS gene containing pGPTV-Bar (Becker et al., 1992) vector system.
For GUS staining trials tissues to be investigated were immerged in an appropriate amount of GUS-staining buffer (100mM Sodium phosphate buffer pH=7.00, 10mM NaEDTA, 1.5mM Potassium hexacyanoferrate(II) trihydrate, 0.25mM Potassium hexacyanoferrate(III), 0.1% (v/v) Triton X-100 and 1mM 5-Bromo-4-chloro-3-indolyl β-D-glucuronide cyclohexylammonium salt) vacuum infiltrated three times for 30s and incubated in the dark at 37°C for 12-48h. After staining samples were cleared and stored in 70% ethanol.

2.4.4 *PhPDR1* RNA interference constructs

Silencing of *PhPDR1* specific transcripts was attempted via the generation of double stranded hairpin RNA fragments utilizing the pKANIBAL vector system (Wesley et al., 2001). Two constructs were designed, one targeting a highly variable region within the NBD2 of *PhPDR1* (C-construct) and one targeting parts of the 3`end and the 3`UTR of *PhPDR1* (R-construct). The 131bp C-fragment was amplified from *PhPDR1* cDNA with 5'-cgatggatcctcgagggaacgcaagcaaaaggg, containing BamHI and XhoI restriction sites (underlined) and 5'-cgatatcgatggtaccctcttgctcaaatcagccgcagtga containing ClaI and KpnI sites (underlined). The 411bp R-fragment was amplified from *PhPDR1* cDNA with 5`cgatggatcctcgagacattatatggactaattgcc, containing BamHI and XhoI restriction sites (underlined) and 5`cgatatcgatggtaccaaaagatactcataacttctcc containing ClaI and KpnI sites (underlined).The resulting amplicons were cloned in sense and antisense direction in the two MCS of pKANIBAL flanking the hairpin intron sequence. Next the pKANIBAL RNAi cassette containing 35S promoter RNAi construct and OCE3 terminator was excised from the vector backbone using the NotI restriction sites and transferred into the binary pGreenII0229 vector system (Hellens et al., 2000), conferring Glufosinate Ammonium resistance as a selection marker in plants.
After stable transformation of W115 plants (see 2.2.5) the degree of down-regulation was estimated via semi-quantitative RT-PCR using the *PhPDR1* specific primers 5`-aaatgctactacagtgcag and 5`-ctgcactgtagtagcattt. Petunia tubulin transcript, partially

amplified with 5`-cattggtcaagccggttattc and 5`-acccttgaagaccagtacagt served as a housekeeping and loading control.

2.4.5 Stable Petunia Transformation

PhPDR1 promoter-GUS constructs and Phpdr1 RNAi constructs were transferred into the W115 background via *Agrobacterium tumefaciens* mediated transformation of leaf explants, callus induction and plant regeneration (Lutke, 2006). 0.45% Phytagel was used instead of 0.9% agar in all media and the concentrations of BAP and NAA in the Selection Medium was adjusted between 1-2mg/l for the former and 0.05-1.5mg/l for the latter to maximize shoot induction for each individual transformation.
Regenerated plantlets were tested for successful construct insertion via PCR on genomic DNA. The primers 5'-acggtccacatgccggtatatacgatg and 5'-gatggcatttgtaggagccaccttcc, targeting the 35S promoter, were used to confirm RNAi construct insertion. The primers 5'-gaattgatcagcgttggtgggaaagc and 5'-ggtaatgcgaggtacggtaggagttg, targeting the GUS gene, were used to confirm GUS construct insertion.

2.4.6 Reverse Screening Approach to Identify Transposon Insertions in *PhPDR1*

The highly mobile, non-autonomous, 284bp transposon dTph1 exists in a number of around 200 copies per individual in petunias of the variety W138. Transposon insertion in the coding region of a gene of interest frequently results in the complete loss of function of the respective gene. An elaborate PCR based screening approach has been developed that allows for the simultaneous screening of several thousand W138 individuals for a transposon insertion in the desired gene (Koes et al., 1995; Vandenbussche and Gerats, 2004). In short, a W138 population is arranged in a cube like fashion and genomic DNA of each individual is extracted and subsequently pooled in slices according to the three dimensions of the cube (Fig10B). Each pool of genomic DNA is then screened via PCR with a radiolabled gene specific primer and a transposon primer, specific for the inverted repeat bordering both sides of the transposon. Since the inverted repeat primer matches both ends of the transposon facing outward, it can be considered bi-directional and hence

the orientation of the transposon, when inserted, does not matter (and the primer simultaneously functions as forward and reverse primer). Separated on an acrylamide gel, single concomitant bands of identical size in one slice of each dimension then indicate a transposon insertion in the gene of interest and the slice number of each dimension gives the exact coordinates for the respective W138 individual within the cube. Two three dimensionally arranged genomic DNA libraries (a kind gift from Tom Gerats, Radboud University Nijmegen), one representing 16x16x16 (4096) W138 individuals and the other representing 10x10x10 (1000) W138 individuals were screened for dTph1 insertions in *PhPDR1* via PCR based method (Vandenbussche and Gerats, 2004). A multitude of radiolabled *PhPDR1* specific primers covering the whole cDNA sequence and separated by less than 500bp, with annealing temperatures above 65°C were used in combination with the un-labled dTph1 inverted repeat specific primer 5`-gaattcgctccgcccctg to scan the entire genomic region of *PhPDR1* in contiguous steps covering less than 1kb each for transposon insertions. The screening primer 5'-ccatttcgtctccaacaatggtatcgg yielded a positive result on the 10x10x10 library. Homozygosity PCRs were performed with the following transposon flanking primers: 5'-tgccaatccttcatgatgtcagtgg and 5'-ccttctctctcctagacagctctgc.

2.4.7 Mycorrhization Trials

Mycorrhized plants were quantified for their level of colonization via the gridline intersect method (Giovannetti and Mosse). Only clearly intraradical structures such coiled cortical hyphae, arbuscles and vesicles were scored as positively mycorrhized. Extraradical hyphae, apressoria and early invading hyphae were not considered. A minimum of 200 intersecting root fragments per sample were investigated microscopically for the presence or absence of intraradical AM fungal structures. For quantification mycorrhized roots were cleaned from growth substrate, cut into 1cm fragments and randomized. A subsample was then cleared in 10% boiling KOH, stained for mycorrhizal structures in 5% boiling black ink (Brilliant Black, Pelikan 4001, Germany) and 5% acetic acid and destained in 5% acetic acid in accordance to a detailed staining protocol (Vierheilig et al., 1998a).

2.4.8 Hyphal Branching Assays

Pre-selected spores of *Gigaspora margarita* were purchased from AGRAUXINE (France), surface sterilized for 3 min in a medium containing 0.2% NaClO and 0.05% Triton X-100, rinsed 5 times with sterile distilled water and stored in a medium containing 100mg/l gentamycin and 200mg/l streptomycin. Prior to use, aliquots were rinsed again 3 times with sterile distilled water to wash off the antibiotics. Single spores were placed on plates containing 2mM $MgSO_4$ solidified with 0.3% Phytagel (Sigma, Switzerland). Plates were incubated vertically in the dark in a Heraus B 5060 CO_2 incubator (Switzerland), set to 32°C and 2% CO_2 for 6-8 days. Branching assays were performed on primary hyphae that had grown in a negative geotropic manner and started producing secondary hyphae, extending laterally from the primary hyphae. In the tip region of the primary hyphae 2 holes, one on the left and one on the right, were produced 5mm from the hyphae in Phytagel plate via suction with a 1ml pipette tip and 5ul of a root exudate concentrate in 10% acetone were applied. For production of the root exudates concentrate, petunia W138 lines and Phpdr1::dTph1 lines were grown in clay granules supplemented with 1xHoagland Solution once a week until they had produced a root mass of 1-2g. Clay granules were then carefully removed from the root system and the plant placed for 24h under constant aeration in 300ml of a hydroponic solution containing 2mM $CaCl_2$ and 2mM KSO_4. The hydroponic solution was then run through a Sep-Pak Classic C18 Cartridge (Waters, Ireland) to adsorb hydrophobic root exudates. Afterwards exudates were eluted from the column with 2ml of acetone and the eluate was dried over nitrogen. Dried exudates were dissolved in 100ul of 50% acetone per g root FW, which was then diluted 1/5 to a final concentration of 10% acetone. 2x5ul of the final root exudate concentrate, an equivalent of 2x10mg root FW exudates, were used in each branching assay.

2.4.9 Axillary Branching Trials

For a comparative analysis of lateral branch production in wild type and Phpdr1 mutant backgrounds, W138, W115, Phpdr1::dTph1 and Phpdr1 RNAi lines were grown for 50

days in 550ml (W138 and Phpdr1::dTph1) or 1500ml (W115 and Phpdr1 RNAi) pots and watered daily with a fertilizing solution containing 0.4% (v/v) Wuxal (Maag Agro, Germany). Before abscission of leaves nodes were marked with a permanent marker for later evaluation. Branches were scored in accordance to a previous branch definition developed for branching studies with the V26 variety of *Petunia hybrida* (Snowden and Napoli, 2003). In short, outgrowths were considered a branch, if they were at least 2cm in length, had at least 3 clearly distinguishable internodes and at least 8 macroscopic leaves.

2.4.10 ^{3}H-GR24 Uptake Assay

Racemic GR24 was produced by Chiralix (The Netherlands) and radiolabeling of GR24 with ^{3}H was performed by ARC (American Radiolabeled Chemicals, USA). For uptake assays W138 and Phpdr1::dTph1 plants were germinated and grown on clay granules under limited space conditions to promote internode elongation. Plantlets between 60mg and 120mg in fresh weight were cleaned from substrate and the root system was cut down to 2cm total length. Only groups of plants that did not differ significantly in their mean of FW were used for comparative studies. Cropped plantlets were incubated in 250ul of incubation medium containing 2mM $CaCl_2$, 2mM KSO_4 and 2mM NaEDTA (to inhibit callus formation and ensure ^{3}H-GR24 uptake via xylem vessels) supplemented with 0.125µCi of ^{3}H-GR24 (equivalent of 0.93ng GR24) for one to three hours at room temperature and 200µmol/m^2*s illumination. After incubation cotyledonary nodes and nodes of the firs true leaves were cut out weighted and partially dissolved in 50µl of 24% (w/v) TCA for several hours. The resulting probes were homogenized in 3ml of Ultima Gold LSC cocktail (Perkin Elmer, USA) and DPMs were quantified in a Tri Carb 2900 Liquid Scintillation Analyzer (Packard, USA). ^{3}H-GR24 uptake was normalized against FW nodal tissue.

2.4.10 Desiccation Trials

W138 and Phpdr1::dTph1 plants were germinated and grown on clay granules and plantlets between 60mg and 120mg in fresh weight were cleaned from substrate and the

root system was cut down to 3cm total length. Only groups of plants that did not differ significantly in their mean of FW were used for comparative studies. Cropped plantlets were incubated in 250ul of incubation medium containing 2mM $CaCl_2$, 2mM KSO_4 and 2mM NaEDTA (to inhibit callus formation and ensure direct uptake of incubation medium via xylem vessels) at 31°C and 220µmol/m^2*s illumination. Plant roots were dried from incubation medium and whole plants were weighted once an hour over a period of 6hours. After 30min of initial adjustment time, FW was determined and used as a reference for all subsequent measurements. FW loss was assumed to represent transpirational water loss.

2.4.11 RNA isolation and cDNA Synthesis

RNA was isolated with the RNeasy Plant Mini Kit (Qiagen, Germany) in accordance to the user manual. Reverse Transcription of RNA to yield cDNA was performed with the M-MLV Reverse Transcriptase (Promega, USA) and a polyT primer (Promega, USA).

2.4.12 Software Based Analysis

Membrane protein topology predictions were calculated using ConPredII (http://bioinfo.si.hirosaki-u.ac.jp/~ConPred2/) based algorithms. Transmembrane topology was visualized with Topo2 (Johns S.J., TOPO2, Transmembrane protein display software ; http://www.sacs.ucsf.edu/TOPO2/) with amino acids classified as follows: hydrophilic (W,S,T,C,Q,G,H,Y,N); hydrophobic (M,L,V,I,P,A,F); positively charged (R,K); negatively charged (D,E).

Calculation of phylogenetic relationships of different Cluster1 PDR homologues was performed using different algorithms accessible at www.phylogeny.fr. Visualization was achieved with the Mega4 software, downloaded from www.megasoftware.net.

General sequence analysis was performed using Vector NTI (Invitrogen, USA). Sequence alignments were created with Multalin (http://bioinfo.genotoul.fr/multalin/).

3 PhPDR2,
Contributing to Trichome-Related Herbivory Defense

Glandular trichomes constitute important components in herbivory defense strategies, in particular among solanaceous species. Insect deterring secondary metabolites predominantly of terpenoid or fatty acid origin are specifically produced in trichome cells and subsequently either excreted into apoplastic regions or accumulated in substantial amounts in subcuticular cavities above the glandular head cell(s). Little is known about how apoplastic or subcuticular cavity loading is accomplished and by what mechanisms reflux of the mostly lipophilic compounds across the plasma membrane (PM) back into the cytosol is prevented.

Here we report on PhPDR2, a Pleiotropic Drug Resistance (PDR) type ABC transporter from Petunia, which, in foliar tissues, is exclusively expressed in glandular trichomes and along the leaf margin. Belowground *PhPDR2* promoter activity concentrates at sites of lateral root emergence. *PhPDR2* is under the control of jasmonic acid dependent pathways that are also known to modulate secondary metabolite production and herbivory defense. Post-transcriptional silencing of *PhPDR2* renders Petunia more susceptible to feeding related damage by the generalist caterpillar larvae of *Spodoptera littoralis*. Plant PDR type ABC transporters are plasma membrane intrinsic primary active pumps. Several PDR homologues have been demonstrated to excrete antimicrobial compounds of terpenoid origin, thus contributing to basal pathogen resistance, but so far they have not been implicated in herbivory defense. We propose that PhPDR2 plays a comparable role in basal herbivory resistance by catalyzing the export of deterring compounds from trichome cells and at sites of emerging lateral roots

.

3.1 Introduction

For plants, being primary producers on this planet and the only organisms able to directly harvest the suns energy to convert carbon-dioxide into high energy sugars, almost all animal life, from microscopic nematodes to large mammals, either directly or indirectly depends on herbivory for survival. Consequently plants have evolved multiple ways to ward off herbivores and ensure survival into the next generation. Ranging from large thorns to fend off big mammals to minute traces of volatile signaling compounds released into the air to attract natural enemies of the insect that is currently feeding on it, plant defense strategies can generally be categorized as either being of a mechanical or chemical nature.

A specialized plant organ that adapted to serve both functions is the trichome. Trichomes of various size, shape and abundance are commonly found on the foliar surfaces and stem surfaces of most land plants. They are uni- to multicellular epidermal outgrowths responsible for several characteristics commonly associated with certain types of plant. For example they confer the distinct smell of many herbs and spices such as mint, basil and thyme, they cause the sting of the stinging nettle, account for the stickiness of the leaves of many nightshade species and the fuzziness of plants like the edelweiss. They are responsible for the psychoactivity of *Cannabis indica* and *Salvia divinorum* as well as the anti-malarial properties of *Artemisia annua*. Trichomes can protect plants from desiccation, UV exposure, cold and herbivory. They can make surfaces water repellent or act as a sponge that retains water. They play an important role in seed dispersal of many species and in fact many of the clothes we wear are made from highly modified trichomes intended to facilitate wind dispersal, namely cotton fibers.

The structure, size and shape of trichomes range from minute bumpy epidermal protrusions through complexly branched unicellular extensions to multicellular appendages, consisting of a base a stalk and a head. However, they are usually just classified in being either of a glandular or non-glandular type. The study of non-glandular trichomes, with Arabidopsis being its foremost model organism, mainly focuses on developmental aspects such as morphogenesis, epidermal patterning and differentiation (Larkin et al., 2003; Schellmann and Hulskamp, 2005; Guimil and Dunand, 2006; Ishida

et al., 2008). On the other hand the study of glandular trichomes, with members of the Laminaceae (foremost basil) and Solanaceae (foremost tobacco and tomato) being the most prominent objects of investigation, is mainly centered around the diverse and highly complex biosynthetic pathways of secondary metabolites. Both research areas exploit the fact that trichomes are easily accessible for morphological, biochemical and molecular investigations.

Glandular trichomes are known to produce and secrete a plethora of secondary metabolites (many of them trichome specific) that vary in their function from attracting pollinators, through deterring herbivores to attracting enemies of herbivores. The substances can be volatile or non-volatile, nourishing or toxic, oily or sticky and include members of many of the main secondary compound classes such as phenylpropanoids, terpenes, and fatty acid derivates. Surprisingly one of the most variant and highly distributed compound classes, alkaloids, is underrepresented in trichomes. It is argued that this is due to the limited supply of nitrogen (in form of amino acids) to the trichomes. Trichomes are not connected to the vasculature and thus have no direct access to soil derived macro- and micro-nutrients. They are primarily supplied by neighboring cells in the form of sucrose that serves both as an energy source and raw material for secondary metabolite synthesis. Being highly specialized on secondary metabolite production, many trichomes are partly or even completely devoid of the photosynthetic machinery.

The production of phenylpropanoids, which include chavicol, eugenol and derivatives that contribute to the typical basil aroma have been intensively studied is in the trichomes of sweet basil varieties (Gang et al., 2001; Gang et al., 2002). Petunia petals have been demonstrated to produce related compounds that play a role in pollinator attraction (Verdonk et al., 2005; Koeduka et al., 2006), but there the biosynthesis is trichome independent.

One of the most commonly found and probably best studied compound classes produced in trichomes are terpenes and isoprenoid derivatives. Several enzymes involved in terpenoid biosynthesis have been identified and analyzed in the peltate trichomes (a type of glandular trichome) of different cultivars of sweet basil (Iijima et al., 2004b; Iijima et al., 2004a), which synthesize a large number monoterpenes and sesquiterpenes. In tobacco cembratrieneols and cembratrienediols are two diterpene classes that are

produced and stored abundantly in glandular trichomes (Wang and Wagner, 2003). Parts of their biosynthetic pathways have been unraveled and they seem to play a substantial role in herbivory defense (Wang et al., 2001). Several sesquiterpene lactones found in substantial concentrations in the glandular trichomes of *Tithonia diversifolia* appear to play a pivotal role in the plants defense strategies against folivor caterpillars, and the cost intensive production is tightly correlated with the annual rhythm of caterpillar appearance (Ambrosio et al., 2008).

Microarray and mutant studies in Arabidopsis revealed that JA is a key component in the defense against leaf-feeders, particularly generalist caterpillars like *Spodoptera littoralis* larvae (Bodenhausen and Reymond, 2007). Interestingly monoterpene biosynthesis in tomato trichomes is substantially stimulated by JA application (van Schie et al., 2007), linking JA-dependent herbivory defense directly to terpene biosynthesis in trichomes. Several other studies also show that JA application alters the production of terpenes and other secondary metabolites in solanaceous species (Hare and Walling, 2006; Hare, 2007). Moreover not only the content of solanaceous glandular trichomes, but also their foliar abundance is directly regulated via JA (Boughton et al., 2005), signifying the importance of trichomes in regard to herbivory avoidance.

Direct evidence for the implication of glandular trichomes in herbivory defense comes from extensive studies on the solanaceaeous species *Datura wrightii,* which is dimorphic in terms of trichome morphology, with one variety producing only non-glandular trichomes and a second variety producing glandular trichomes (Van Dam and Hare, 1998). Individuals with glandular trichomes have a sticky leaf surface and are more resistant to folivory by the caterpillar larvae of *Manducta sexta*. It could be shown that the glandular trichomes exude acyl sugars coupled to fatty acid moieties, which are responsible for decreased feeding damage and consumption rate by the larvae. In a later study it was demonstrated that these compounds confer resistance to several native herbivores in the field as well as under laboratory conditions (Hare, 2005), stressing their importance under aspects of chemical ecology. Acyl sugars containing branched chain fatty acids are commonly found in the glandular trichome exudates of many solanaceous species including petunia (Slocombe et al., 2008) and are generally regarded as important components in chemical defense mechanisms against herbivores.

Since many of the compounds produced by glandular trichomes are potentially cytotoxic for the plant as well, they are commonly sequestered into a subcuticular cavity directly above the glandular head cell(s) and thus removed from the cytosol. Loading of the subcuticular cavity causes the head to swell up to proportions that can exceed the actual head cell(s) in size and thus glandular trichomes can be regarded as secondary metabolite factories with vast storage facilities in the attic. Having substantial amounts of toxic compounds stored in a balloon like fashion at the tip of the trichome has the added advantage that it creates an effective first line of defense. Insects intending to feed will cause the first trichome heads to burst and release their cargo, even before they have had a chance to start feeding. If on the other hand toxic or deterring compounds are incorporated directly into the foliar tissue as in the case of silicone in many grasses, or of nicotine in tobacco, they will not be effective until the animal is already feeding on it and the concentration of the substances is limited due to their cytotoxicity. But even stored in subcuticular cavities, potentially toxic compounds are not completely removed from the cell. The only barrier separating the cavity from the head cell cytosol is the PM, which is more or less permeable for lipophilic substances such as terpenes and fatty acid derivatives. Therefore it must be assumed that due to steep concentration gradients a continuous reflux from the cavity into the cytosol is taking place.

Not much is known about the transport mechanisms involved in gland loading and to our knowledge the question of how to deal with metabolite reflux has not yet been addressed. Direct primary active transport is cost intensive in terms of ATP expenditure, but might be one way in which loading is achieved. Particularly to counteract reflux, ATP dependent pumps like ABC transporters seem highly suitable, for they are not directly dependent on electrochemical gradients. When deployed in high number directly into the PM below the cavity they could efficiently scavenge molecules at the very instant that they managed to diffuse back across the membrane. Several characteristics, such as affinities for terpenoids, responsiveness to JA, PM localization and general implications in biotic stress responses (see General Introduction for details) make PDR-type ABC transporters interesting candidates in this respect. Here we report on PhPDR2, a PDR type ABC transporter, which, initially identified as a mycorrhiza responsive protein in the

roots of Petunia, is highly abundant in foliar glandular trichomes and might contribute to chemical herbivory defense.

3.2 Results

3.2.1 Cloning and Structural Characterization of *PhPDR2*

PhPDR2 full length cDNA was cloned via a degenerate primer approach from total cDNA extracted from mycorrhized roots of Petunia hybrida line W115 (Fig 3.1). In short, degenerate primers targeting highly conserved PDR specific regions were designed and short cDNA fragments amplified from NBD1 and NBD2 of putative PDRs. The resulting fragments for each NBD were aligned and family specific primers were designed on the consensus sequence, which allowed amplification of large 2kb fragments between NBD1 and NBD2. 5`RACE and 3`RACE PCRs were performed on fragments of interest in order to obtain full length coding regions and un-translated regions (UTRs) (Fig 3.1).

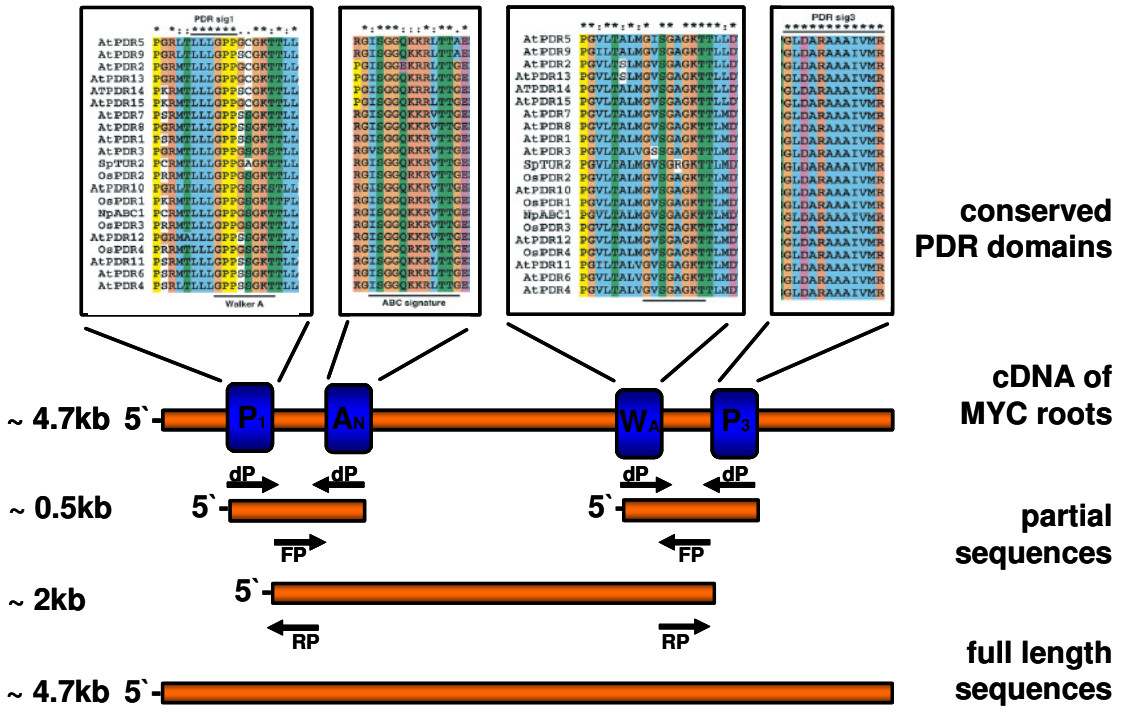

Figure 3.1: Cloning strategy to obtain full length PDR sequences from the cDNA of mycorrhized roots. Degenerate primers (dP) were designed to anneal to highly conserved PDR and/or ABC specific regions to amplify ~0.5kb fragments from NBD1 and NBD2. On NBD1 PDR signature1 (P1) and the ABC signature (AN) were targeted and on NBD2 Walker A (WA) box and PDR signature3 (P3) were targeted. Alignment of the respective regions from several PDR homologues displays level of conservation and is adapted from van den Brule et al. 2002. The resulting fragments were aligned and family specific primers (FP) designed on the consensus sequence. These resulted in amplicons of ~2kb on which RACE primers (RP) were designed to amplify 5`and 3`ends.

The 4680bp cDNA of *PhPDR2* (Appendix 6.4) comprises an open reading frame (ORF) of 4290bp, a 5`UTR of 136bp and a 3`UTR of 253bp followed by the poly A tail. The predicted polypeptide of 1429 amino acid residues (Appendix 6.5) features a reverse domain organization of NBD1-TMD1-NBD2-TMD2, which is exclusively found in PDR type ABC transporters and typical ABC specific motifs such as Walker A box, Walker B box and ABC signatures on both NBDs are conserved.

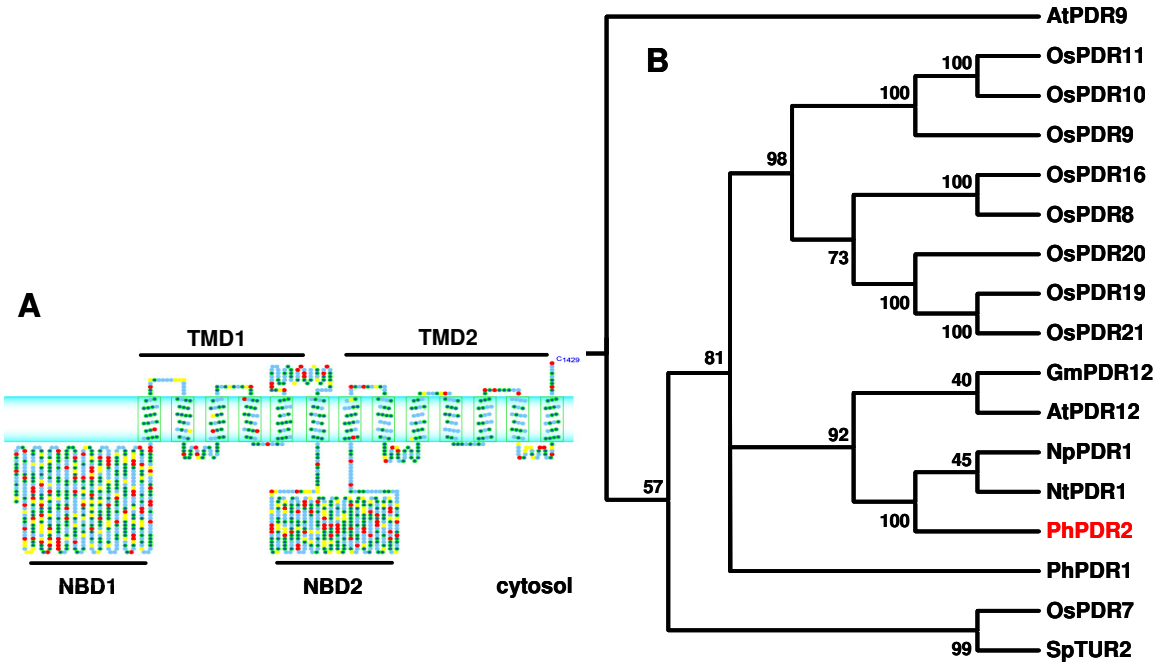

Figure 3.2: Predicted protein topology and phylogenetic analysis of PhPDR2.
(A) Putative transmembrane topology of PhPDR2. PhPDR2 features a PDR specific reverse orientation with an initial nucleotide binding domain (NBD1) followed by 6 membrane spanning alpha helices, which constitute the first transmembrane domain (TMD1). TMD1 is followed by NBD2 and TMD2, the latter consisting of 7 membrane spanning alpha helices. TMDs contain mainly hydrophobic (green circles) and hydrophilic (blue circles) residues, whereas the NBDs additionally contain many positively charged (red circles) and negatively charged (yellow circles) residues.
(B) Position of PhPDR2 within PDR Cluster1 homologues of rice (OsPDRs), Arabidopsis (AtPDRs), tobacco (NtPDR), soy (GmPDR), Petunia (PhPDR), *Nicotiana plumbaginifolia* (NpPDR) and *Spirodela polyrrhiza* (SpTUR). Numbers next to bifurcations represent bootstrap values. Bootstrap supports below 40 were not integrated. Cluster2 homologue AtPDR9 serves as an outgroup.

Furthermore all four PDR signatures of PhPDR2 are in perfect consensus with the ones found in other PDRs. TMD1 contains six predicted membrane spanning alpha helices and TMD2 contains seven, bringing the total number to an amount of 13 (Fig 3.2A). This is

quite unusual, for PDR type transporters are commonly predicted to have two TMDs with six alpha helical structures each. Phylogenetic analysis places PhPDR2 within Cluster1 of the PDR sub-clusters (Fig 3.2B) and in close proximity to NtPDR1 and NpPDR1, which are both are proposed to be associated with pathogen response (Sasabe et al., 2002; Stukkens et al., 2005).

3.2.2 Expression Profile of *PhPDR2*

In an initial RT-PCR based expression profile, *PhPDR2* transcript was detected ubiquitously in roots, flowers, leaves and stems (Fig 3.3A). Expression was highest in leaves and upregulated in roots upon mycorrhization (Fig 3.3A). Investigation of *PhPDR2* expression in response to various hormonal and stress related treatments revealed that transcript accumulated markedly in the roots and shoots of seedlings treated with JA (Fig 3.3B). In addition a moderate increase in transcript abundance was detectable in roots after treatment with yeast extract, serving as a general fungal elicitor (Fig 3.3B). Both JA and elicitor responsiveness are in congruence with patterns observed for its close relatives *NtPDR1* and *NpPDR1*.

In order to obtain a more detailed picture of *PhPDR2* expression with respect to tissue specificity, a 1.2 kb genomic fragment upstream of the *PhPDR2* coding sequence (Appendix 6.6) was fused with the GUS promoter gene and stably transformed in the petunia W115 background. Two constructs were created, one starting within the 3`UTR and one containing the first codons downstream of the start ATG. Several lines of both constructs yielded identical staining patterns and were stable into the T3 generation (data not shown). Surprisingly despite high transcript abundance within leaves as investigated via RT-PCR, *PhPDR2* promoter activity was exclusively found in leaf glandular trichomes and around the leaf margins (Fig 3.4B and Fig 3.4C). Expression was also confined to trichomes in stem tissues (data not shown). In developing flowers promoter activity was restricted to the stigma tips and the expanding petals (Fig 3.4A). Below ground the pattern of promoter activity was more diffuse, with patches of high activity throughout epidermal and cortical layers next to areas devoid of any detectable activity

(data not shown). However in any case activity was always reported to be highest in and around developing and emerging lateral root primordia (Fig 3.4D and Fig 3.4E).

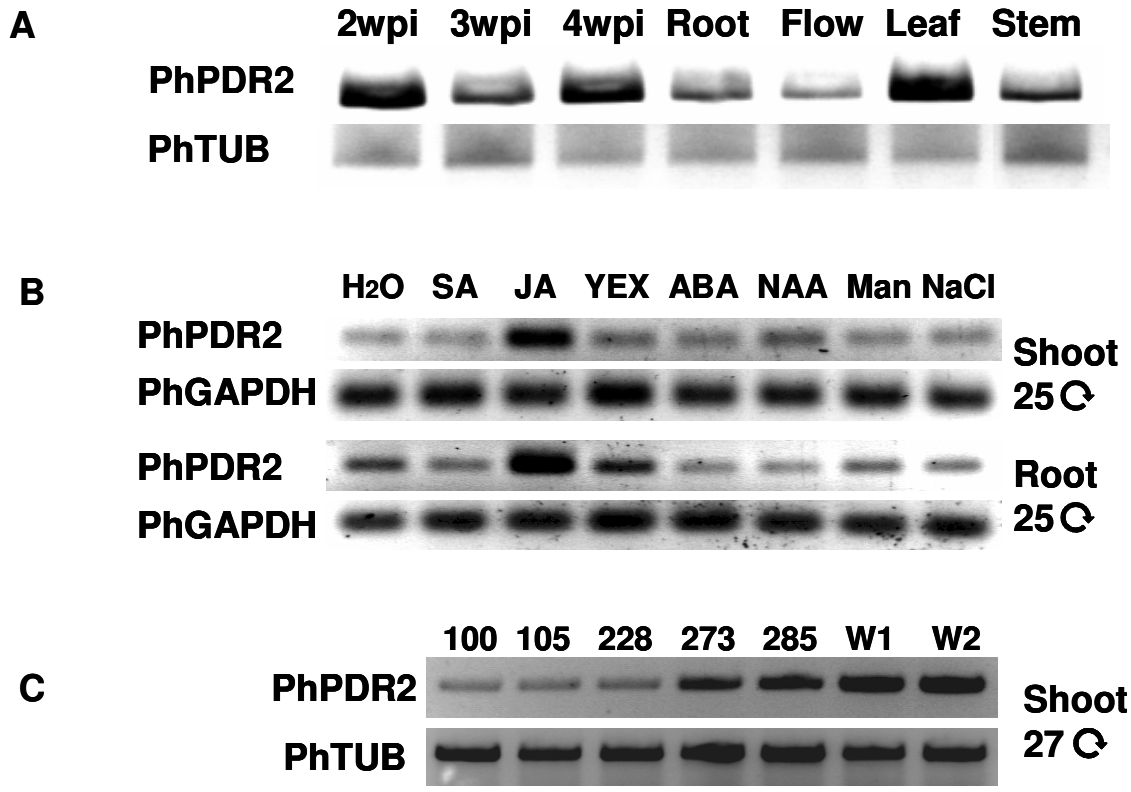

Figure 3.3: Semiquantitative *PhPDR2* transcript analysis via RT-PCR.
(A) Relative *PhPDR2* transcript abundance in mycorrhized roots 2-4 weeks post inoculation (2wpi-4wpi), non-mycorrhized roots (Root), whole flowers (Flow), fully expanded leaf tissue (Leaf) and primary stem tissue (Stem) of fully developed W115 plants. Petunia tubulin (PhTUB) transcript served as a housekeeping control. Cycle number is displayed on the right hand side.
(B) Relative treatment dependent transcript abundance in whole roots and whole shoots of 2 week old W115 seedlings grown on plate after 24h treatment with final concentrations of water (H_2O), 100uM salicylic acid (SA), 5ul/plate methyl-jasmonate (JA), 10 g/l yeast extract (YEX), 10uM abscisic acid (ABA), 25uM alpha-naphthaeneacetic acid (NAA), 250mM Manitol (Man) and 125mM sodium chloride (NaCl). Petunia glycerin-aldehyde-3-phosphate dehydrogenase (PhGAPDH) transcript served as a housekeeping control. Cycle number is displayed on the right hand side.
(C) Semiquantitative analysis of residual *PhPDR2* expression in several independent W115 lines transformed with the Phpdr2-R silencing construct (100-285). Two independent non-transformed W115 individuals (W1 and W2) were used as negative control. Petunia tubulin (PhTUB) served as a housekeeping control.

Taken together these data suggest that *PhPDR2* expression is most dominant in tissues actively secreting volatile and non-volatile secondary metabolites. Petunia petals are known to produce and excrete scent-conferring benzene derivates (Verdonk et al., 2005).

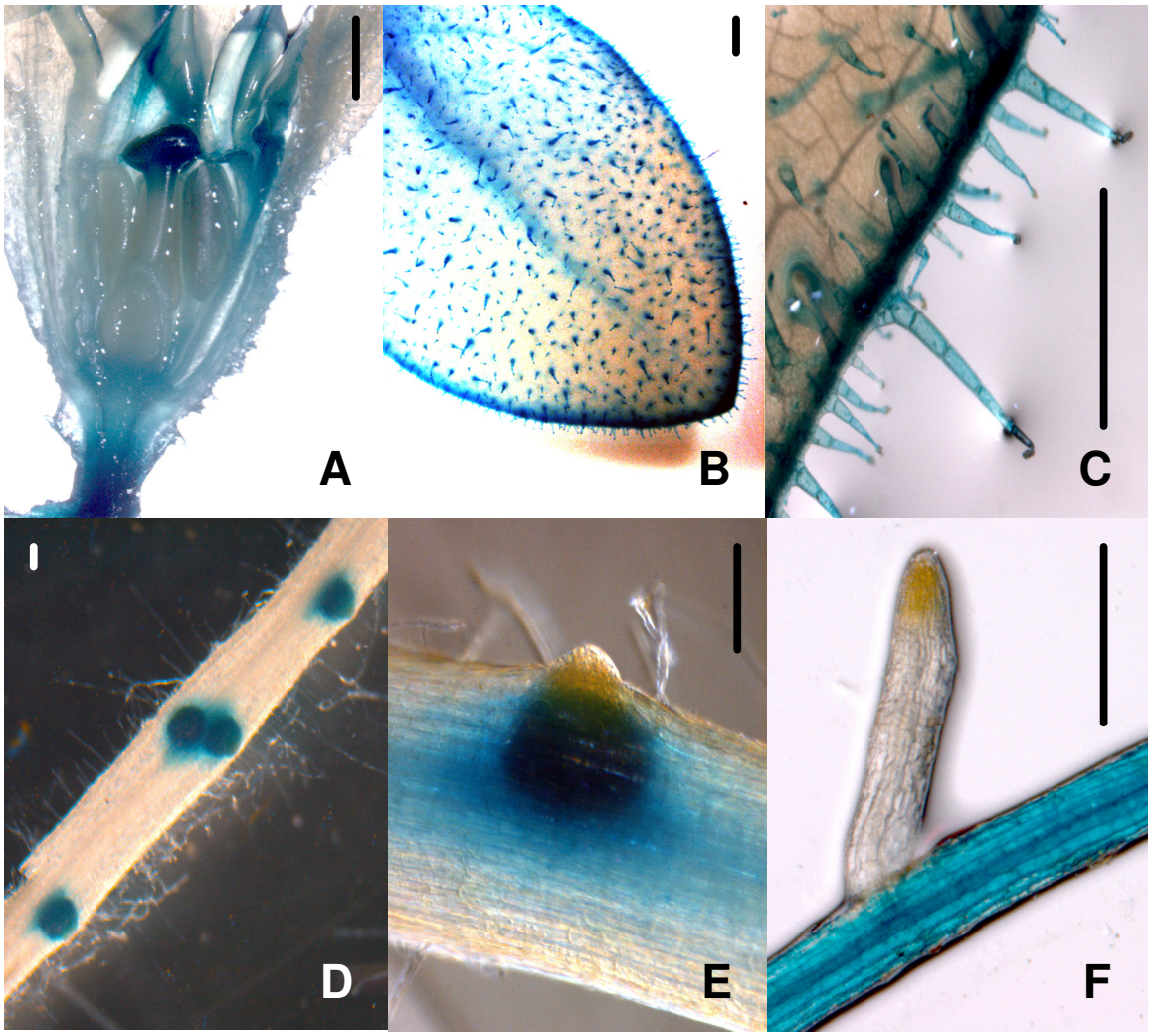

Figure 3.4: Tissue specific *PhPDR2* expression analysis in developing plants via *PhPDR2* promoter-GUS fusion constructs in the W115 background.
(A) Unextended flowers display a signal in the stigma tip and the petals. Scale bar = 1mm
(B) In expanding leaves *PhPDR2* promoter activity is confined to the leaf margins and the glandular trichomes. Scale bar = 1mm
(C) A close-up of the margin of a fully developed leaf shows that the signal is present in all cells of the stalk and the tip of the glandular trichome, as well as along the leaf edge. Scale bar = 1mm
(D and E) Belowground Expression is detectable predominantly in developing and emerging lateral root primordia. Scale bars = 0.1mm
(F) Fully emerged lateral roots are commonly devoid of any signal. Scale bar = 1mm

Stigma tips commonly excrete sticky metabolites presumably, to facilitate pollen attachment. Glandular trichomes are commonly described as being tiny factories of diverse secondary metabolites that are either stored within the cell, directly secreted into the apoplast or accumulated in substantial amounts in the subcuticular space between the apical cavity and the sub-glandular PM. Developing lateral roots must penetrate the root

cortex and rhizodermis from which they emerge, creating a local wound that might attract pathogens and herbivores. Thus the respective areas are known to contain increased contents of protective secondary compounds.

3.2.3 RNAi Mediated Silencing of *PhPDR2* and Screening for Transposon Insertions in *PhPDR2*

With the goal of investigating and revealing putative functions of PhPDR2, two approaches to obtain *PhPDR2* knock-down or knock-out plants were pursued. First silencing of *PhPDR2* expression was attempted via RNA-interference-mediated mechanisms and second large populations of dTph1 harboring W138 individuals were screened for transposon insertions within coding regions of the *PhPDR2* gene.

Silencing of *PhPDR2* transcription was achieved via the transformation of W115 individuals with a pKANIBAL-based vector system containing a 407bp cDNA fragment that includes the 3`end and the 3`UTR of *PhPDR2* in sense and antisense orientation. Several independent lines displaying high to moderate *PhPDR2* transcript silencing were recovered and two lines, Phpdr2-100 and Phpdr2-105, chosen for further analysis (Fig 3.3C).

Screening of two independent W138 populations, one consisting of 4086 individuals and the other of 1000 individuals, resulted in several putative hits. One in particular displayed a near perfect alignment with *PhPDR2* cDNA (Fig 3.5A). However the presence of eight nucleotide mismatches as well as three nucleotide deletions in the screen-derived genomic area corresponding to a *PhPDR2* cDNA fragment of 587bp, lead to the conclusion that the transposon insertion was not within the *PhPDR2* gene, but rather within a close homologue of *PhPDR2*. 5`RACE PCR with primers previously used to amplify the 5`region and 5`UTR of *PhPDR2* resulted in an amplicon of a novel PDR homologue, which was named PhPDR3 (Appendix 6.7). Alignment of the predicted AA sequence of the PhPDR3 fragment to the respective sequence of PhPDR2 revealed that over a stretch of 334 amino acid residues the consensus only contained six mismatches, which corresponds to an identity of 98.2% over the investigated area (Fig 3.5B). So far we have not been able to obtain the full length coding region of *PhPDR3*, allowing no

conclusion as to whether this high grade of identity is representative for the whole sequence.

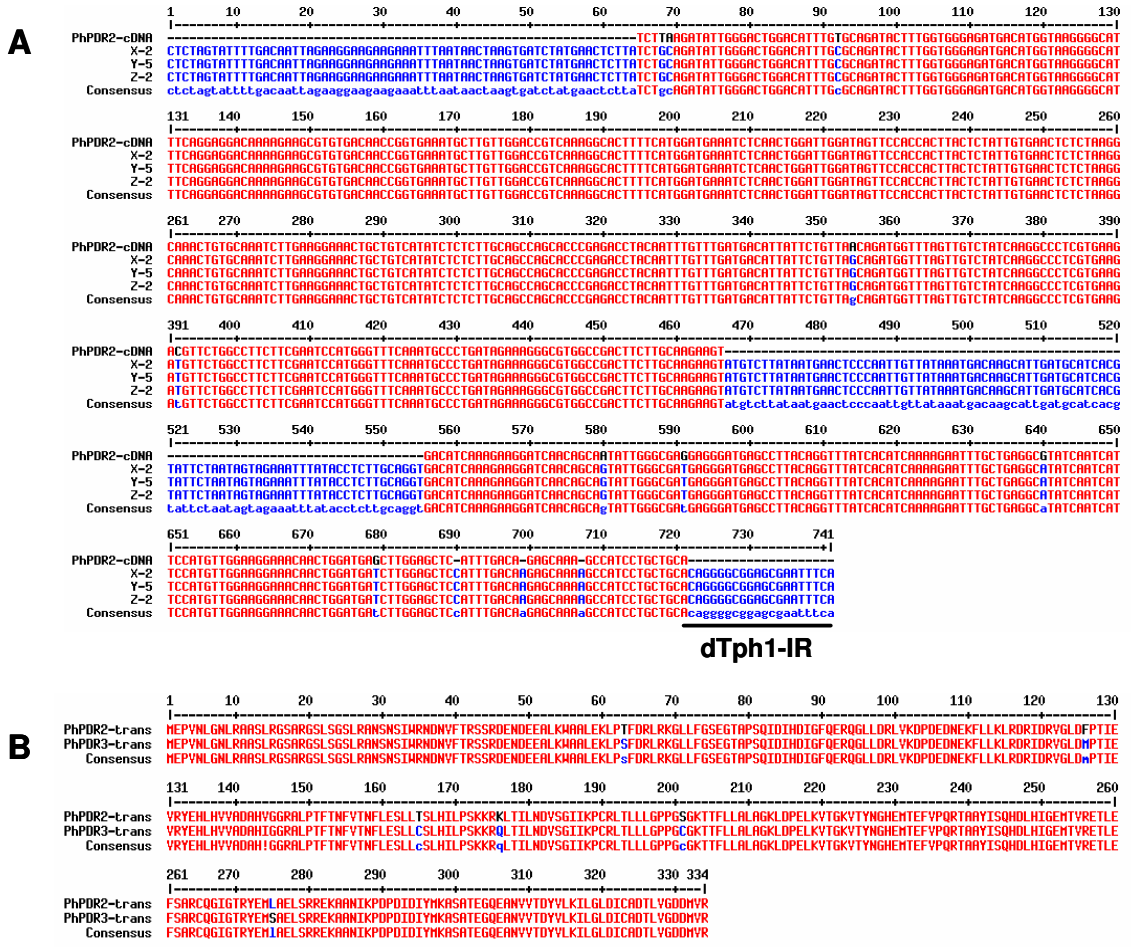

Figure 3.5: Screening for transposon insertions in *PhPDR2* and discovery of *PhPDR3*.
(A) 3D-gDNA library screening result for dTph1 transposable element insertions in the *PhPDR2* gene. A W115 *PhPDR2* cDNA fragment is aligned against 3 W138 genomic fragments obtained via re-amplification from unique congruent bands from the X, Y and Z dimension of the original screening gel. Red sections indicate coding sequence consensus, whereas blue sections indicate intron consensus of the genomic fragments. Single blue and black base pairs depict mismatches between *PhPDR2* cDNA and the genomic fragments, insinuating that the genomic fragments are part of a novel *PhPDR* gene closely related to *PhPDR2*. DTph1 inverted repeat is underlined.
(B) Amino acid alignment of the N-terminal region of PhPDR2 and the N-terminal region of PhPDR3, which was discovered in the above screen. Red sections indicate perfect consensus whereas single blue and black amino acids indicate mismatches. PhPDR2 and PhPDR3 display a 98% identity over the observed region.

Surprisingly, even the 5`UTRs of both genes, which are usually not subject to selective restraints and thus prone to diversifying mutations, bear high resemblance between

PhPDR2 and *PhPDR3*. Genome-walking approaches on the upstream genomic regions of *PhPDR3* lead to the isolation of a 1.5kb promoter fragment (Appendix 6.8), which does not bear any resemblance to the *PhPDR2* promoter, suggesting that despite structural resemblance, tissue specific expression between *PhPDR2* and *PhPDR3* might vary. The discovery of such a close PhPDR2 homologue calls for a critical re-evaluation of RT-PCR based findings of *PhPDR2* transcript abundance in respect to tissue specificity and treatment responsiveness. With high likelihood, primers previously designed to exclusively amplify *PhPDR2* cDNA will have also annealed to *PhPDR3* sequences.

3.2.4 *PhPDR3* Promoter-GUS Analysis

Tissue specific investigation of *PhPDR3* promoter activity via stable transformation of W115 plants with a promoter-GUS fusion-construct revealed that *PhPDR3* was confined to belowground organs and the hypocotyls. No promoter activity could be detected in either stem or foliar tissues (Fig 3.6A). Throughout the root system *PhPDR3* was ubiquitously expressed in varying degrees (Fig 3.6A). Prominent peaks of promoter activity could be detected in root hairs (Fig 3.6D), emerging lateral roots (Fig 3.6C) and root tips (Fig 3.6E). When plants were grown under conditions promoting hypcotyl elongation, areas displaying strong locally restricted signals became apparent along the hypocotyls that correlate with adventitious root primordia (Fig 3.6B). Emerging adventitious roots also exhibited strong *PhPDR3* promoter activity (data not shown). In comparison to *PhPDR2* promoter activity, there seemed to be no apparent overlap at these specific sites, despite structural similarities between both proteins. *PhPDR2* expression was absent in root hairs and root tips. In emerging lateral roots *PhPDR2* expression was restricted to the parental root (Fig 3.4E) while PhPDR3 expression is strongest in the tip of the protruding lateral outgrowth. However, substantial areas of the root system stained for both *PhPDR2* and *PhPDR3* promoter activity and it is not clear yet whether either is preferentially expressed in epidermal cortical or conductive layers. Analysis of transversal thin sections at different developmental stages and under different growth conditions will be necessary to further dissect specific expression patterns of

PhPDR2 and *PhPDR3*, which might ultimately allow for a clear spatial and functional distinction of these two close homologues.

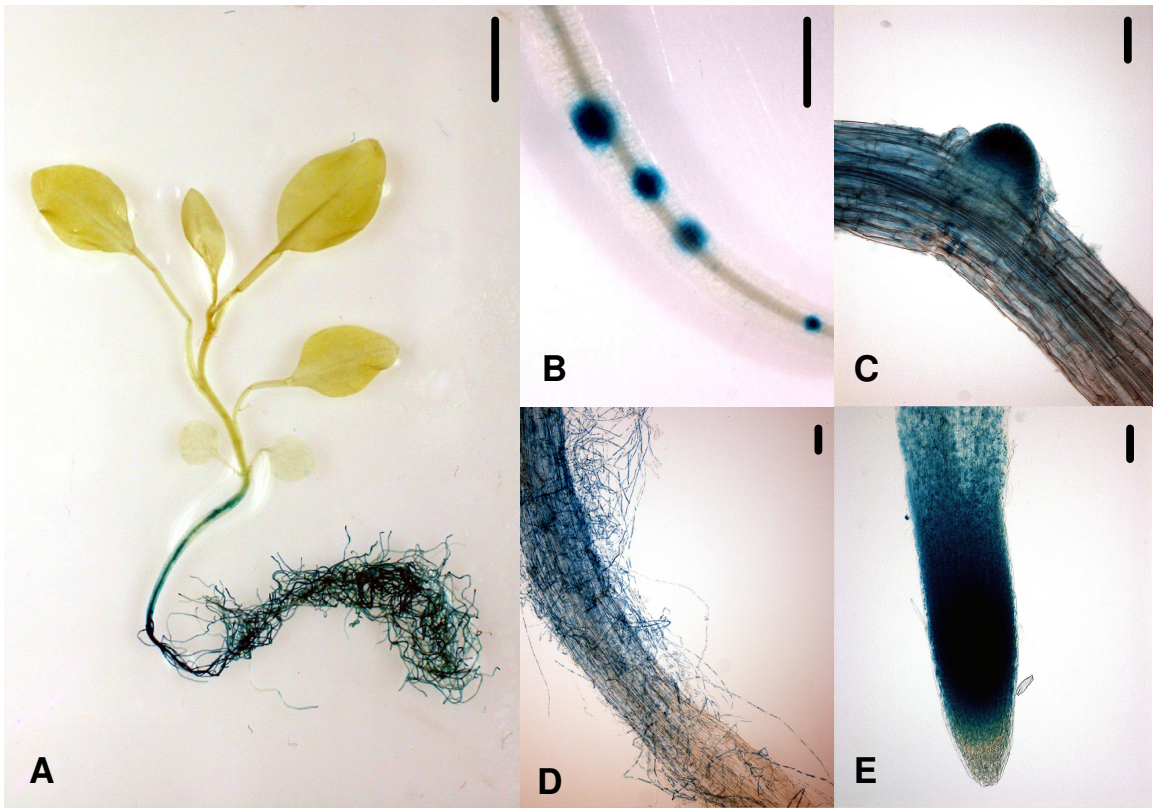

Figure 3.6: Tissue specific *PhPDR3* expression analysis in developing plants via *PhPDR3* promoter-GUS fusion constructs in the W115 background.
(A) Whole plant staining reveals that PhPDR3 is confined to belowground organs and the hypocotyl. In the root system PhPDR3 seems ubiquitously expressed. Scale bar = 1cm
(B) In the hypocotyl region the signal is strongest in developing adventitious root primordia. Scale bar = 1mm
(C) Strong expression in emerging lateral roots Scale bar = 0.1 mm
(D) root hairs Scale bar = 0.1 mm
(E) and root tips Scale bar = 0.1 mm

3.2.5 *Spodoptera littoralis* Feeding Trials

Dominant *PhPDR2* expression in leaf and stem glandular trichomes, together with the observation that expression is distinctively promoted by JA treatment, lead to the hypothesis that PhPDR2 might be involved in chemical herbivory defense. Postulating that PhPDR2 contributes to the loading of subcuticular cavities with insect deterring secondary metabolites we investigated the feeding behavior of caterpillars of the generalist herbivore *Spodoptera littoralis* on Phpdr2-100 and Phpdr2-105 lines in

comparison to W115 wild type lines. The following results were obtained in cooperation with Prof. Ted Turlings and associates from the University of Neuchatel. The data represent merely one series of experiments and thus have to be regarded as preliminary results. Repetitions, optimizations and extensions of the respective experiments are under way in order to allow for an objective validation or reconsideration of the findings presented here.

Two experiments were performed, first a feeding trial for five days with the intent of assessing the damage inflicted by a caterpillar and its weight gain from feeding either on W115 or Phpdr2 lines. Second a clip-cage experiment to quantify the weight gain of single caterpillars after 6 hours of forced feeding on the respective petunia lines.

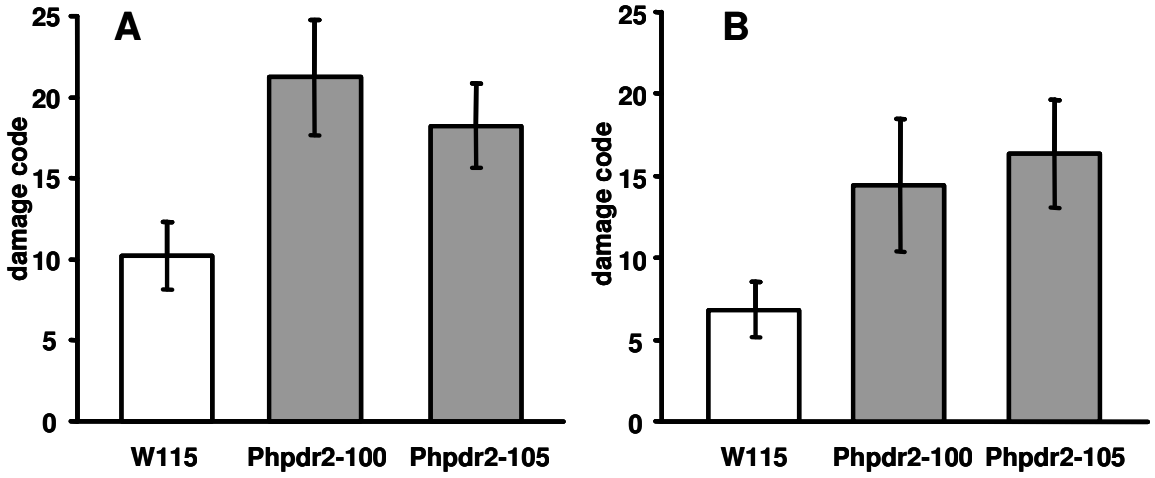

Figure 3.7: *Spodoptera littoralis* feeding trials on 3 week old W115 plantlets and Phpdr2 RNAi lines in the W115 background.
(A) Relative foliar damage inflicted by *Spodoptera littoralis* larvae after 5days of feeding on either wild type (white column) or Phpdr2 silenced plants (grey columns). The mortality rate for larvae on W115 plants was 75%, whereas it was 50% on Phpdr2-100 and Phpdr2-105. Error bars indicate standard error (n=24)
(B) Relative foliar damage inflicted by *Spodoptera littoralis* larvae after 5days of feeding on either wild type or Phpdr2 silenced plants. Only plants were assessed on which no live larvae could be retrieved after the feeding period. Error bars indicate standard error (n=12-18).

After having left single caterpillars for five days on well developed plantlets, a clear difference in the amount of feeding-related damage between PhPDR2 wild type and Phpdr2 silenced lines was detectable (Fig 3.7A). The damage of each individual plant was assessed via a relative damage code that categorizes the amount of visible caterpillar-inflicted injury on a scale of 0 to 100. On average the feeding action of *Spodoptera*

littoralis resulted in a damage code of around 10 on W115 lines whereas the damage code was almost double, around 21 for Phpdr2-100 and around 18 for Phpdr-105, in the mutant background. However it must be noted that these findings might be biased by a high rate of mortality of *Spodoptera littoralis* caterpillars throughout the experiment that differed between W115 and Phpdr2 lines. 75% of all larvae could not be retrieved from W115 plants after 5 days. For both Phpdr2 silenced lines the mortality rate was 50%, indicating an increased chance of survival for *Spodoptera littoralis* on plants impaired in PhPDR2 function. If the damage is compared only between plants on which the larvae survived, the difference is far less pronounced and not statistically significant anymore (data not shown). This might be due to individual reciprocal differences in herbivory related fitness for both plant and caterpillar individuals and it must be kept in mind that only 25% of W115 plants are accounted for in this data set. If however only the individuals were considered on which live caterpillars could not be retrieved (Fig 3.7B) it became apparent that individual larvae inflicted more than twice the damage on a plant impaired in PhPDR2 function before they died (presumably of poisoning) and that only half the amount of individuals actually did succumb to the prevailing feeding conditions on mutant plants, if compared to the corresponding WT.

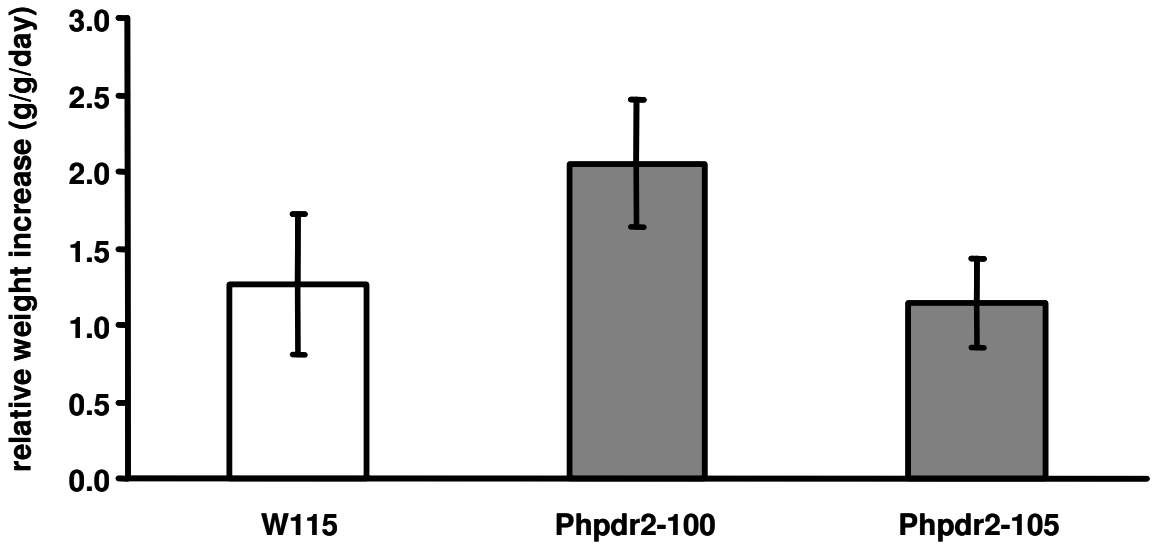

Figure 3.8: Relative weight gain of *Spodoptera littoralis* larvae after having fed for 5 days on 3 week old W115 plantlets (white column) and Phpdr2 RNAi lines in the W115 background (grey columns). Error bars indicate standard error (n=6-12).

In addition to damage assessment, the surviving larvae were weighted and their relative weight gain recorded (Fig 3.8). No significant difference in weight gain between the three groups was detectable, though there was a slight tendency towards more pronounced weight gain for caterpillars having fed on Phpdr2-100. In conclusion Phpdr2 silenced lines were more prone to feeding-inflicted damage from *Spodoptera littoralis*. More larvae were able to survive on Phpdr2 silenced lines and even those which did not survive inflicted considerably more damage on mutant lines before they died than they did on wild type lines. However no significant difference in weight gain for the surviving larvae could be demonstrated.

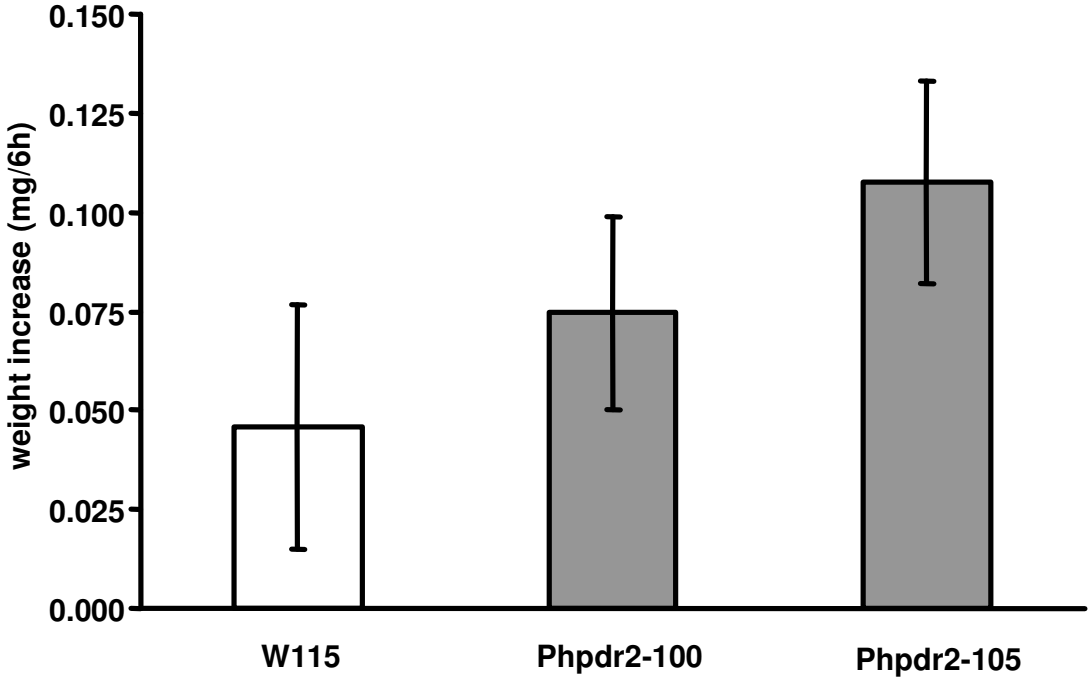

Figure 3.9: Absolute weight gain of *Spodoptera littoralis* larvae after having been contained in a clip-cage for 6h on expanding leaves of W115 plantlets (white column) and 2 independent Phpdr2 RNAi lines in the W115 background (grey columns). Error bars indicate standard error (n=24).

In a different approach to test a potentially different feeding affinity of *Spodoptera littoralis* in respect to PhPDR2 function, single caterpillars were confined for 6h to a small cage attached to a young leaf and their weight was recorded before and after the experiment (Fig 3.9). Again no significant difference could be recorded between the three

groups. However the variation was relatively larger for the control group on W115 wild type lines, suggesting that either the capability to deter *Spodoptera littoralis* fluctuates considerably between W115 individuals that are genetically identical, or that individual larvae display variable tolerance against Petunia herbivory defense mechanisms. These considerations might also account to a certain degree for the fact that larvae that did survive for five days on W115 lines caused similar damage as did larvae that survived on mutant lines.

Taken together these findings revealed a trend towards Phpdr2 lines being more susceptible to the generalist herbivore *Spodoptera littoralis*. Even though these data are not conclusive, they nevertheless point towards an involvement of PhPDR2 in trichome specific herbivory defense.

3.3 Discussion

Several studies have pointed out implications of PDR-type ABC transporters in biotic stress responses. Nonhost pathogen resistance in particular seems to be governed in part by PDR mediated excretion of antimicrobial compounds from epidermal tissues, rendering mutants susceptible to otherwise incompatible pathogens. Many of the resistance conferring properties of PDR proteins (transcript concentration at local infection sites, transcript abundance and presumably substrate abundance) are regulated via JA.

JA also plays a dominant role in the control of induced wounding and herbivory resistance and putative PDR substrate classes such as terpenoids and phenylpropanpoids are known to contribute to herbivory defense. Furthermore the common PM localization of PDRs, together with their direct energetization via ATP makes them ideal candidates to catalyze processes like the loading of subcuticular cavities in glandular trichomes or the fortification of cuticular surfaces with insect deterring metabolites. Both require mechanisms that are able to build up and maintain substantial concentration gradients across bilipid membranes. Thus it is surprising to find that so far no connection between herbivory defense and PDR transporters has yet been investigated or established. Here we report on a PDR-type ABC transporter from Petunia, *PhPDR2* that is highly expressed in leaf and stem glandular trichomes as well as emerging lateral root primordia. Downregulation of *PhPDR2* activity via RNA interference mediated mechanisms renders the plant more susceptible to the generalist foliage feeder *Spodoptera littoralis* suggesting a contribution to trichome specific herbivory defense.

PhPDR2 was isolated and cloned from the cDNA of mycorrhized Petunia roots. However, despite its expression in roots being promoted by the presence of AM fungi, we could not confirm a direct association of *PhPDR2* promoter activity and intracortical or extracortical mycorrhizal structures. Moreover transcriptional silencing of *PhPDR2* did not result in aberrant colonization patterns from either quantitative or qualitative perspectives. We speculate that the enhanced transcription of *PhPDR2* in response to AM fungal invasion rather owes to an unspecific elicitation of *PhPDR2* by the fungus. Alternatively it cannot be ruled out that the initially observed responsiveness of *PhPDR2*

to fungal colonization via RT-PCR is solely due to *PhPDR3* background amplification. *PhPDR3* is predominantly found belowground, but its reaction to mycorrhization has not yet been investigated. Still *PhPDR2* reacts positively to the exogenous application of yeast extract, which contains a variety of fungal elicitors and might explain the observed induction in the presence of AM fungi. Furthermore elicitor responsiveness might suggest implications in fungal pathogen resistance. This would be consistent with the functions of its close tobacco homologues NpPDR1 and NpPDR1. Like *PhPDR2*, both are also elicitor responsive and incorporated in JA signaling pathways. NpPDR1 in particular also resides in foliar trichomes, but in contrast to *PhPDR2* is induced in the whole leaf upon JA treatment or pathogen inoculation. NpPDR1 is proposed to transport the antifungal diterpene agent sclareol (and possible related compounds) across the PM into the apoplast at local infection sites, conferring resistance to the nonhost opportunist pathogen *Botritis cineria*. Nppdr1 silenced lines are prone to spontaneous often lethal infections of Botritis and prove hypersensitive to sclareol. Susceptibility of Phpdr2 lines to sclareol has not been investigated, but no spontaneous infections under non-sterile conditions could ever be detected. Furthermore partial sequences of an *NpPDR1* homologue that is more closely related to *PhPDR2* than *NpPDR1* could be amplified from *Nicotiana plumbaginifolia* roots (data not shown), suggesting that NpPDR1 is not a functional orthologue of PhPDR2. This is more likely the case for NtPDR1 since they share a significant overlap in amino acid sequence within the highly variable region of NBD2 (data not shown). Unfortunately analysis of NtPDR1 is restricted to transcript studies on suspension cultured BY-2 cells, rendering direct comparison futile.

As examined via RT-PCR, *PhPDR2* seems to be ubiquitously present in all main plant organs, but the presence of the very close homologue PhPDR3 makes PCR based transcript profiling unreliable due to potential *PhPDR3* background amplification. The creation of stable *PhPDR2* promoter-GUS fusion lines allowed for the specific investigation of promoter activity and revealed that aboveground, *PhPDR2* is restricted to leaf and stem trichomes as well as stigma tips and developing petals (Fig 3.6). Furthermore there seems to be a small rim of expression along the leaf margins. Expression below ground displays a more diffuse and unpredictable pattern, but peaks of activity can be observed in and around emerging lateral root primordia.

Expression of *PhPDR2* in the reproductive organs might be related to the transport of volatile substances that play a role in pollinator attraction. The odorant W115 lines produce an array of volatile benzenoids, which presumably serve in one of its ancestral species, *Petunia axillaris*, as attractants for its nocturnal hawkmoth pollinator. However expression is most pronounced in developing petals and in the stigma tip before it becomes receptive. Attraction of putative pollinators at that stage would be counterproductive. A possible explanation is that, in congruence to its expression in trichomes, it also has protective function in floral structures. Developing flowers are tender plant organs that are prone to predation (McCall and Irwin, 2006). And even though Petunia can continuously produce flowers, damage of a reproductive unit can seriously corrupt reproductive success (McCall, 2008). Native tobacco compromised in its ability to produce nicotine is impaired in its ability to protect developing flowers and hence more susceptible to florivory (Kessler et al., 2008).

In analogy the strong expression in emerging lateral roots can be interpreted as a means to protect young newly forming plant structures that are particularly attractive to herbivores. Prior to emergence lateral roots have to actively penetrate cortical and epidermal cell layers causing a local wound and the release of cellular contents into the rhizosphere. These sites are preferential entry points for several soil-borne pathogens (Sprague et al., 2007; Govindarajan et al., 2008) and it is quite likely that root herbivores are equally attracted to lateral root emergence sites.

Dominant *PhPDR2* expression in leaf and stem glandular trichomes, together with the observation that expression is distinctively promoted by JA treatment, lead to the hypothesis that PhPDR2 might be involved in chemical defense against aboveground herbivores. JA is a major mediator of herbivory defense which is in part regulated by a differential production of secondary metabolites (Hare, 2007; Steppuhn et al., 2008) and in part by an increase in trichome density (Boughton et al., 2005). Glandular trichomes are well known to produce and accumulate substantial amounts of insect deterring secondary metabolites such as terpenoids, phenylpropanoids and alkaloids (Ambrosio et al., 2008; Schilmiller et al., 2008). Since many of these compounds are also toxic for the plant in high concentrations, they are commonly excreted from glandular cells into a subcuticular storage cavity at the tip of the trichome that consequently swells up and

might even exceed the actual trichome cells in size. This way they are sequestered from the cytosol and strategically well positioned to fulfill their part in insect defense. Upon contact with a herbivore intending to feed on the trichome-protected foliage, the glandular cuticle bursts, releasing its cocktail of volatile and non-volatile chemicals. Considering the stark concentration gradient of a plethora of secondary metabolites that must exist between the subcuticular cavity and the trichome cytosol, a constant passive reflux of non-polar compounds across the PM sections separating both can be assumed. If not counteracted, this reflux would invariably result in an impediment of secondary metabolite production due to feedback inhibition or general cellular poisoning. Putative candidate transporters for the loading and reloading of subglandular cavities are PM intrinsic primary active extrusion pumps that are not directly dependent on electrochemical gradients and thus can participate in the establishment and maintenance of immense concentration differences across biological membranes. PDR-type ABC transporters fulfill these requirements and have furthermore been demonstrated to display a high transport affinity for secondary metabolites of terpenoid and possibly phenylpropanoid origin.

If consistent with general PDR localization, PhPDR2 localizes to the PM, it might well contribute to the loading and trapping of secondary metabolites in subcuticular cavities of glandular trichomes. Petunia glandular trichomes are multicellular complexes consisting of a stalk several cells in length and a head, which features the cuticular gland. *PhPDR2* is expressed in all trichome cells and not restricted to the apical cell where glandular loading takes place. This suggests that PhPDR2 is not a highly specialized protein solely intended to guard over secondary metabolite traffic across the subglandular PM, but rather serves more general functions, which is also consistent with its expression in other non-glandular albeit secretory tissues.

The hypothesis that PhPDR2 contributes to the sequestration of herbivore repelling compounds within the trichome system is supported by our data obtained from caterpillar feeding trials. Larvae of the generalist folivore *Spodoptera littoralis* have a lower mortality rate when feeding on Phpdr2 lines and commonly inflict more feeding related damage on Phpdr2 leaves. Since *PhPDR2* is exclusively expressed in trichomes and margins of W115 leaves, the observed difference in feeding behavior of *Spodoptera*

littoralis must be trichome related. Analysis of secondary metabolite contents in glandular trichomes of Phpdr2 lines is yet outstanding, but we assume a deficit of one or several compounds in the trichome head that renders the plant more susceptible to herbivory via *Spodoptera littoralis.* Since it is not a specialized feeder of Petunias, we furthermore postulate that PHPDR2-associated substrates exhibit a rather broad toxic spectrum and might even be bulk compounds present in substantial quantities. Several solanaceous species have been analyzed for their secondary metabolite contents in trichomes. Most prominent compound classes among solanaceae are either isoprenoid derived (Hare, 2007; Kapteyn et al., 2007; Besser et al., 2009) or acyl sugars containing branched-chain fatty acids (Slocombe et al., 2008). Since several PDR homologues exhibit terpenoid transport capacities, members of the former are more likely substrates for PhPDR2. Also unknown is whether PhPDR2 related substances are more of a volatile or non-volatile nature. Subcellular localization studies will have to confirm that PhPDR2 does indeed localize to the PM and it would be interesting to know whether there is a specific accumulation of *PhPDR2* transcript below the subcuticular cavity.

Another area for further investigation is the relationship of PhPDR2 to PhPDR3. Their unusually high sequence identity suggests that they diverged only recently and it is highly likely that they display overlapping substrate affinities and possibly even redundant functions. However not being detectable in trichomes or foliar tissues in general, it can be ruled out that PhPDR3 also contributes to aboveground herbivory defense. Furthermore belowground *PhPDR2* and *PhPDR3* exhibit distinct and only marginally overlapping expression patterns, suggesting functional divergence despite structural similarities.

3.4 Materials and Methods

3.4.1 Plant Growth Conditions

All Petunia lines were grown under long day conditions with 16h of continuous light at 40% relative humidity. Plants were either grown in soil (ED 73 Einheitserde) or in clay granules (Oil Dry US Special from Damolin) supplemented once a week with 1x Hoagland solution. On plate plants were grown on growth medium containing 2.2g/l MS (M0222.0050 Duchefa, The Netherlands) and 15g/l sucrose, supplemented either with 9g/l PHYTO AGAR (Duchefa, The Netherlands) or 4.5g/l Phytagel (Sigma, Switzerland) under long day conditions with 16h of continuous light. Prior to plating seeds were surface sterilized for 3min in 70% ethanol and rinsed four times with sterile distilled water.

All transgene lines were selected for T-DNA insertion either on plates containing 10mg/l Glufosinate Ammonium or in soil by spraying germinated seeds for 3 times with a BASTA (BASF, Germany) solution containing 320µM Glufosinate Ammonium over a period of 1 week. Non-transformed wild type lines served as controls for positive selection.

3.4.2 *PhPDR2* Cloning Strategy

Partial sequences of putative PDR transcripts were amplified from total cDNA obtained from the roots of W115 individuals 4 weeks after inoculation with the AM fungus *Glomus intraradices*. NBD1 amplicons of around 0.5kb were obtained with the following degenerate primers: 5`-MGWATGACTCTDYTKYTKGGACCTCC targeting PDR signature1 and 5`-GYTTCYTYTGNCCHCCHGAAATWCC targeting the ABC signature. NBD2 amplicons of around 0.5kb were obtained with the following degenerate primers: 5`-GGGWGTYAGTGGWGCWGGWAARAC targeting the Walker A box and 5`-CTCATNACAATDGCWGCWGCTCTWGC targeting PDR signature3. Fragments for the respective NBDs were aligned and the following consensus primers were designed

to amplify putative PDR coding regions spanning NBD1 and NBD2: 5`-tattgggacttgaaatttgtgccgatac and 5`-gctccactaacacccatcagagctgtc.

Amplification of upstream and downstream sequences of *PhPDR1* full length transcript was achieved via 5`RACE and 3`RACE PCRs using the SMART-RACE cDNA Amplification Kit (Clontech, Takara Bio Company, USA) according to the manufacturer's specifications. 5`RACE primer and 5`nested RACE primer had the following sequence: 5'-atggattcgaagaaggccagaacgtcttc and 5'-cccttaccatgtcatctcccaccaaag. 3`RACE primer and nested 3`RACE primer sequences were: 5'-gatcagggtgcctctgaagatagattgg and 5'-caggaggatatattgagggtagaatccaca. 5`RACE of a 1.1kb *PhPDR3* fragment was achieved with the same primer sets as previously used for *PhPDR2*.

3.4.3 *PhPDR2* and *PhPDR3* Promoter-GUS Constructs and GUS Staining Assay

Amplification of a 1.2kb promoter fragment upstream of the *PhPDR2* gene was accomplished via use of the Genome Walker Universal Kit (Clontech, Takara Bio Company, USA) with the primer 5'-caagagctgcccatttaagtgcttcttc and the nested primer 5'-cgcttaaacttccccttgcacttcctc. The fragment was T/A cloned into pGEM-T-Easy vector system (Promega, USA) and subsequently reamplified with the primer 5'-ggaaccaagctttgtgtaggaaaattttgc containing a HindIII restriction site (underlined) and the primer 5'-tacatctagagacccccctctagctcag containing an XbaI restriction site (underlined). An alternative *PhPDR2* promoter construct including the *PhPDR2* start ATG and the first 19bp of the first exon in frame with the GUS gene was created using the primers 5'-ggaaccaagctttgtgtaggaaaattttgc containing a HindIII restriction site (underlined) and the primer 5'-tcgatctagatacctaagtttactggttccat containing an XbaI restriction site (underlined). The respective restriction sites were used to clone the *PhPDR2* promoter fragments into the GUS gene containing pGPTV-Bar (Becker et al., 1992) vector system.

A 1.5kb PhPDR3 promoter fragment was obtained with similar methods using the genome walker primer 5'-cgcttaaacttccccttgcacttcctc and the nested genome walker primer 5'-gccgctcgtaagttacctaagtttactgg. Addition of pGPTV-Bar compatible restriction sites was achieved with the following primers 5'-ggaaccaagctttaaaaacgtcaagcaagc

containing a HindIII restriction site (underlined) and the primer 5'-tcgatctagatatgaaccaatcaaaatgc containing an XbaI restriction site (underlined).

For GUS staining trials tissues to be investigated were immerged in an appropriate amount of GUS-staining buffer (100mM Sodium phosphate buffer pH=7.00, 10mM NaEDTA, 1.5mM Potassium hexacyanoferrate(II) trihydrate, 0.25mM Potassium hexacyanoferrate(III), 0.1% (v/v) Triton X-100 and 1mM 5-Bromo-4-chloro-3-indolyl β-D-glucuronide cyclohexylammonium salt vacuum infiltrated three times for 30s and incubated in the dark at 37°C for 12-48h. After staining samples were cleared and stored in 70% ethanol.

3.4.4 *PhPDR2* RNA Interference Constructs

Silencing of *PhPDR1* specific transcripts was attempted via the generation of double stranded hairpin RNA fragments utilizing the pKANIBAL vector system (Wesley et al., 2001). A 407bp fragment containing parts of the 3`end and the 3`UTR of *PhPDR2* was amplified from *PhPDR2* cDNA with the following primers: 5`cgatggatcctcgagctgatgatgaaacagtggaa, containing BamHI and XhoI restriction sites (underlined) and 5`cgatatcgatggtaccgaataaatatgccgctttca containing ClaI and KpnI sites (underlined).The resulting amplicons were cloned in sense and antisense direction in the two MCS of pKANIBAL flanking the hairpin intron sequence. Next the pKANIBAL RNAi cassette containing 35S promoter RNAi construct and OCE3 terminator was excised from the vector backbone using the NotI restriction sites and transferred into the binary pGreenII0229 vector system (Hellens et al., 2000), conferring Glufosinate Ammonium resistance as a selection marker in plants.

After stable transformation of W115 plants (see 2.2.5) the degree of down-regulation was estimated via semi-quantitative RT-PCR using the *PhPDR2* specific primers 5`-ggaatgtattctgccttacc and 5`-gtaatctccaaattgtgatgc. Petunia tubulin transcript, partially amplified with 5`-cattggtcaagccggttattc and 5`-acccttgaagaccagtacagt served as a housekeeping and loading control.

3.4.5 Stable Petunia Transformation

PhPDR2 promoter-GUS constructs, PhPDR3 promoter-GUS constructs and Phpdr2 RNAi constructs were transferred into the W115 background via *Agrobacterium tumefaciens* mediated transformation of leaf explants, callus induction and plant regeneration (Lutke, 2006). 0.45% Phytagel was used instead of 0.9% agar in all media and the concentrations of BAP and NAA in the Selection Medium was adjusted between 1-2mg/l for the former and 0.05-1.5mg/l for the latter to maximize shoot induction for each individual transformation.

Regenerated plantlets were tested for successful construct insertion via PCR on genomic DNA. The primers 5'-acggtccacatgccggtatatacgatg and 5'-gatggcatttgtaggagccaccttcc, targeting the 35S promoter, were used to confirm RNAi construct insertion. The primers 5'-gaattgatcagcgttggtgggaaagc and 5'-ggtaatgcgaggtacggtaggagttg, targeting the GUS gene, were used to confirm GUS construct insertion.

3.4.6 Reverse Screening Approach to Identify Transposon Insertions in *PhPDR2*

Two three dimensionally arranged genomic DNA libraries (a kind gift from Prof. Tom Gerats, Radboud University Nijmegen), one representing 16x16x16 (4096) W138 individuals and the other representing 10x10x10 (1000) W138 individuals were screened for dTph1 insertions in *PhPDR2* via PCR based method (Vandenbussche and Gerats, 2004). A multitude of radiolabled *PhPDR2* specific primers covering the whole cDNA sequence and separated by less than 500bp, with annealing temperatures above 65°C were used in combination with the unlabled dTph1 inverted repeat specific primer 5`-gaattcgctccgcccctg to scan the entire genomic region of *PhPDR2* in contiguous steps covering less than 1kb each for transposon insertions. The screening result presented in this work derived from the primer 5`-agcaacagagggacaagaagcaaatgttg.

3.4.7 Insect Feeding Trials

W115 wild type lines as well as Phpdr2-100 and Phpdr2-105 RNAi lines were grown in soil to a height of about 15cm. Single *Spodoptera littoralis* larva of a weight of around 1mg were placed on each plant, which was covered with a transparent plastic container to prevent escape of the insect. Larvae were weight prior to feeding trial, left on a plant for 5 days and then weight again in order to calculate relative weight gain. Foliar feeding damage was assessed via a subjective and comparative damage code on a scale from 0 (no damage) to 100 (no more leaf). Additionally single larva of a weight of around 1mg were confined to a small container (clip-cage), which was attached to a young expanding leaf, allowing the larva to feed for 6h, without being able to move away from the chosen feeding site. Larvae were weight before and after the forced feeding trial in order to calculate absolute weight gains.

3.4.8 Software Based Analysis

Membrane protein topology predictions were calculated using ConPredII (http://bioinfo.si.hirosaki-u.ac.jp/~ConPred2/) based algorithms. Transmembrane topology was visualized with Topo2 (Johns S.J., TOPO2, Transmembrane protein display software ; http://www.sacs.ucsf.edu/TOPO2/) with amino acids classified as follows: hydrophilic (W,S,T,C,Q,G,H,Y,N); hydrophobic (M,L,V,I,P,A,F); positively charged (R,K); negatively charged (D,E).

Calculation of phylogenetic relationships of different Cluster1 PDR homologues was performed using different algorithms accessible at www.phylogeny.fr. Visualization was achieved with the Mega4 software, downloaded from www.megasoftware.net.

General sequence analysis was performed using Vector NTI (Invitrogen, USA). Sequence alignments were created with Multalin (http://bioinfo.genotoul.fr/multalin/).

4 General Conclusion

The original aim of this PhD thesis was to investigate putative implications of ABC-type or MATE-type secondary metabolite transporters in the establishment and function of arbuscular mycorrhiza in *Petunia hybrida*. Both a forward and a reverse screening approach were initiated in order to identify and characterize transport proteins with affinities for symbiosis related compounds. The forward genetic screen, designed to specifically single-out mutants impaired in strigolactone transport, proved to be insufficiently robust and reliable for a large scale and high throughput analysis of large dTph1 transposon-harboring W138 populations, and thus was discarded already in its developmental stage. Instead it was decided to focus on a reverse genetic approach, exclusively targeting PDR-type ABC transporters, which, owing to several common characteristics (see General Introduction), appeared at the time as the most probable candidates. It must by noted however that by limiting the scope of our investigations to a single subfamily (namely PDRs) of a single transporter family (namely ABC transporters) we substantially narrowed our perspective right from the start, running the risk of missing the majority of secondary metabolite transport related aspects in mycorrhization. With a degenerate primer approach we managed to obtain several PDR candidate transcripts from the cDNA of mycorrhized Petunia roots, two of which were characterized in detail and constitute the backbone of the presented work.

Despite being positively responsive on the transcriptional level to the inoculation with AM fungi, PhPDR2 proved to lack any detectable function in symbiosis associated matters. *PhPDR2* promoter-GUS analysis did not reveal any significant overlap of *PhPDR2* promoter activity and mycorrhizal structures in colonized roots. Furthermore post-transcriptional silencing of *PhPDR2* did not affect the dynamics or extent of the belowground symbiotic interactions. Instead PhPDR2 is emerging as a putative contributor to aboveground chemical herbivory defense. Being elicitor-responsive and highly induced by elevated JA concentrations, we postulated that, in congruence with the roles of several other characterized PDRs, PhPDR2 might be involved in biotic stress responses. Interestingly foliar expression of *PhPDR2* is restricted to the leaf margins and glandular trichomes, insinuating involvement in herbivory rather than pathogen defense.

Indeed downregulation of *PhPDR2* via RNA interference-mediated mechanisms rendered Petunia leaves more susceptible to feeding-related damage by the generalist caterpillar larvae of *Spodophtora littoralis*. Presumed to be localizing to the plasma membrane, PhPDR2 is proposed to support the loading of subcuticular cavities and apoplastic regions of Petunia glandular trichomes with herbivore-deterring secondary metabolites such as terpenoids or acyl sugar derivatives. It has long been acknowledged that plant PDR-type transporters are important factors in biotic stress responses, but so far their major role was believed to be confined to constitutive and induced nonhost resistance based on the excretion of antimicrobial compounds. Just very recently it was demonstrated that PDRs are also of importance in conferring durable resistance to appropriate biotrophic pathogens, even though it is currently unknown whether it is transport of secondary metabolites that is responsible. Here we present first data that links PDR function to chemical defense against organisms above the microbial scale. Defense related secondary metabolite production constitutes one of the hallmarks of glandular trichome functions, but whereas the biosynthesis of several classes of secondary compounds has been intensively studied in the trichomes of several species, the question of transport and subcuticular cavity loading has so far not been addressed. Knowledge of how gland filling and avoidance of metabolite reflux into subglandular cells is achieved is of importance from aspects of chemical ecology, but might even have more substantial repercussions in the biotechnology field. Bioengineering of secondary metabolites of medical or industrial value in glandular trichomes has become an area of intense focus in plant biotechnology. However production efficiency depends to a certain degree on the sequestration of the final compounds. Modifying export capacities of trichomes engineered to produce certain substances in excess might be a key step in improving yield and increasing the stability of the system.

In the course of PhPDR2 characterization, a very close homologue, PhPDR3, was discovered. Despite high structural identity PhPDR2 and PhPDR3 exhibit different expression patterns suggesting divergent functions. *PhPDR3* expression is strong in root hairs and root tips, including the tips of emerging lateral roots and adventitious roots, all of which are tissues devoid of *PhPDR2* expression. Furthermore *PhPDR3* is completely absent aboveground with the exception of the hypocotyl. Nothing can yet be said about

any potential function about PhPDR3, but the identification of a W138 line harboring a dTph1 transposon insertion in the coding region of *PhPDR3* might facilitate its characterization.

PhPDR1 expression was found to be confined to root and stem tissues. General expression levels were very low, but root-specific transcript abundance positively correlated with amounts of fungal colonization, making PhPDR1 a high priority candidate in the context of this thesis. Auxin and SA had stimulatory effects on *PhPDR1* expression. *PhPDR1* promoter-GUS analysis further defined above ground expression, limiting *PhPDR1* presence to the stem vasculature, particularly to the areas directly below the leaf axils. Co-staining for *PhPDR1* promoter activity and intraradical AM fungal presence disclosed a significant overlap. However *PhPDR1* promoter activity appeared highest in cortical cells adjacent to arbusculated cells and in regions flanking colonized sections. Cells containing developing or fully expanded arbuscles did not exhibit a strong signal, suggesting that PhPDR1 is not of importance in arbuscle development and might not catalyze transport events across the periarbuscular membrane. Instead PhPDR1 appears to transport substances that stimulate intracortical proliferation of AM fungi. Petunias devoid of functional PhPDR1 copies exhibited lower and delayed colonization rates without the morphology of mycorrhizal structures being affected. In addition pre-symbiotic signaling was impaired in the mutant background. Reminiscent of a lack of strigolactone exudation, germinated AM fungal spores displayed a reduced branching response when subjected to root exudates of Phpdr1 mutant plants in comparison to the wild type. The deduced hypothesis that PhPDR1 might be implicated in the transport of strigolactones was consolidated by the finding that Phpdr1 mutant plants were impaired in the control of axillary bud outgrowth. Similar to Petunia mutants with defects in strigolactone biosynthesis, they produced lateral branches at higher frequencies, suggesting that the allocation of branching-inhibiting strigolactones to the axillary buds is partially dependent on PhPDR1 function. To further investigate this hypothesis we performed whole plant uptake assays with a synthetic radiolabeled strigolactone derivative (GR24). Quantification of GR24 contents in the nodal regions of wild type and Phpdr1 mutant plants revealed that exogenously applied strigolactones accumulate to a significantly higher degree in the mutant background, indicating aberrant

export capacities in certain tissues. These findings might also help to explain a seemingly unrelated phenotype observed in Phpdr1 lack of function plants. At late developmental stages or under conditions of high evaporative demands the mutants are prone to wilting, presumably due to the development of malformed conductive elements. So far a role for strigolactones in vasculature differentiation has not been established, but a high branching mutant in pea, with so far unknown genetic defects, exists that also displays apical wilting. Histological analysis of stem sections showed that the pea mutant produced more numerous xylem vessels at the expense of vessel diameter, resulting in significantly reduced conductive capacities. Hence we postulate that strigolactones, in addition to negatively regulating lateral branching, also negatively control xylem expansion. By doing so, the conductive capacities of the stem vasculature is dynamically adjusted to the transpirational demands of the plant, which is directly linked the number and size of foliated lateral branches.

In conclusion, two novel members of Cluster1 of the PDR-type ABC transporter subfamily were partially characterized in Petunia within the frame of this thesis, insinuating yet unrecognized functions for PDRs in herbivory defense, symbiotic interactions and plant development. Despite their high structural similarity PhPDR2 and PhPDR1 fulfill completely unrelated task within the plant, but it is nevertheless likely that their respective substrates belong to similar compound classes. Herbivory deterring metabolites of terpenoid origin are the most likely candidates for PhPDR2, while there is considerable evidence that apocarotenoid derivatives of the strigolactone family are substrates of PhPDR1.

Inclusion of PhPDR1 and PhPDR2 into the PDR subfamily extends its implications beyond the scope of nonhost pathogen resistance (NpPDR1, NtPDR1, AtPDR8 and AtPDR12), appropriate pathogen resistance (LR34), heavy metal tolerance (AtPDR8 and AtPDR12), abiotic stress responses (SpTUR2, OsPDR9 and NtPDR3) and postulated organic acid excretion (OsPDR21), making Pleiotropic Drug Resistance transporters one of the most resourceful subfamily of ABC-transporters. To a large degree this might be explained by the versatility of the secondary metabolite classes that constitute PDR substrates. Considering that PDR transporters are absent in animals, their evolution and diversification might have been influenced by the restraints associated with the lack of

mobility of most plants and fungi, which forces them to directly cope with a multitude of environmental stresses without having the option of simply fleeing from them.

5 List of References

Ahkami, A.H., Lischewski, S., Haensch, K.-T., Porfirova, S., Hofmann, J., Rolletschek, H., Melzer, M., Franken, P., Hause, B., Druege, U., and Hajirezaei, M.R. (2008). Molecular physiology of adventitious root formation in Petunia hybrida cuttings: involvement of wound response and primary metabolism. New Phytol.**181,** 613-25.

Akiyama, K. (2007). Chemical identification and functional analysis of apocarotenoids involved in the development of arbuscular mycorrhizal symbiosis. Biosci Biotechnol Biochem **71,** 1405-1414.

Akiyama, K., Matsuoka, H., and Hayashi, H. (2002). Isolation and identification of a phosphate deficiency-induced C-glycosylflavonoid that stimulates arbuscular mycorrhiza formation in melon roots. Mol Plant Microbe Interact **15,** 334-340.

Akiyama, K., Matsuzaki, K.-i., and Hayashi, H. (2005). Plant sesquiterpenes induce hyphal branching in arbuscular mycorrhizal fungi. Nature **435,** 824-827.

Ambrosio, S.R., Oki, Y., Heleno, V.C.G., Chaves, J.S., Nascimento, P.G.B.D., Lichston, J.E., Constantino, M.G., Varanda, E.M., and Da Costa, F.B. (2008). Constituents of glandular trichomes of Tithonia diversifolia: relationships to herbivory and antifeedant activity. Phytochemistry **69,** 2052-2060.

Angenent, G.C., Stuurman, J., Snowden, K.C., and Koes, R. (2005). Use of Petunia to unravel plant meristem functioning. Trends Plant Sci **10,** 243-250.

Arite, T., Iwata, H., Ohshima, K., Maekawa, M., Nakajima, M., Kojima, M., Sakakibara, H., and Kyozuka, J. (2007). DWARF10, an RMS1/MAX4/DAD1 ortholog, controls lateral bud outgrowth in rice. Plant J **51,** 1019-1029.

Bainbridge, K., Sorefan, K., Ward, S., and Leyser, O. (2005). Hormonally controlled expression of the Arabidopsis MAX4 shoot branching regulatory gene. Plant J **44,** 569-580.

Balzi, E., and Goffeau, A. (1995). Yeast multidrug resistance: the PDR network. J Bioenerg Biomembr **27,** 71-76.

Balzi, E., Wang, M., Leterme, S., Van Dyck, L., and Goffeau, A. (1994). PDR5, a novel yeast multidrug resistance conferring transporter controlled by the transcription regulator PDR1. J Biol Chem **269,** 2206-2214.

Bari, R., and Jones, J. (2008). Role of plant hormones in plant defence responses. Plant Mol Biol.**69,**473-88

Becker, D., Kemper, E., Schell, J., and Masterson, R. (1992). New plant binary vectors with selectable markers located proximal to the left T-DNA border. Plant Mol Biol **20,** 1195-1197.

Besser, K., Harper, A., Welsby, N., Schauvinhold, I., Slocombe, S., Li, Y., Dixon, R.A., and Broun, P. (2009). Divergent regulation of terpenoid metabolism in the trichomes of wild and cultivated tomato species. Plant Physiol **149,** 499-514.

Besserer, A., Becard, G., Jauneau, A., Roux, C., and Sejalon-Delmas, N. (2008). GR24, a synthetic analog of strigolactones, stimulates the mitosis and growth of the arbuscular mycorrhizal fungus Gigaspora rosea by boosting its energy metabolism. Plant Physiol **148,** 402-413.

Bhalerao, R.P., and Bennett, M.J. (2003). The case for morphogens in plants. Nat Cell Biol **5,** 939-943.

Bird, D., Beisson, F., Brigham, A., Shin, J., Greer, S., Jetter, R., Kunst, L., Wu, X., Yephremov, A., and Samuels, L. (2007). Characterization of Arabidopsis ABCG11/WBC11, an ATP binding cassette (ABC) transporter that is required for cuticular lipid secretion. Plant J **52,** 485-498.

Blakeslee, J.J., Bandyopadhyay, A., Lee, O.R., Mravec, J., Titapiwatanakun, B., Sauer, M., Makam, S.N., Cheng, Y., Bouchard, R., Adamec, J., Geisler, M., Nagashima, A., Sakai, T., Martinoia, E., Friml, J., Peer, W.A., and Murphy, A.S. (2007). Interactions among PIN-FORMED and P-glycoprotein auxin transporters in Arabidopsis. Plant Cell **19,** 131-147.

Bodenhausen, N., and Reymond, P. (2007). Signaling pathways controlling induced resistance to insect herbivores in Arabidopsis. Mol Plant Microbe Interact **20,** 1406-1420.

Booker, J., Auldridge, M., Wills, S., McCarty, D., Klee, H., and Leyser, O. (2004). MAX3/CCD7 is a carotenoid cleavage dioxygenase required for the synthesis of a novel plant signaling molecule. Curr Biol **14,** 1232-1238.

Booker, J., Sieberer, T., Wright, W., Williamson, L., Willett, B., Stirnberg, P., Turnbull, C., Srinivasan, M., Goddard, P., and Leyser, O. (2005). MAX1 encodes a cytochrome P450 family member that acts downstream of MAX3/4 to produce a carotenoid-derived branch-inhibiting hormone. Dev Cell **8,** 443-449.

Boughton, A.J., Hoover, K., and Felton, G.W. (2005). Methyl jasmonate application induces increased densities of glandular trichomes on tomato, Lycopersicon esculentum. J Chem Ecol **31,** 2211-2216.

Buee, M., Rossignol, M., Jauneau, A., Ranjeva, R., and Becard, G. (2000). The pre-symbiotic growth of arbuscular mycorrhizal fungi is induced by a branching factor partially purified from plant root exudates. Mol Plant Microbe Interact **13,** 693-698.

Campbell, E.J., Schenk, P.M., Kazan, K., Penninckx, I.A.M.A., Anderson, J.P., Maclean, D.J., Cammue, B.P.A., Ebert, P.R., and Manners, J.M. (2003). Pathogen-responsive expression of a putative ATP-binding cassette transporter gene conferring resistance to the diterpenoid sclareol is regulated by multiple defense signaling pathways in Arabidopsis. Plant Physiol **133,** 1272-1284.

Carlsbecker, A., and Helariutta, Y. (2005). Phloem and xylem specification: pieces of the puzzle emerge. Current Opinion in Plant Biology Cell signalling and gene regulation **8,** 512-517.

Chen, J.-C., Jiang, C.-Z., Gookin, T.E., Hunter, D.A., Clark, D.G., and Reid, M.S. (2004). Chalcone synthase as a reporter in virus-induced gene silencing studies of flower senescence. Plant Mol Biol **55,** 521-530.

Cook, C.E., Whichard, L.P., Turner, B., Wall, M.E., and Egley, G.H. (1966). Germination of Witchweed (Striga lutea Lour.): Isolation and Properties of a Potent Stimulant. Science **154,** 1189-1190.

Crouzet, J., Trombik, T., Fraysse, A.S., and Boutry, M. (2006). Organization and function of the plant pleiotropic drug resistance ABC transporter family. FEBS Lett **580,** 1123-1130.

David-Schwartz, R., Badani, H., Smadar, W., Levy, A.A., Galili, G., and Kapulnik, Y. (2001). Identification of a novel genetically controlled step in mycorrhizal colonization: plant resistance to infection by fungal spores but not extra-radical hyphae. Plant J **27,** 561-569.

David-Schwartz, R., Gadkar, V., Wininger, S., Bendov, R., Galili, G., Levy, A.A., and Kapulnik, Y. (2003). Isolation of a premycorrhizal infection (pmi2) mutant of tomato, resistant to arbuscular mycorrhizal fungal colonization. Mol Plant Microbe Interact **16,** 382-388.

Dodd, I.C., Ferguson, B.J., and Beveridge, C.A. (2008). Apical Wilting and Petiole Xylem Vessel Diameter of the rms2 Branching Mutant of Pea are Shoot Controlled and Independent of a Long-Distance Signal Regulating Branching. Plant Cell Physiol. **49,** 791-800.

Ducos, E., Fraysse, A.S., and Boutry, M. (2005). NtPDR3, an iron-deficiency inducible ABC transporter in Nicotiana tabacum. FEBS Letters **579,** 6791-6795.

Eichhorn, H., Klinghammer, M., Becht, P., and Tenhaken, R. (2006). Isolation of a novel ABC-transporter gene from soybean induced by salicylic acid. J Exp Bot **57,** 2193-2201.

Fester, T., Wray, V., Nimtz, M., and Strack, D. (2005). Is stimulation of carotenoid biosynthesis in arbuscular mycorrhizal roots a general phenomenon? Phytochemistry **66,** 1781-1786.

Fester, T., Schmidt, D., Lohse, S., Walter, M.H., Giuliano, G., Bramley, P.M., Fraser, P.D., Hause, B., and Strack, D. (2002). Stimulation of carotenoid metabolism in arbuscular mycorrhizal roots. Planta **216,** 148-154.

Floss, D.S., Schliemann, W., Schmidt, J., Strack, D., and Walter, M.H. (2008a). RNA interference-mediated repression of MtCCD1 in mycorrhizal roots of Medicago truncatula causes accumulation of C27 apocarotenoids, shedding light on the functional role of CCD1. Plant Physiol **148,** 1267-1282.

Floss, D.S., Hause, B., Lange, P.R., Kuster, H., Strack, D., and Walter, M.H. (2008b). Knock-down of the MEP pathway isogene 1-deoxy-D-xylulose 5-phosphate synthase 2 inhibits formation of arbuscular mycorrhiza-induced apocarotenoids, and abolishes normal expression of mycorrhiza-specific plant marker genes. Plant J **56,** 86-100.

Gadkar, V., David-Schwartz, R., Nagahashi, G., Douds, D.D., Wininger, S., and Kapulnik, Y. (2003). Root exudate of pmi tomato mutant M161 reduces AM fungal proliferation in vitro. FEMS Microbiol Lett **223,** 193-198.

Galliot, C., Stuurman, J., and Kuhlemeier, C. (2006). The genetic dissection of floral pollination syndromes. Curr Opin Plant Biol **9,** 78-82.

Gang, D.R., Beuerle, T., Ullmann, P., Werck-Reichhart, D., and Pichersky, E. (2002). Differential production of meta hydroxylated phenylpropanoids in sweet basil peltate glandular trichomes and leaves is controlled by the activities of specific acyltransferases and hydroxylases. Plant Physiol **130,** 1536-1544.

Gang, D.R., Wang, J., Dudareva, N., Nam, K.H., Simon, J.E., Lewinsohn, E., and Pichersky, E. (2001). An investigation of the storage and biosynthesis of phenylpropenes in sweet basil. Plant Physiol **125,** 539-555.

Garcia-Garrido, J.M., and Ocampo, J.A. (2002). Regulation of the plant defence response in arbuscular mycorrhizal symbiosis. J Exp Bot **53,** 1377-1386.

Geisler, M., and Murphy, A.S. (2006). The ABC of auxin transport: the role of p-glycoproteins in plant development. FEBS Lett **580,** 1094-1102.

Genre, A., Chabaud, M., Timmers, T., Bonfante, P., and Barker, D.G. (2005). Arbuscular mycorrhizal fungi elicit a novel intracellular apparatus in Medicago truncatula root epidermal cells before infection. Plant Cell **17,** 3489-3499.

Gerats, A.G., Huits, H., Vrijlandt, E., Marana, C., Souer, E., and Beld, M. (1990). Molecular characterization of a nonautonomous transposable element (dTph1) of petunia. Plant Cell **2,** 1121-1128.

Gerats, T., and Vandenbussche, M. (2005). A model system for comparative research: Petunia. Trends Plant Sci **10,** 251-256.

Giovannetti, M., and Mosse, B. An Evaluation of Techniques for Measuring Vesicular Arbuscular Mycorrhizal Infection in Roots. New Phytologist **84,** 489-500.

Gomez-Roldan, V., Fermas, S., Brewer, P.B., Puech-Pages, V., Dun, E.A., Pillot, J.-P., Letisse, F., Matusova, R., Danoun, S., Portais, J.-C., Bouwmeester, H., Becard, G., Beveridge, C.A., Rameau, C., and Rochange, S.F. (2008). Strigolactone inhibition of shoot branching. Nature **455,** 189-194.

Govindarajan, M., Balandreau, J., Kwon, S.-W., Weon, H.-Y., and Lakshminarasimhan, C. (2008). Effects of the inoculation of Burkholderia vietnamensis and related endophytic diazotrophic bacteria on grain yield of rice. Microb Ecol **55,** 21-37.

Guimil, S., and Dunand, C. (2006). Patterning of Arabidopsis epidermal cells: epigenetic factors regulate the complex epidermal cell fate pathway. Trends Plant Sci **11,** 601-609.

Gutjahr, C., Banba, M., Croset, V., An, K., Miyao, A., An, G., Hirochika, H., Imaizumi-Anraku, H., and Paszkowski, U. (2008). Arbuscular Mycorrhiza-Specific Signaling in Rice Transcends the Common Symbiosis Signaling Pathway. Plant Cell **20,** 2989-3005.

Hans, J., Hause, B., Strack, D., and Walter, M.H. (2004). Cloning, characterization, and immunolocalization of a mycorrhiza-inducible 1-deoxy-d-xylulose 5-phosphate reductoisomerase in arbuscle-containing cells of maize. Plant Physiol **134,** 614-624.

Hare, J.D. (2005). Biological activity of acyl glucose esters from Datura wrightii glandular trichomes against three native insect herbivores. J Chem Ecol **31,** 1475-1491.

Hare, J.D. (2007). Variation in herbivore and methyl jasmonate-induced volatiles among genetic lines of Datura wrightii. J Chem Ecol **33,** 2028-2043.

Hare, J.D., and Walling, L.L. (2006). Constitutive and jasmonate-inducible traits of Datura wrightii. J Chem Ecol **32,** 29-47.

Harrison, M.J. (1999). MOLECULAR AND CELLULAR ASPECTS OF THE ARBUSCULAR MYCORRHIZAL SYMBIOSIS. Annu Rev Plant Physiol Plant Mol Biol **50,** 361-389.

Harrison, M.J., Dewbre, G.R., and Liu, J. (2002). A phosphate transporter from Medicago truncatula involved in the acquisition of phosphate released by arbuscular mycorrhizal fungi. Plant Cell **14,** 2413-2429.

Hause, B., Mrosk, C., Isayenkov, S., and Strack, D. (2007). Jasmonates in arbuscular mycorrhizal interactions. Phytochemistry **68,** 101-110.

Hellens, R.P., Edwards, E.A., Leyland, N.R., Bean, S., and Mullineaux, P.M. (2000). pGreen: a versatile and flexible binary Ti vector for Agrobacterium-mediated plant transformation. Plant Mol Biol **42,** 819-832.

Humphrey, A.J., and Beale, M.H. (2006). Strigol: biogenesis and physiological activity. Phytochemistry **67,** 636-640.

Iijima, Y., Gang, D.R., Fridman, E., Lewinsohn, E., and Pichersky, E. (2004a). Characterization of geraniol synthase from the peltate glands of sweet basil. Plant Physiol **134,** 370-379.

Iijima, Y., Davidovich-Rikanati, R., Fridman, E., Gang, D.R., Bar, E., Lewinsohn, E., and Pichersky, E. (2004b). The biochemical and molecular basis for the divergent patterns in the biosynthesis of terpenes and phenylpropenes in the peltate glands of three cultivars of basil. Plant Physiol **136,** 3724-3736.

Imaizumi-Anraku, H., Takeda, N., Charpentier, M., Perry, J., Miwa, H., Umehara, Y., Kouchi, H., Murakami, Y., Mulder, L., Vickers, K., Pike, J., Downie, J.A., Wang, T., Sato, S., Asamizu, E., Tabata, S., Yoshikawa, M., Murooka, Y., Wu, G.-J., Kawaguchi, M., Kawasaki, S., Parniske, M., and Hayashi, M. (2005). Plastid proteins crucial for symbiotic fungal and bacterial entry into plant roots. Nature **433,** 527-531.

Isayenkov, S., Mrosk, C., Stenzel, I., Strack, D., and Hause, B. (2005). Suppression of allene oxide cyclase in hairy roots of Medicago truncatula reduces jasmonate levels and the degree of mycorrhization with Glomus intraradices. Plant Physiol **139,** 1401-1410.

Ishida, T., Kurata, T., Okada, K., and Wada, T. (2008). A genetic regulatory network in the development of trichomes and root hairs. Annu Rev Plant Biol **59,** 365-386.

Ishikawa, S., Maekawa, M., Arite, T., Onishi, K., Takamure, I., and Kyozuka, J. (2005). Suppression of tiller bud activity in tillering dwarf mutants of rice. Plant Cell Physiol **46,** 79-86.

Ito, H., and Gray, W.M. (2006). A gain-of-function mutation in the Arabidopsis pleiotropic drug resistance transporter PDR9 confers resistance to auxinic herbicides. Plant Physiol **142,** 63-74.

Jasinski, M., Stukkens, Y., Degand, H., Purnelle, B., Marchand-Brynaert, J., and Boutry, M. (2001). A plant plasma membrane ATP binding cassette-type transporter is involved in antifungal terpenoid secretion. Plant Cell **13,** 1095-1107.

Javot, H., Penmetsa, R.V., Terzaghi, N., Cook, D.R., and Harrison, M.J. (2007). A Medicago truncatula phosphate transporter indispensable for the arbuscular mycorrhizal symbiosis. Proc Natl Acad Sci U S A **104,** 1720-1725.

Johnson, X., Brcich, T., Dun, E.A., Goussot, M., Haurogne, K., Beveridge, C.A., and Rameau, C. (2006). Branching genes are conserved across species. Genes controlling a novel signal in pea are coregulated by other long-distance signals. Plant Physiol **142,** 1014-1026.

Kapteyn, J., Qualley, A.V., Xie, Z., Fridman, E., Dudareva, N., and Gang, D.R. (2007). Evolution of Cinnamate/p-coumarate carboxyl methyltransferases and their role in the biosynthesis of methylcinnamate. Plant Cell **19,** 3212-3229.

Kessler, D., Gase, K., and Baldwin, I.T. (2008). Field experiments with transformed plants reveal the sense of floral scents. Science **321,** 1200-1202.

Kim, D.-Y., Bovet, L., Maeshima, M., Martinoia, E., and Lee, Y. (2007). The ABC transporter AtPDR8 is a cadmium extrusion pump conferring heavy metal resistance. Plant J **50,** 207-218.

Kistner, C., and Parniske, M. (2002). Evolution of signal transduction in intracellular symbiosis. Trends Plant Sci **7,** 511-518.

Kistner, C., Winzer, T., Pitzschke, A., Mulder, L., Sato, S., Kaneko, T., Tabata, S., Sandal, N., Stougaard, J., Webb, K.J., Szczyglowski, K., and Parniske, M. (2005). Seven Lotus japonicus genes required for transcriptional reprogramming of the root during fungal and bacterial symbiosis. Plant Cell **17,** 2217-2229.

Klein, I., Sarkadi, B., and Varadi, A. (1999). An inventory of the human ABC proteins. Biochim Biophys Acta **1461,** 237-262.

Klein, M., Burla, B., and Martinoia, E. (2006). The multidrug resistance-associated protein (MRP/ABCC) subfamily of ATP-binding cassette transporters in plants. FEBS Lett **580,** 1112-1122.

Kobae, Y., Sekino, T., Yoshioka, H., Nakagawa, T., Martinoia, E., and Maeshima, M. (2006). Loss of AtPDR8, a plasma membrane ABC transporter of Arabidopsis thaliana, causes hypersensitive cell death upon pathogen infection. Plant Cell Physiol **47,** 309-318.

Koeduka, T., Fridman, E., Gang, D.R., Vassao, D.G., Jackson, B.L., Kish, C.M., Orlova, I., Spassova, S.M., Lewis, N.G., Noel, J.P., Baiga, T.J., Dudareva, N., and Pichersky, E. (2006). Eugenol and isoeugenol, characteristic aromatic constituents of spices, are biosynthesized via reduction of a coniferyl alcohol ester. Proc Natl Acad Sci U S A **103,** 10128-10133.

Koes, R., Souer, E., van Houwelingen, A., Mur, L., Spelt, C., Quattrocchio, F., Wing, J., Oppedijk, B., Ahmed, S., and Maes, T. (1995). Targeted gene inactivation in petunia by PCR-based selection of transposon insertion mutants. Proc Natl Acad Sci U S A **92,** 8149-8153.

Kogel, K.-H., Franken, P., and Hückelhoven, R. (2006). Endophyte or parasite - what decides? Current Opinion in Plant Biology **9,** 358-363.

Kosuta, S., Chabaud, M., Lougnon, G., Gough, C., Denarie, J., Barker, D.G., and Becard, G. (2003). A diffusible factor from arbuscular mycorrhizal fungi induces symbiosis-specific MtENOD11 expression in roots of Medicago truncatula. Plant Physiol **131,** 952-962.

Kramer, E.M. (2004). PIN and AUX/LAX proteins: their role in auxin accumulation. Trends in Plant Science **9,** 578-582.

Krattinger, S.G., Lagudah, E.S., Spielmeyer, W., Singh, R.P., Huerta-Espino, J., McFadden, H., Bossolini, E., Selter, L.L., and Keller, B. (2009). A Putative ABC Transporter Confers Durable Resistance to Multiple Fungal Pathogens in Wheat. Science **323**, 1360-1363.

Krupinska, K., Haussuhl, K., Schafer, A., van der Kooij, T.A.W., Leckband, G., Lorz, H., and Falk, J. (2002). A novel nucleus-targeted protein is expressed in barley leaves during senescence and pathogen infection. Plant Physiol **130,** 1172-1180.

Larkin, J.C., Brown, M.L., and Schiefelbein, J. (2003). How do cells know what they want to be when they grow up? Lessons from epidermal patterning in Arabidopsis. Annu Rev Plant Biol **54,** 403-430.

Lee, M., Lee, K., Lee, J., Noh, E.W., and Lee, Y. (2005). AtPDR12 contributes to lead resistance in Arabidopsis. Plant Physiol **138,** 827-836.

Leppert, G., McDevitt, R., Falco, S.C., Van Dyk, T.K., Ficke, M.B., and Golin, J. (1990). Cloning by gene amplification of two loci conferring multiple drug resistance in Saccharomyces. Genetics **125,** 13-20.

Levy, J., Bres, C., Geurts, R., Chalhoub, B., Kulikova, O., Duc, G., Journet, E.-P., Ane, J.-M., Lauber, E., Bisseling, T., Denarie, J., Rosenberg, C., and Debelle, F. (2004). A putative Ca2+ and calmodulin-dependent protein kinase required for bacterial and fungal symbioses. Science **303,** 1361-1364.

Leyser, O. (2005). The fall and rise of apical dominance. Current Opinion in Genetics & Development Pattern formation and developmental mechanisms **15,** 468-471.

Leyser, O. (2009). The Control of Shoot Branching: An example of plant information processing. Plant Cell Environ.[Epub ahead of print]

Lopez-Raez, J.A., Charnikhova, T., Gomez-Roldan, V., Matusova, R., Kohlen, W., De Vos, R., Verstappen, F., Puech-Pages, V., Becard, G., Mulder, P., and Bouwmeester, H. (2008). Tomato strigolactones are derived from carotenoids and their biosynthesis is promoted by phosphate starvation. New Phytol **178,** 863-874.

Luo, B., Xue, X.-Y., Hu, W.-L., Wang, L.-J., and Chen, X.-Y. (2007). An ABC transporter gene of Arabidopsis thaliana, AtWBC11, is involved in cuticle development and prevention of organ fusion. Plant Cell Physiol **48,** 1790-1802.

Lutke, W.K. (2006). Petunia (Petunia hybrida). Methods Mol Biol **344,** 339-349.

Maier, W., Peipp, H., Schmidt, J., Wray, V., and Strack, D. (1995). Levels of a terpenoid glycoside (blumenin) and cell wall-bound phenolics in some cereal mycorrhizas. Plant Physiol **109,** 465-470.

Maria J. Harrison, R.A.D. (1994). Spatial patterns of expression of flavonoid/isoflavonoid pathway genes during interactions between roots of Medicago truncatula and the mycorrhizal fungus Glomus versiforme. The Plant Journal **6,** 9-20.

Matusova, R., Rani, K., Verstappen, F.W.A., Franssen, M.C.R., Beale, M.H., and Bouwmeester, H.J. (2005). The strigolactone germination stimulants of the plant-parasitic Striga and Orobanche spp. are derived from the carotenoid pathway. Plant Physiol **139,** 920-934.

McCall, A.C. (2008). Florivory affects pollinator visitation and female fitness in Nemophila menziesii. Oecologia **155,** 729-737.

McCall, A.C., and Irwin, R.E. (2006). Florivory: the intersection of pollination and herbivory. Ecol Lett **9,** 1351-1365.

Mentewab, A., and Stewart, C.N. (2005). Overexpression of an Arabidopsis thaliana ABC transporter confers kanamycin resistance to transgenic plants. Nat Biotechnol **23,** 1177-1180.

Meyers, S., Schauer, W., Balzi, E., Wagner, M., Goffeau, A., and Golin, J. (1992). Interaction of the yeast pleiotropic drug resistance genes PDR1 and PDR5. Curr Genet **21,** 431-436.

Moons, A. (2003). Ospdr9, which encodes a PDR-type ABC transporter, is induced by heavy metals, hypoxic stress and redox perturbations in rice roots. FEBS Lett **553,** 370-376.

Moons, A. (2008). Transcriptional profiling of the PDR gene family in rice roots in response to plant growth regulators, redox perturbations and weak organic acid stresses. Planta **229,** 53-71.

Nagahashi, G., and Douds, D.D. (1999). Rapid and sensitive bioassay to study signals between root exudates and arbuscular mycorrhizal fungi. Biotechnology Techniques **13,** 893-897.

Nagy, R., Karandashov, V., Chague, V., Kalinkevich, K., Tamasloukht, M.b., Xu, G., Jakobsen, I., Levy, A.A., Amrhein, N., and Bucher, M. (2005). The characterization of novel mycorrhiza-specific phosphate transporters from Lycopersicon esculentum and Solanum tuberosum uncovers functional redundancy in symbiotic phosphate transport in solanaceous species. Plant J **42,** 236-250.

Napoli, C. (1996). Highly Branched Phenotype of the Petunia dad1-1 Mutant Is Reversed by Grafting. Plant Physiol **111,** 27-37.

Ongaro, V., and Leyser, O. (2008). Hormonal control of shoot branching. J Exp Bot **59,** 67-74.

Otsu, C.T., daSilva, I., de Molfetta, J.B., da Silva, L.R., de Almeida-Engler, J., Engler, G., Torraca, P.C., Goldman, G.H., and Goldman, M.H.S. (2004). NtWBC1, an ABC transporter gene specifically expressed in tobacco reproductive organs. J Exp Bot **55,** 1643-1654.

Panikashvili, D., Savaldi-Goldstein, S., Mandel, T., Yifhar, T., Franke, R.B., Hofer, R., Schreiber, L., Chory, J., and Aharoni, A. (2007). The Arabidopsis DESPERADO/AtWBC11 transporter is required for cutin and wax secretion. Plant Physiol **145,** 1345-1360.

Parniske, M. (2008). Arbuscular mycorrhiza: the mother of plant root endosymbioses. Nat Rev Microbiol **6,** 763-775.

Paszkowski, U. (2006). Mutualism and parasitism: the yin and yang of plant symbioses. Current Opinion in Plant Biology Biotic interactions / edited by Anne Osbourn and Sheng Yang He **9,** 364-370.

Paszkowski, U., Kroken, S., Roux, C., and Briggs, S.P. (2002). Rice phosphate transporters include an evolutionarily divergent gene specifically activated in arbuscular mycorrhizal symbiosis. Proc Natl Acad Sci U S A **99,** 13324-13329.

Pighin, J.A., Zheng, H., Balakshin, L.J., Goodman, I.P., Western, T.L., Jetter, R., Kunst, L., and Samuels, A.L. (2004). Plant cuticular lipid export requires an ABC transporter. Science **306,** 702-704.

Pozo, M.J., and Azcon-Aguilar, C. (2007). Unraveling mycorrhiza-induced resistance. Curr Opin Plant Biol **10,** 393-398.

Rausch, C., Daram, P., Brunner, S., Jansa, J., Laloi, M., Leggewie, G., Amrhein, N., and Bucher, M. (2001). A phosphate transporter expressed in arbuscle-containing cells in potato. Nature **414,** 462-470.

Rea, P.A. (2007). Plant ATP-binding cassette transporters. Annu Rev Plant Biol **58,** 347-375.

Reddy, S., Schorderet, M., Feller, U., and Reinhardt, D. (2007). A petunia mutant affected in intracellular accommodation and morphogenesis of arbuscular mycorrhizal fungi. Plant J **51,** 739-750.

Remy, W., Taylor, T.N., Hass, H., and Kerp, H. (1994). Four hundred-million-year-old vesicular arbuscular mycorrhizae. Proc Natl Acad Sci U S A **91,** 11841-11843.

Rugutt, J.K., Yarabe, H.H., Shamsi, S.A., Billodeaux, D.R., Fronczek, F.R., and Warner, I.M. (2000). GR 24 enantiomers: synthesis, NMR spectroscopy, X-ray crystallography, and separation by chiral electrokinetic capillary chromatography. Anal Chem **72,** 3887-3895.

Sasabe, M., Toyoda, K., Shiraishi, T., Inagaki, Y., and Ichinose, Y. (2002). cDNA cloning and characterization of tobacco ABC transporter: NtPDR1 is a novel elicitor-responsive gene. FEBS Lett **518,** 164-168.

Sato, D., Awad, A.A., Takeuchi, Y., and Yoneyama, K. (2005). Confirmation and quantification of strigolactones, germination stimulants for root parasitic plants Striga and Orobanche, produced by cotton. Biosci Biotechnol Biochem **69,** 98-9102.

Schellmann, S., and Hulskamp, M. (2005). Epidermal differentiation: trichomes in Arabidopsis as a model system. Int J Dev Biol **49,** 579-584.

Schilmiller, A.L., Last, R.L., and Pichersky, E. (2008). Harnessing plant trichome biochemistry for the production of useful compounds. Plant J **54,** 702-711.

Shibuya, K., Barry, K.G., Ciardi, J.A., Loucas, H.M., Underwood, B.A., Nourizadeh, S., Ecker, J.R., Klee, H.J., and Clark, D.G. (2004). The central role of PhEIN2 in ethylene responses throughout plant development in petunia. Plant Physiol **136,** 2900-2912.

Sieburth, L.E., and Deyholos, M.K. (2006). Vascular development: the long and winding road. Current Opinion in Plant Biology Growth and development / edited by David R Smyth and Thomas Berleth **9,** 48-54.

Simons, J.L., Napoli, C.A., Janssen, B.J., Plummer, K.M., and Snowden, K.C. (2007). Analysis of the DECREASED APICAL DOMINANCE genes of petunia in the control of axillary branching. Plant Physiol **143,** 697-706.

Slocombe, S.P., Schauvinhold, I., McQuinn, R.P., Besser, K., Welsby, N.A., Harper, A., Aziz, N., Li, Y., Larson, T.R., Giovannoni, J., Dixon, R.A., and Broun, P. (2008). Transcriptomic and Reverse Genetic Analysesof Branched-Chain Fatty Acid and Acyl Sugar Production in Solanum pennellii and Nicotiana benthamiana,. Plant Physiol **148,** 1830-1846.

Smart, C.C., and Fleming, A.J. (1996). Hormonal and environmental regulation of a plant PDR5-like ABC transporter. J Biol Chem **271,** 19351-19357.

Snowden, K.C., and Napoli, C.A. (2003). A quantitative study of lateral branching in petunia. Functional Plant Biology **30,** 987-994.

Snowden, K.C., Simkin, A.J., Janssen, B.J., Templeton, K.R., Loucas, H.M., Simons, J.L., Karunairetnam, S., Gleave, A.P., Clark, D.G., and Klee, H.J. (2005). The Decreased apical dominance1/Petunia hybrida CAROTENOID CLEAVAGE DIOXYGENASE8 gene affects branch production and plays a role in leaf senescence, root growth, and flower development. Plant Cell **17,** 746-759.

Sorefan, K., Booker, J., Haurogne, K., Goussot, M., Bainbridge, K., Foo, E., Chatfield, S., Ward, S., Beveridge, C., Rameau, C., and Leyser, O. (2003). MAX4 and RMS1 are orthologous dioxygenase-like genes that regulate shoot branching in Arabidopsis and pea. Genes Dev **17,** 1469-1474.

Spitzer, B., Zvi, M.M.B., Ovadis, M., Marhevka, E., Barkai, O., Edelbaum, O., Marton, I., Masci, T., Alon, M., Morin, S., Rogachev, I., Aharoni, A., and Vainstein, A. (2007). Reverse genetics of floral scent: application of tobacco rattle virus-based gene silencing in Petunia. Plant Physiol **145,** 1241-1250.

Sprague, S.J., Watt, M., Kirkegaard, J.A., and Howlett, B.J. (2007). Pathways of infection of Brassica napus roots by Leptosphaeria maculans. New Phytol **176,** 211-222.

Stein, M., Dittgen, J., Sanchez-Rodriguez, C., Hou, B.-H., Molina, A., Schulze-Lefert, P., Lipka, V., and Somerville, S. (2006). Arabidopsis PEN3/PDR8, an ATP binding cassette transporter, contributes to nonhost resistance to inappropriate pathogens that enter by direct penetration. Plant Cell **18,** 731-746.

Steinkellner, S., Lendzemo, V., Langer, I., Schweiger, P., Khaosaad, T., Toussaint, J.-P., and Vierheilig, H. (2007). Flavonoids and strigolactones in root exudates as signals in symbiotic and pathogenic plant-fungus interactions. Molecules **12,** 1290-1306.

Steppuhn, A., Schuman, M.C., and Baldwin, I.T. (2008). Silencing jasmonate signalling and jasmonate-mediated defences reveals different survival strategies between two Nicotiana attenuata accessions. Mol Ecol **17,** 3717-3732.

Stirnberg, P., Furner, I.J., and Ottoline Leyser, H.M. (2007). MAX2 participates in an SCF complex which acts locally at the node to suppress shoot branching. Plant J **50,** 80-94.

Stracke, S., Kistner, C., Yoshida, S., Mulder, L., Sato, S., Kaneko, T., Tabata, S., Sandal, N., Stougaard, J., Szczyglowski, K., and Parniske, M. (2002). A plant receptor-like kinase required for both bacterial and fungal symbiosis. Nature **417,** 959-962.

Stukkens, Y., Bultreys, A., Grec, S., Trombik, T., Vanham, D., and Boutry, M. (2005). NpPDR1, a pleiotropic drug resistance-type ATP-binding cassette transporter from Nicotiana plumbaginifolia, plays a major role in plant pathogen defense. Plant Physiol **139,** 341-352.

Stuurman, J., and Kuhlemeier, C. (2005). Stable two-element control of dTph1 transposition in mutator strains of Petunia by an inactive ACT1 introgression from a wild species. Plant J **41,** 945-955.

Sugiyama, A., Shitan, N., Sato, S., Nakamura, Y., Tabata, S., and Yazaki, K. (2006). Genome-wide analysis of ATP-binding cassette (ABC) proteins in a model legume plant, Lotus japonicus: comparison with Arabidopsis ABC protein family. DNA Res **13,** 205-228.

Tawaraya, K., Hashimoto, K., and Wagatsuma, T. (1998). Effect of root exudate fractions from P-deficient and P-sufficient onion plants on root colonisation by the arbuscular mycorrhizal fungus Gigaspora margarita. Mycorrhiza **8,** 67-70.

Teale, W.D., Paponov, I.A., and Palme, K. (2006). Auxin in action: signalling, transport and the control of plant growth and development **7,** 847-859.

Tejeda-Sartorius, M., Martinez de la Vega, O., and Delano-Frier, J.P. (2008). Jasmonic acid influences mycorrhizal colonization in tomato plants by modifying the expression of genes involved in carbohydrate partitioning. Physiol Plant **133,** 339-353.

Trombik, T., Jasinski, M., Crouzet, J., and Boutry, M. (2008). Identification of a cluster IV pleiotropic drug resistance transporter gene expressed in the style of Nicotiana plumbaginifolia. Plant Mol Biol **66,** 165-175.

Uggla, C., Moritz, T., Sandberg, G., and Sundberg, B. (1996). Auxin as a positional signal in pattern formation in plants. Proc Natl Acad Sci U S A **93,** 9282-9286.

Ukitsu, H., Kuromori, T., Toyooka, K., Goto, Y., Matsuoka, K., Sakuradani, E., Shimizu, S., Kamiya, A., Imura, Y., Yuguchi, M., Wada, T., Hirayama, T., and Shinozaki, K. (2007). Cytological and biochemical analysis of COF1, an Arabidopsis mutant of an ABC transporter gene. Plant Cell Physiol **48,** 1524-1533.

Umehara, M., Hanada, A., Yoshida, S., Akiyama, K., Arite, T., Takeda-Kamiya, N., Magome, H., Kamiya, Y., Shirasu, K., Yoneyama, K., Kyozuka, J., and Yamaguchi, S. (2008). Inhibition of shoot branching by new terpenoid plant hormones. Nature **455,** 195-200.

Van Dam, N.M., and Hare, J.D. (1998). Biological Activity of Datura wrightii Glandular Trichome Exudate Against Manduca Sexta Larvae. Journal of Chemical Ecology **24,** 1529-1549.

Van den Broeck, D., Maes, T., Sauer, M., Zethof, J., De Keukeleire, P., D'hauw, M., Van Montagu, M., and Gerats, T. (1998). Transposon Display identifies individual transposable elements in high copy number lines. Plant J **13,** 121-129.

van den Brule, S., and Smart, C.C. (2002). The plant PDR family of ABC transporters. Planta **216,** 95-9106.

van den Brule, S., Muller, A., Fleming, A.J., and Smart, C.C. (2002). The ABC transporter SpTUR2 confers resistance to the antifungal diterpene sclareol. Plant J **30,** 649-662.

van Schie, C.C.N., Haring, M.A., and Schuurink, R.C. (2007). Tomato linalool synthase is induced in trichomes by jasmonic acid. Plant Mol Biol **64,** 251-263.

Vandenbussche, M., and Gerats, T. (2004). TE-based mutagenesis systems in plants: a gene family approach. Methods Mol Biol **260,** 115-127.

Vandenbussche, M., Zethof, J., Souer, E., Koes, R., Tornielli, G.B., Pezzotti, M., Ferrario, S., Angenent, G.C., and Gerats, T. (2003). Toward the analysis of the petunia MADS box gene family by reverse and forward transposon insertion mutagenesis approaches: B, C, and D floral organ identity functions require SEPALLATA-like MADS box genes in petunia. Plant Cell **15,** 2680-2693.

Vandenbussche, M., Janssen, A., Zethof, J., van Orsouw, N., Peters, J., van Eijk, M.J.T., Rijpkema, A.S., Schneiders, H., Santhanam, P., de Been, M., van Tunen, A., and Gerats, T. (2008). Generation of a 3D indexed Petunia insertion database for reverse genetics. Plant J. [Epub ahead of print]

Verdonk, J.C., Haring, M.A., van Tunen, A.J., and Schuurink, R.C. (2005). ODORANT1 regulates fragrance biosynthesis in petunia flowers. Plant Cell **17,** 1612-1624.

Verdonk, J.C., Ric de Vos, C.H., Verhoeven, H.A., Haring, M.A., van Tunen, A.J., and Schuurink, R.C. (2003). Regulation of floral scent production in petunia revealed by targeted metabolomics. Phytochemistry **62,** 997-991008.

Verrier, P.J., Bird, D., Burla, B., Dassa, E., Forestier, C., Geisler, M., Klein, M., Kolukisaoglu, Ü., Lee, Y., Martinoia, E., Murphy, A., Rea, P.A., Samuels, L., Schulz, B., Spalding, E.J., Yazaki, K., and Theodoulou, F.L. (2008). Plant

ABC proteins - a unified nomenclature and updated inventory. Trends in Plant Science **13,** 151-159.

Vierheilig, H. (2004). Further root colonization by arbuscular mycorrhizal fungi in already mycorrhizal plants is suppressed after a critical level of root colonization. J Plant Physiol **161,** 339-341.

Vierheilig, H., Coughlan, A., Wyss, U., and Piche, Y. (1998a). Ink and vinegar, a simple staining technique for arbuscular-mycorrhizal fungi. Appl Environ Microbiol **64,** 5004-5007.

Vierheilig, H., Bago, B., Albrecht, C., Poulin, M.J., and Piche, Y. (1998b). Flavonoids and arbuscular-mycorrhizal fungi. Adv Exp Med Biol **439,** 9-33.

Wang, E., and Wagner, G.J. (2003). Elucidation of the functions of genes central to diterpene metabolism in tobacco trichomes using posttranscriptional gene silencing. Planta **216,** 686-691.

Wang, E., Wang, R., DeParasis, J., Loughrin, J.H., Gan, S., and Wagner, G.J. (2001). Suppression of a P450 hydroxylase gene in plant trichome glands enhances natural-product-based aphid resistance. Nat Biotechnol **19,** 371-374.

Wasternack, C. (2007). Jasmonates: an update on biosynthesis, signal transduction and action in plant stress response, growth and development. Ann Bot (Lond) **100,** 681-697.

Wegmuller, S., Svistoonoff, S., Reinhardt, D., Stuurman, J., Amrhein, N., and Bucher, M. (2008). A transgenic dTph1 insertional mutagenesis system for forward genetics in mycorrhizal phosphate transport of Petunia. Plant J. [Epub ahead of print]

Wesley, S.V., Helliwell, C.A., Smith, N.A., Wang, M.B., Rouse, D.T., Liu, Q., Gooding, P.S., Singh, S.P., Abbott, D., Stoutjesdijk, P.A., Robinson, S.P., Gleave, A.P., Green, A.G., and Waterhouse, P.M. (2001). Construct design for efficient, effective and high-throughput gene silencing in plants. Plant J **27,** 581-590.

Yano, K., Yoshida, S., Muller, J., Singh, S., Banba, M., Vickers, K., Markmann, K., White, C., Schuller, B., Sato, S., Asamizu, E., Tabata, S., Murooka, Y., Perry, J., Wang, T.L., Kawaguchi, M., Imaizumi-Anraku, H., Hayashi, M., and Parniske, M. (2008). CYCLOPS, a mediator of symbiotic intracellular accommodation. Proc Natl Acad Sci U S A **105,** 20540-20545.

Yasuno, N., Takamure, I., Kidou, S.-I., Tokuji, Y., Ureshi, A.-N., Funabiki, A., Ashikaga, K., Yamanouchi, U., Yano, M., and Kato, K. (2008). Rice shoot branching requires an ATP-binding cassette subfamily G protein. New Phytol.

Zhu, Y.-Q., Xu, K.-X., Luo, B., Wang, J.-W., and Chen, X.-Y. (2003). An ATP-binding cassette transporter GhWBC1 from elongating cotton fibers. Plant Physiol **133,** 580-588.

6 Appendix

6.1 *PhPDR1* cDNA Sequence

aagaaagaaaaaaccaacaaaaaaagggaaaa**atg**gagggtggtgaagaactctttagggtgagtagtgcacgtttgagtagt
tcaaatgtgtggaggaatagtgcaatggatgtgttttcaagatcttcaagagaagctgatgatgaagaagcattaaaatgggctgc
acttgagaaacttccaacttatcttcgtattagaagaggcattctcactgaagaagaaggccaatctagagaagttgatataactaa
gcttgatttggttgaaaggaggaatccgttagagaggcttatcaagattactgatgaagataatgagaagttcttgttgaagctcaa
agaacgcattgatagagttggtcttgatcttcctacaatcgaagtacggttcgagcatttgagtgtagatgcagaagctcgggttgg
tagtagagctttaccaacagtattcaacttcactgttaacatcttagaggatttcttgaattatcttcacattcttccaaatagaaagcaa
ccattgccaatccttcatgatgtcagtggaatcatcaagccaggaagaatgacactgctcttaggaccaccaagttctggaaaaac
cacattgctattagctttggctgggaaacttgataaagatctcaaagtttcaggaagagttacatataatggccatgacatgaatga
gtttgtagcacaaagatcatctgcttatataagccaatatgatcttcatataggagaaatgacagtcagggaaacactggctttttct
gctagatgtcaaggagttggagccaaatatgaaatttggcagagctgtctaggagagagaaggaagcgaatattaagccagat
cctgatgttgatatatttatgaaggcagcatggaatgaaggacaggaggctaatgttgtaacagattatactctaaagatattggga
cttgaaatttgtgccgataccattgttggagacgaaatggttcgaggaatttctgggggacagagaaagagactaacaacaggg
gagatgatggttggaccagcaagagcacttttatggatgagatatcaactggtttagacagttcaacaacctatcagattgtaaatt
caattaggcaatcaatacacattcttcaaggaactgctgtaatctcacttctgcagcctgcaccagaaacttatgacttgttcgatgat
attattcttctatcagatggacaaattgtgtaccaaggtccccgagaaaatgtactcgagttctttgagtacatgggcttcatatgccc
cgagaggaaaggagttgctgatttcttacaagaagtaacctcaaggaaggatcaagagcaatactgggcacgtcgtgaggagt
cttataagtttattacagtgcgcgaattttctgaagcatttcaagcatttcacattggaaggaagcttggtgatgagcttgctgtacctt
ttgacaaatccaagagccaccctgccgctctaaccaccaagaggtatggtgttagcaagaaagaactcttaaaagcctgtacag
ctagagaataccttcttatgaagaggaattcgttcgtctatatattcaagatgatacaactaacattgatggcttctataacaatgaca
ctgttcttaccaactgagatgcacagaaacacaacaatagatggtgctgtattcttgggtgcactgttctatgcattgatcatgattat
gttcaatggattctcagaacttgccctcagtataatgaagcttccatccttttacaaacatcgcgatctacttttctttcctccttgggca
tatgctttgcctacttggatcctcaagataccgatcacacttgtagaagttgccatttgggtgtgtatgacttattatgtaattggattcg
aggcagatgttgggaggtttttcaaacagctacttctgctcatatgtgttaaccagatggcctctgggctatttcgactcatgggagc
tcttggaaggaatatcattgttgcaaatacatttggatcatttgtactactcacggttcttgtgatgggtggattcgttctgtcaagagat
gatgtgaaaaaatggtggatatggggttattggatttcgcctatgatgtatgcacagaatgctatagctgtgaatgaatttctaggga
agagttgggcacatgttcctcctaactccacgtccacggagacattaggggtatctttcttgaaatcgcgtggaatctttccagatg
caagatggtattggattggagcaggagcgcttattggatatgtttttctcttcaatttcctgtttgcagtggccttagcttatctcaaccc
atttggtaaacctcaggcagttctttcggaagaaactgtggccgaaaggaacgcaagcaaaaggggtgaggttattgaactatct
tcgcttggaaagagctcttctgaaaaaggaaatgatgttcggcgaagtgcatcttccaggtcaatgtcctcaagagtaggaagcat
cactgcggctgatttgagcaagagaaggggaatgatccttccttttgagccccttttctattacttttgatgatatcagatatgcagtag
atatgccacaggaaatgaaagctcaaggttttaccgaggaccggcttgaactcttgagaggtgtgagcggtgcttttaggccagg
agttttgacagctctgatgggtgttagtggagctggtaagaccaccccttatggatgtattagctggtcggaagactggtggatacat
tgacggaacgatcagtatatcagggtacccaaagcagcaagaaacgtttgctcggatagcaggatactgtgagcaaactgacat
tcattcacctcatgttacagtatacgaatcattgcagttctctgcttggcttcgactgcctcgtgaagttgacactgcaacccgaaag
atgttcattgaagaggtcatggaactcatagagctaatccccctgagagacgcacttgttggattgcctggagtgaatggtctttca
actgaacaacgaaaacggctcacagttgcagttgaacttgttgccaacccttctataatattcatggatgagccaacctctggatta
gatgctagagcagctgctatagtgatgagaactgttagaaacactgtagatacaggtcgaacagtggtatgtacaatccatcagc
ctagcattgacatatttgatgcttttgatgagctcctactcctgaaacgaggaggcgaagaaatttatgtcggcccattaggacgcc
agtcttctcaccttattaagtattttgagggaattgatggagtaccaaaaatcaaagatggttataatccagcaacatggatgttgga
gataacttcagtagcgcaagaaggagctcttggaaatgactttacagaattgtacaagaactcagagttgtataggagaaacaaa
gcattgatcaaggaactgagtgtgccagcctcatgttcaaaggacctgtactttccaactaaatactcccagtctttcttcacccaat

gcatggcttgtttctggaaacagcactggtcatactggagaaatcctccttataccgcagttaggattatgtttacattcttcattgctc
tcatgttcggaacaatattttgggatcttggctccagaagggaaaggcaacaagatcttcttaatgcaataggttcaatgtatattgc
agtcttgtttcttggtgtacaaaatgctactacagtgcagccggttattgccattgagagaacagtcttttatagggaaagagcagct
ggaatgtattcagctatgccttatgcttttggacaggttatgattgagctcctttacctttcctccaaacgatcatttatggtgttatagt
ctatgccatgattggatttgaatggacagttgccaagttcttttggtatctgttcttcatgtactttaccttgttatacttcacattgtatgg
gatgatgacagtagcagttactcctaatcatagcattgcggccatcatttcatctgcattttatgcagtatggaacctttctgtggatt
catcgttccaaaaacaagaatgccagtgtggtggagatggtactattacatttgccccatttcctggacattatatggactaattgcc
tcacaatttggagacatacaagacagacttgacacaaatgagacagtggaacaattcatagagaatttctttgatttcaaacatgatt
ttgtgggatatgttgctctcattcttgttgggatttctgttcttttctcttcatttttgcattttcaattaaaacatttaatttccagaaaaga**t**
aggttggtccaggtatacacatgaaaagagcgtttatcaagatatgtgtatattaggataataatataatctttctttttcctctttttttact
tattgtggttttctcaagtttggaatagatagaaccaaaagtctgtactctgtatttaagaacaacttttgtacacattgttatgtattgga
gaagttatgagtatcttttgcaaaaaaaaaaaaaaaaaaaaa

Start ATG and Stop TAG are marked in bold and underlined

6.2 PhPDR1 Amino Acid Sequence

meggeelfrvssarlsssnvwrnsamdvfsrssreaddeealkwaaleklptylrirrgilteeegqsrevditkldlverrnpl
erlikitdednekfllklkeridrvgldlptievrfehlsvdaearvgsralptvfnftvniledflnylhilpnrkqplpilhdvsgi
ikpgrmtlllgppssgkttlllalagkldkdlkvsgrvtynghdmnefvaqrssayisqydlhigemtvretlafsarcqgvga
kyeilaelsrrekeanikpdpdvdifmkaawnegqeanvvtdytlkilgleicadtivgdemvrgisggqrkrlttgemmv
gparalfmdeistgldssttyqivnsirqsihilqgtavisllqpapetydlfddiillsdgqivyqgprenvleffeymgficper
kgvadflqevtsrkdqeqywarreesykfitvrefseafqafhigrklgdelavpfdkskshpaalttkrygvskkellkactar
eyllmkrnsfvyifkmiqltlmasitmtlflptemhrnttidgavflgalfyalimimfngfselalsimklpsfykhrdllffp
pwayalptwilkipitlvevaiwvcmtyyvigfeadvgrffkqllllicvnqmasglfrlmgalgrniivantfgsfvlltvlv
mggfvlsrddvkkwwiwgywispmmyaqnaiavneflgkswahvppnststetlgvsflksrgifpdarwywigaga
ligyvflfnflfavalaylnpfgkpqavlseetvaernaskrgevielsslgkssekgndvrrsassrsmssrvgsitaadlskrr
gmilpfeplsitfddiryavdmpqemkaqgftedrlellrgvsgafrpgvltalmgvsgagkttlmdvlagrktggyidgtisi
sgypkqqetfariagyceqtdihsphvtvyeslqfsawlrlprevdtatrkmfieevmelieliplrdalvglpgvnglsteqrk
rltvavelvanpsiifmdeptsgldaraaaivmrtvrntvdtgrtvvctihqpsidifdafdellllkrggeeiyvgplgrqsshli
kyfegidgvpkikdgynpatwmleitsvaqegalgndftelyknselyrrnkalikelsvpascskdlyfptkysqsfftqc
macfwkqhwsywrnppytavrimftffialmfgtifwdlgsrrerqqdllnaigsmyiavlflgvqnattvqpviaiertvf
yreraagmysampyafgqvmiellylflqtiiygvivyamigfewtvakffwylffmyftllyftlygmmtvavtpnhsia
aiissafyavwnlfcgfivpktrmpvwwrwyyyicpiswtlygliasqfgdiqdrldtnetveqfienffdfkhdfvgyvali
lvgisvlflfifafsiktfnfqkr

6.3 *PhPDR1* Promoter Sequence

acaccacctgtaaaaaaatagtaaaaacagcacccagaagaagattaggcttctacaagccttaatttttttctaaacaaggcttatt
gcctttgaactgaaactttaataatttacataacatcaataattcatagtgattcaaacaagttaatacatgtctaaaacaagtctaaaa
catcaacaatctattattactactccgttgcctcagaactagactcagaacccgactcagacgatgagctgtattgacgtttgcttttg
cctttccccgggctcttggtcttgctcttgctcttgctcttgctcttgcctttgcccttgcccttgcccttctttcgcttgtccgcactacc
acacataatattctgcatcatttcccgcatggctctcatattttcctcattgcgcagacgttcttcttcactctttctcttaagctcttcgatt
tcaacaaccgcaaaaatgttcatctccaaaaattgatacaacaacaaagttcattatcactactaccaaaataggatccacaaaaat
gttcatttccaacttacaattattcaacaacaacaatattcaacaaccacaaaaaaattcattaactccattatcaactttcaaattttcc

aacaatatcaaccccaataccaagactacacactatacttttcaattcaaaatctaatttttattcaatttaaacaacaaaattaacccc
aacaatatcctcattatttttttctttctcgttttcaatttttgcctacaaagttaacaactcaacattccataacaactccaaaggctaaat
ccaaaacaaaaccaaagtttcaaagtgtatcactattttctcaattttctaccaaaatccaaaacaacaatttacaactaaaccaaca
agttgccatataaatttataatttttatataccaaataacccaacaatttacaactttcattactcacatatgaatgttcattactcacttga
aaacataaatagaaaaataaaaaaaagaaaaaaatagaaaaaaacgtaacctgtttgtagctgccggatttaagtacaacaccct
gcgggtccggtggtctctccactggatctgcaacaaaaaaaaagaacgttagggtttgtaagttttggatgaaaaaaatgagaaat
atgaaatttttagaagtatttatatttaaagaattaggataaaattaacatgtaatcagtaagacttgagataaaagcaagacagaag
tatatatggggttgttgaggatgcctaatgagttagtttgaacaaaatcataaccacaaagttcctcaacttatgcatatttattctcta
agctattattctttattatgtcttttattagtatatatgacttttgtttttacctattttggttgaacagtagtgggaggatgatcatgaaacat
aacctcaaatattcaattatgataataattaagctagttagcggtcaacaaactttggcatcactgattttgtttgcatcaactcttacgt
caaatcactaaaatagtatctctcgaagctgaccctctattatattctatagtctccattaaatacatctctctacctacgtatatataaat
cacaccctcctttacaaaactttcaagcatcaaagcccctcctaccagaaaaggaggaggatttaaatgatcaaaaagattccattt
gaattatacttaccagtttttaaactctcatttgtcttttgtctcattgagctacaaaataaaagtacctactttcctcttaatgtgaagtaa
gaaagaaaaaaccaacaaaaaaagggaaaa**atg**

PhPDR1 transcipt start in bold and underlined

6.4 *PhPDR2* cDNA Sequence

agcaactcttacttttttcctttcattctttttatttttctctttcagatcattcacttgaaaaaaacgaaaactcaagaacatatttctgagcta
gaggggtctgaaaatataatttgcatgttgattggttcata**atg**gaaccagtaaacttaggtaacttacgagcggctagtttgaga
ggaagtgcaaggggaagtttaagcggaagtttaagagcaaatagtaactctatatggagaaatgataatgttttcactcgttcatca
agagatgaaaatgatgaagaagcacttaaatgggcagctcttgaaaaacttccaacatttgatcgtttaagaaaaggtttgttgtttg
gatctgaaggtacagcaccttctcaaattgatatacatgatattggttttcaagaaagacaaggtttgcttgataggcttgtgaaagat
cctgatgaagataatgagaagttcttgttgaaactcagagatagaattgacagagttgggctggattttccaacaatagaagtaag
atatgagcatctacatgttgtggcagatgcacatgtaggaggcagagctttgcctacatttacaaactttgtgactaattttcttgagt
cattgttgacctctctccatatcctaccaagtaaaaagaggaagctcactattcttaatgatgtgagtggtatcattaagccttgcaga
ctgactttgcttttgggacctcctggttctggcaaaactacttttttattagctttggctggaaagcttgatcctgaacttaaggtaactg
ggaaggtaacctataatggacatgaaatgactgaatttgtaccacaaagaactgctgcttatattagccagcatgatttgcatattgg
agaaatgactgtgagagaaaccttggaattctctgccagatgccaaggcattggcactcgttatgagatgttggctgaactgtcaa
gaagagagaaggcagctaatatcaagccagaccctgatattgatatctatatgaaggcatcagcaacagagggacaagaagca
aatgttgtaacagattatgttcttaagatattgggactggacatttgtgcagatactttggtgggagatgacatggtaaggggcatttc
aggaggacaaaagaagcgtgtgacaaccggtgaaatgcttgttggaccgtcaaaggcacttttcatggatgaaatctcaactgg
attggatagttccaccacttactctattgtgaactctctaaggcaaactgtgcaaatcttgaaggaaactgctgtcatatctctcttgca
gccagcacccgagacctacaatttgtttgatgacattattctgttaacagatggtttagttgtctatcaaggccctcgtgaagacgttc
tggccttcttcgaatccatgggtttcaaatgccctgatagaaagggcgtggccgacttcttgcaagaagtgacatcaaagaaggat
caacagcaatattgggcgaggagggatgagccttacaggtttatcacatcaaaagaatttgctgaggcgtatcaatcattccatgtt
ggaaggaaacaactggatgagcttggagctcatttgacagagcaaagccatcctgctgcattgtcaaatcaaaagtacggtattg
ggaagaaacaactcttaaaggtctgcactgaaagagaatacctgctaatgaagaggaactcatttctttttatattcaagttctttcag
cttttaattatggcaatcctgacgatgaccatgtttctccgaactgagatgcaccataatactgaggaggatggtggaacatacgtt
ggtgctctctttttttgtaatcgttatgattatgtttaatggaatgactgagcttggcatggtacttttttaagcttcccgtcttctacaagca
aagagacctcttcttttacccctcatgggcttatgcaattccctcatggatactcaaaatccctataacatttgttgaagttgctctttgg
gtgttcctcacttactatgtcattggatttgatccgaacccagaaagattgttcaaacagttcttcctactcataatagtaaaccagatg
gcatcagggttgtttcgattcataggggcagctggcaggaccttgggtattgctgctacatttggagcttttgctctgcttttacaattt
gcattgggtggattcgtcctttcacgagatatgatgaagaaatggtggatatggggttactggacttcaccgatgatgtattctgtga
atgcaatccttgtgaatgaatttcatgggaaaaggtggagacgtattgcaccaaatggaactgagccacttggagatgctgttgta

agaggccgaggcttcttcccagatgcatcctggtactggataggtgtaggggcacttattggattcacagtcctctttaacatcttgt
atagtcttgcgctcgcttatctcaacccaattggtaagccgcaagctatgatgccagaagacagtgaagatgccaaaacaactag
cactgagaaagaaggttacaatagtgagggtcagaataagaaaaggggaatggttcttccctttgaaccacattccatcacctttg
atgatgttatttactctgttgacatgcctcaggaaatgaaagatcagggtgcctctgaagatagattggtacttctgaatggtgtaagt
ggagctttcaggcccggtgttttgacagctttgatgggagttagtggggctggaaaaacaacattgatggacgtattggctggaa
gaaaaacaggaggatatattgagggtagaatccacatttctggctatcccaagaagcaagaaacatttgcacgtatatctggatac
tgtgagcagaatgatatccattcaccttatgttacagtttatgagtcattagtatactccgcttggatgcgtttacctcatgatgttgacg
aaagaaccagaaagatgtttgttgaggaagttatggatcttgtggagctaagaccaataagatcagccttagttggtttgccagga
gtcgacggtctctcaactgagcaacgcaaaaggttgaccattgcagtggaactagttgcaaacccctctatcattttcatggatga
accaacatcagggctggatgcaagggcagctgcaattgtcatgagagctgttaggaacacagttgacactggaagaaccgttgt
ttgtaccatccatcagcctagcatcgacatttttgaagcctttgatgagctatttctaatgaaacgaggaggacaagagatatatgtt
ggtccattgggtcgcaattcatgccacttgatcaaatactttgagtcaatgcctggggtaagtaaaataaaaagatggctacatcca
gcaacttggatgttagaagtcacaaccccgggccaggaaacgatgtttggagtcgattttactgatttatacaaaaaatcagacctt
tacgggaggaacaaagcgctgattactgaactgagtgtgcctcgccctggtacaaaagacctgcattttgatactcaatactcaca
gccattttggacccaatgtatggcttgcctttggaagcaacattggtcatactggcgtaatcctgcttataccgcagtcagatttctgt
tcacagtcatgatatccttggtctttgggacaatgttctgggatcttggttctaaagtgagtagggcccaagatctatctaacgcgat
gggatgcttgtatgctgctgttctcttcattggtacacaaaatgcatcatcagtgcagcctgttgtagccgttgagcgtacagtatttt
acagagaaagagctgctggaatgtattctgccttaccctatgcctttgcccaggctttcattgaaatcccatatatatttgtgcaagct
actttctgtggtaccattatctatgctatgattggatttgaatggacagttgaaaagtacttttggtacttgttcttcatgtttttcaccctc
atgtactatacctactatggtatgatgaccgttgctattaccccaaacgtgaatgttgctcaagttgtctccgctttcttctacggcttat
ggaatcttttctcaggattcatcgttccacgacctcgtatggccatatggtggagatggtactactggatttgtcctactgcctggac
cttatatggtttgattgcatcacaatttggagattaccaaaataaacttactgatgatgaaacagtggaacaatacttgagacgcttct
tcggcttcaaacatgaatttctaccagtagttggagttgtgactgctggatttactgttctttttgccttcacatttgcttttggtatcaag
gcattcaacttccagacaaga**tag**aagaagacttgctgaacatttattaggacaatttgaaggagaacaatgttgtctcaagtgctc
gtgaaatggtggagactcggtcagtacaaggatgtttttttttttccacaagtatgtatgggcgagagatcataatgttatgacttgaa
gaagtgtattttctgttataaattgtttatgaaacttagcttttgtgtaatacagtaggtaataatttgttaatgttaaatgaaagcggcata
tttattccaaaaaaaaaaaaaaaaaaaaa

Start ATG and Stop TAG are marked in bold and underlined

6.5 PhPDR2 Amino Acid Sequence

mepvnlgnlraaslrgsargslsgslransnsiwrndnvftrssrdendeealkwaaleklptfdrlrkgllfgsegtapsqidih
digfqerqglldrlvkdpdednekfllklrdridrvgldfptievryehlhvvadahvggralptftnfvtnflesllltslhilpskk
rkltilndvsgiikpcrltlllgppgsgkttfllalagkldpelkvtgkvtynghemtefvpqrtaayisqhdlhigemtvretlef
sarcqgigtryemlaelsrrekaanikpdpdidiymkasategqeanvvtdyvlkilgldicadtlvgddmvrgisggqkkr
vttgemlvgpskalfmdeistgldssttysivnslrqtvqilketavisllqpapetynlfddiilltdglvvyqgpredvlaffes
mgfkcpdrkgvadflqevtskkdqqqywarrdepyrfitskefaeayqsfhvgrkqldelgahlteqshpaalsnqkygig
kkqllkvctereyllmkrnsflfifkffqllimailtmtmflrtemhhnteedggtyvgalffvivmimfngmtelgmvlfkl
pvfykqrdlffypswayaipswilkipitfvevalwvfltyyvigfdpnperlfkqfflliivnqmasglfrfigaagrtlgiaatf
gafalllqfalggfvlsrdmmkkwwiwgywtspmmysvnailvnefhgkrwrriapngteplgdavvrgrgffpdasw
ywigvgaligftvlfnilyslalaylnpigkpqammpedsedakttstekegynsegqnkkrgmvlpfephsitfddviysv
dmpqemkdqgasedrlvllngvsgafrpgvltalmgvsgagkttlmdvlagrktggyiegrihisgypkkqetfarisgyc
eqndihspyvtvyeslvysawmrlphdvdertrkmfveevmdlvelrpirsalvglpgvdglsteqrkrltiavelvanpsii
fmdeptsgldaraaaivmravrntvdtgrtvvctihqpsidifeafdelflmkrggqeiyvgplgrnschlikyfesmpgvsk
ikrwlhpatwmlevttpgqetmfgvdftdlykksdlygrnkalitelsvprpgtkdlhfdtqysqpfwtqcmaclwkqhw

sywrnpaytavrflftvmislvfgtmfwdlgskvsraqdlsnamgclyaavlfigtqnassvqpvvavertvfyreraagm
ysalpyafaqafieipyifvqatfcgtiiyamigfewtvekyfwylffmfftlmyytyygmmtvaitpnvnvaqvvsaffy
glwnlfsgfivprprmaiwwrwyywicptawtlygliasqfgdyqnkltddetveqylrrffgfkheflpvvgvvtagftvl
faftfafgikafnfqtr

6.6 *PhPDR2* Promoter Sequence

cctggaaccaagctttgtgtaggaaaattttgcaaacgttttaccacatccttgactgactatatttgagccaatgatttgtgctggac
gacgcttgtcccgacatccatttaatttggaataattcacattctagtaattacatgaaaataagtgtcgaaggaataggcacaaaat
taaatgttatgagacttgaagaaatagaatgaacatgtgaaatgctattactagtatcaactaagcaaacttaattatctttcgaaaat
ggagttgaagtagtaaagagaaagaaaattttctataagaacaagaatgtacagaatcttttgcttacgcgtgatttccttttatgtg
gatttagtgtgctattggatagtcacaaggtccatgagaattggaagaaattaagccagtcaaacaagggatgcctttcgtagaaa
gacaaataagatagacaacattggtatacactatgtactctccgtccattttatttgtctcatttatttttacatgctttttataaaaatatta
ataaaaatgtacttttactatattaatccatctttataaaaatattaattcttgtttctatttttaaaattaattaatactgtgggcaaatttaa
aaaaaataattaattttatcttaaactcttaaataaataaataatttgaaacaattatttataataagagacaaataaatagattgaagag
tgcatgtaggacaacttaataatgaggggaaagatacttgtctcgaagggcaattggtaggggccatcgcttctcataatgcaa
gttctttaacatttttatattaacaataatattaagctaagtgggtaggggccatctctttcacatttttaatattaacaagaatctgtagct
caggataggccatcaagacttttatttaacgagtcaaacaacgtggaatttgaaaaatgaaaaataaaaaatgaaacgctttaatt
agtctatacaatagcccgccttttcctgtacatgtaacatgctatacattatatattatataatcccttggcctttagaattattgcagca
actcttacttttccttcattcttttattttctctttcagatcattcacttgaaaaaaacgaaaacccaagaacatatttctgagctagag
ggggtctgaaaatataatttgcatgttgattggtccata**atg**

PhPDR2 transcipt start in bold and underlined

6.7 PhPDR3 Partial cDNA Sequence

agcaacacttaatttttccttcatttttttttcctctttcaactcattcacttgaagaaaacaaaaatcaagaacatttttcttagctaaag
gtggtctgaaaaatatttgcattttgattggttcata**atg**gaaccagtaaacttaggtaacttacgagcggctagtttgagaggaagt
gcaaggggaagtttaagcggaagtttaagagcaaatagtaactctatatggagaaatgataatgttttcactcgttcatcaagagat
gaaaatgatgaagaagcacttaaatgggcagctcttgaaaaacttccatcatttgatcgtttaagaaaaggtttgttgtttggatctga
aggtacagcaccttctcaaattgatatacatgatattggttttcaagaaagacaaggcttgcttgataggcttgtgaaagatccggat
gaagataatgagaagttcttgttgaaactcagagatagaattgacagagttgggctggatatgccaacaatagaagtaagatatga
gcatctacatgttgtggcagatgcacatataggaggcagagctttgcctacatttacaaactttgtgactaattttcttgagtcattgtt
gtgctctctccatatcctaccaagtaaaaagaggcagctcactattcttaatgatgtgagtggtatcattaagccttgtagattgacttt
gcttttgggacctcctggttgtggcaaaactacttttttattagctttggctggaaagcttgatcctgaacttaaggtaactgggaagg
taacctataatggacatgaaatgactgaatttgtaccacaaagaactgctgcttatattagccagcatgatttgcatattggagaaat
gactgtgagagaaaccttggaattctcggccagatgccaaggcattggcactcgttatgagatgtcggctgaactgtcaagaaga
gagaaagcagctaatatcaagccagaccctgatattgatatctatatgaaggcatcagcaacagagggacaagaagcaaatgtt
gttacagattacgttcttaagatattgggactggacatttgcgcagatactttggtgggagatgacatggtaagg

Start ATG is marked in bold and underlined

6.8 PhPDR3 Promoter Sequence

atctaagtaaaaacgtcaagcaagctcaaattattcaaattttcaccggcaacaatgccaaaaacttgtttctcccaaacccaaaca
caagtatatgcggtcgttcaagtagtaaagtgattaaatcaagtatcgtcccacaaagactaatgttagctactaactaaattaaatg
attttgaattatcaaaacaagcaaagttggctttatggattaaagatattgctaaaatttaaaattaaaattataactaaatcaagtaattt
gatcaaagcacataagtgaaattttggttaacgagggttattggattgatttctcttcggtagttaattgttatagttaaaaggattttgg
ttaacaaggggagaaaatattctagggctatgggatatatgtcaatcctgctgaattctacatgtaatttgaataatgaatttatctgg
gttattaattgacaggattaattttacctatagaaatctttcaatttcctactcatttattcaagttaatctagcgcctatgtttctatagaatt
agaattaacaaaaatgcattgaaattttatgtataatgattaagcaaggcaaaatggtatattccaatcctagttgtgaatccgttccc
cgatacccaggttcaagaacttatcctattcaatcctattgcaatcaaaaattctctttcccaattttaattcaagattcgtagaggagt
atttaaatgttggcccaaacaatcaaataattcagcacatcatatgaataaaataacccaaagtgataattaattaaatccaactaact
tctaaatatcaacattcattataaactcataactccagaacaaaaatttaattacacatagtcatagtaaaaatccaaccattaatttgc
aaaactccgagaatccttgctgtctacgacatccggtggttctaattctagtcacgcacattcctcaatacgacaattaaaatgtgag
taacagttaagcaacttcgatgcaagaatctgcagctcagcacaggccatgaggagttttatttaataaatcaaaacagcgtgga
atctggatgcactattgttattaacaattaagcaacttcgattcaaaaaactgcagctcagcacaggccatgaggagttttatttaat
gagtcaaaacaacgtggaaagtggatgcactattgttattttaatatacgtatctttaaccatatcttttcagctatacttaattcaaata
gccgtttaatagaaaaacgaaacgttttaattaatctattcagtagcccgccttttttctatacatgtatattataaatatccatttagcctt
tagacttaatgcagcaacacttaatttttccttcatttttttttcctctttcaactcattcacttgaagaaaacaaaaatcaagaacatttt
cttagctaaaggtggtctgaaaaatatttgcattttgattggttcata**atg**

PhPDR3 transcipt start in bold and underlined

List of Abbreviations

2,4-D	2,4-Dichlorophenoxyacetic acid
^{3}H	tritium
°C	degree celcius
µ	micro
AA	amino acid
ABA	abscisic acid
ABC	ATP binding cassette
AFLP	amplified fragment length polymorphism
AM	arbuscular mycorrhiza
AMF	arbuscular mycorrhizal fungi
AOH	ABC1 homologue
ATP	adenosine tri-phosphate
b	base
BAC	bacterial artificial chromosome
BAP	6-Benzylaminopurine
BF	branching factor
BLAST	Basic Local Alignment Search Tool
bp	base pair
c	centi
CCD	carotenoid cleavage dioxigenase
cDNA	complementary DNA
CHS	chalcone synthase
CN	cotyledonary node
DA	Dalton
DAD	decreased apical dominance
DPM	disintegrations per minute
DNA	deoxyribonucleic acid
dTph1	nonautonomous petunia specific 284bp transposable element
DTT	Dithiothreitol
DXR	1-deoxy-D-xylulose-5-phosphate reductoisomerase
DXS	1-deoxy-D-xylulose-5-phosphate synthase
ER	endoplasmatic reticulum
EST	expressed sequence tag
FW	fresh weight
g	gram
GR24	synthetic strigolactone derivative
gDNA	genomic DNA
GFP	green fluorescent protein
GUS	beta-glucoronidase
h	hour
HR	hypersensitive response
JA	jasmonic acid
k	kilo

l	liter
LR34	leaf resistance locus 34
m	mol
M	molar
MAX	more axillary branching
MCS	multiple cloning site
MDR	multi drug resistance related (protein)
min	minute
MRP	multi drug resistance protein
MYC	mycorrhiza
n	nano
NAA	1-Naphthaleneacetic acid
NBD	nucleotide binding domain
NOD	nodulation
ORF	open reading frame
p	pico
PAL	phenyl ammonium lyase
PAM	periarbuscular membrane
PCR	polymerase chain reaction
PDR	pleiotropic drug resistance (protein)
PDS	phytoene desaturase
PEN	penetration
Pi	inorganic phosphate
PM	plasma membrane
PMP	peroxisomal membrane protein
PPA	pre-penetration apperatus
RACE	rapid amplification of cDNA ends
RCN	reduced culm number
RMS	ramosous
RNA	ribonucleic acid
RNAi	RNA interference
RT	reverse transcription
s	second
SA	salicylic acid
SAM	shoot apical meristem
SAR	systemic acquired resistance
SYM	symbiosis
TCA	tri-chlor acetic acid
T-DNA	transfer DNA
TMD	transmembrane domain
UTR	untranslated region
v	volume
VIGS	virus induced gene silencing
w	weight
WBC	white brown complex (protein)
wpi	weeks post inoculation

Acknowledgements

Foremost of all I would like to thank Prof. Enrico Martinoia for giving me the opportunity to take on this challenging project and for being supportive in whatever ways necessary, while at the same time allowing me to steer my own course through this PhD.
Second I would like to thank Prof. Beat Keller for agreeing to be member of my thesis committee and critically evaluating this work.
Then I want to thank Dr. Didier Reinhardt for being a great collaborator and external supervisor, whom I could always address for council in matters concerning mycorrhiza.
Furthermore I would like to thank Prof. Tom Gerats and Dr. Michiel Vandenbussche for providing me with two 3D-gDNA libraries to screen, the knowledge how to successfully screen and the W138 individuals derived from my screens. I am grateful to them for hosting me in Nijmegen and teaching me the basics of Petunia genetics, for always being open for discussion, and for introducing me to the Petunia community, which I would also like to thank in its entirety.
I would like to thank all my lab colleagues, for putting up with me and keeping up my spirits. In particular I want to thank Bo Burla for continuously assisting me in perseverative computer and software problems and Barbara Weder as well as Maja Schellenberg for assisting me in practical matters.
Thanks to Dr. Julien Bachelier, for his support in sectioning and for starting a hopefully fruitful collaboration with me.
I want to thank Karl Huwiler for horticultural advice and for taking care of my Petunias.
Thanks to Reto Schild for helping me to find many a chemical and piece of equipment.
Thanks to Daniel Bollier and the workshop crew for custom designing and building several gadgets and fixing whatever broke down.
Thanks to Dr. Jake Alexander for critically reading this manuscript and mental support.
Thanks to the NCCR Plant survival for financial support.
Last, but certainly not least warmest thanks to Tamami Kretzschmar and Momoka Kretzschmar, for always supporting me and managing to take my mind off the lab even in desperate times.

Curriculum Vitae

Name: KRETZSCHMAR
First Name: Tobias
Date of birth: 08.02.1978
Place of birth: Karl-Marx-Stadt (D)

2005-2009 Graduate Studies under the supervision of Prof. Dr. Enrico Martinoia at the Institute of Plant Biology of the University of Zürich entitled: "Pleiotropic Drug Resistance Type ABC Transporters in *Petunia hybrida*: Novel Roles in Symbiotic interactions, Branch Development and Herbivory Defense"

2003-2004 Diploma Thesis under the supervision of Prof. Dr. Ekkehard Neuhaus at the Technical University of Kaiserslautern in Germany entitled: "Biochemical and Physiological Characterization of a Vacuolar Dicarboxylate Transporter in *Arabidopsis thaliana*"

2002-2003 Scientific Internship under the supervision of Prof. Dr. John Holtum at the James Cook University in Townsville, Australia entiltles: "Biochemical Characterization of Hexose Transport Across the Tonoplast of *Ananas comosus*"

1999-2002 Undergaduate studies in Biology at the Technical University of Kaiserslautern in Germany.

1996 Abitur (Secondary school diploma qualifying for university admission) in Biology, History, English and Ethics from the Gymnasium am Rittersberg in Kaiserslautern, Germany.